

A pre-clinical study of SG pseudo-peptide inhibitors for the treatment of  
Alzheimer's disease: single molecule force spectroscopy and cell viability

by

Morgan Robinson

A thesis

presented to the University of Waterloo

in fulfillment of the

thesis requirement for the degree of

Master of Science

in

Biology

Waterloo, Ontario, Canada, 2017

©Morgan Robinson 2017

**Author's Declaration**

This thesis consists of material all of which I authored or co-authored: see Statement of Contributions included in the thesis. This is a true copy of the thesis, including any required final revisions, as accepted by my examiners.

I understand that my thesis may be made electronically available to the public.

## **Statement of Contributions**

This work was completed by me however certain portions include contributions from other students and scientists. A portion of the work presented here has been accepted for publication in a peer-reviewed journal for which I am co-first author. All work is my own unless otherwise reported in this statement of contribution. Below are specific contributions from persons other than me:

Chapter 2: Biochemical schematics of inhibitors presented appear in a publication for which I am a first co-author however the figures themselves were produced by collaborators at the University of Calgary. The text in this section was written by me in its entirety.

Chapter 3: Half of the data collection (including experimental preparation and operation of the atomic force microscope) was gathered with the help of undergraduate co-op student Jennifer Lou. All data was processed and analysed by me. The work presented here was submitted to peer-reviewed journal for publication during the time I prepared this manuscript however the text here was written by me in its entirety. The figures shown in this section were taken from the associated manuscript; all these figures were produced by me, except Figure 7 which was drawn by Dr. Brenda Yasie Lee.

Chapter 4: The protocols used for cell viability work in this thesis were developed in part based on preliminary experiments conducted by undergraduate co-op student, Jennifer Lou, however all data presented in this section was collected, analysed and discussed by me.

## Abstract

Alzheimer's disease (AD) is one of the single greatest healthcare challenges facing our society today with no treatments available that cure, prevent or slow the disease. Neurodegeneration in AD is observed alongside pathology featuring amyloid- $\beta$  ( $A\beta$ ) deposits in the brain.  $A\beta$  monomers themselves have minimal toxicity but misfold into  $\beta$ -sheets and aggregate to form neurotoxic soluble oligomers, than aggregate further into less toxic insoluble fibrils and plaques. To treat or prevent AD one potential strategy has been suggested which involves the use of rationally designed pseudopeptides that bind  $A\beta$  with high affinity, inhibit aggregation into toxic  $A\beta$  oligomers and allow for natural clearance. A class of pseudopeptide  $A\beta$  inhibitors, designated "SG", have been proposed with the use of computer aided drug design (CADD) by medicinal chemists at the University of Calgary led by Dr. Arvi Rauk. It is the aim of this thesis to verify, experimentally, that SG inhibitors behave as expected, moving these potential AD drug candidates further along the drug development pipeline.

In this thesis a brief overview of  $A\beta$  pathology and therapeutics directed against  $A\beta$  are discussed followed by a review of the literature relevant to SG inhibitor design. The results from two separate experiments evaluating SG inhibitor target engagement and neuroprotection against  $A\beta$  are then discussed. In the first experiment, a nanoscale biophysics approach was used to assess the ability of SG inhibitors to bind  $A\beta$  and prevent dimerization – the first step in toxic oligomer formation. This single-molecule biophysics assay built on an atomic force microscopy (AFM) platform demonstrated that all the inhibitors engage the target and prevent  $A\beta$  dimerization. In the second set of experiments, a series of *in vitro* cell viability studies with HT-22 murine derived hippocampal cells was performed to assess SG inhibitor toxicity and the ability of SG inhibitor to mitigate  $A\beta$  toxicity. Most SG inhibitors exhibited no apparent toxicity to HT-22 cells however myristic acid modification for delivery of inhibitors to the brain caused dose dependent toxicity. Importantly, two of the five inhibitors demonstrated a small but promising effect on preventing  $A\beta$  oligomer neurotoxicity as demonstrated by one third increase of HT-22 cell viability in MTT assays. The inhibitor SGA1 may cause a slight increase in the toxicity of  $A\beta$  prepared under fibril forming conditions. Overall the work described here presents experimental evidence that indicates SG inhibitors as a potential therapeutic for  $A\beta$

toxicity and informs recommendations for SG inhibitor design to improve safety and efficacy for future lead candidates.

## **Acknowledgements**

I would like to acknowledge first and foremost my supervisor Dr. Zoya Leonenko. Your support, guidance and example have forever changed the direction of my life, for which I am grateful.

An acknowledgement is in order to the other scientists who contributed to the success of this project: Dr. Michael Beazely for agreeing to be on my committee and providing guidance, expertise and the tools necessary for the successful completion of cell viability assays in this thesis; Dr. Arvi Rauk for kindly supplying the inhibitors and providing advice and expertise whenever needed; Dr. Bernard Glick for agreeing to be on my examination committee and allowing the use of your fume hood for sample preparation; and finally, Dr. Scott Taylor for synthesizing the APS used in these experiments.

I would also like to thank Dr. Francis Hane and Dr. Brenda Yasie Lee for training on the Atomic Force Microscope and the other members of the Nanoscale Biophysics Group, Nyasha Gondora and Nawaz Amhed for training with mammalian cell culture, and Jennifer Lou for your help with experiments, your advice and most of all your friendship.

In addition, I would like to acknowledge the broader University of Waterloo community for the many examples of excellence in the pursuit of true knowledge.

Finally, I would like to acknowledge my family and friends who have provided me with essential support during these times. You are the reason I strive for greatness, the faith you place in me is well received, much love.

## **Dedication**

I would like to dedicate this work to my grandmother, Shirley Jefferies, although your memory has faded, your love lives on in mine.

## Table of Contents

Authors Declaration .....	ii
Statement of contributions.....	iii
Abstract.....	iv
Acknowledgements.....	vi
Dedication .....	vii
Table of Contents.....	viii
List of Figures .....	x
List of Tables .....	xi
List of Abbreviations .....	xii
<b>Chapter 1: Introduction .....</b>	<b>1</b>
1.1 Alzheimer's disease.....	1
1.2 Amyloid- $\beta$ pathology.....	3
1.3 A $\beta$ physiology and the aetiology of AD.....	7
1.4 Therapeutics targeting A $\beta$ .....	11
<b>Chapter 2: Rational design of A<math>\beta</math> aggregation inhibitors .....</b>	<b>16</b>
2.1 Testing A $\beta$ aggregation inhibitors.....	16
2.2 Peptide inhibitors.....	17
2.3 Delivery challenges due to the blood-brain barrier .....	20
2.4 SG inhibitors .....	24
<b>Chapter 3: Single molecule biophysical study of A<math>\beta</math> dimerization .....</b>	<b>30</b>
<b>3.1 Methods.....</b>	<b>30</b>
3.1.1 Atomic force microscopy .....	30
3.1.2 Atomic and single molecular force spectroscopy.....	32
3.1.3 Surface modification for SMFS .....	34
3.1.4 Data acquisition and statistical analysis .....	36
<b>3.2 Results &amp; Discussion .....</b>	<b>37</b>
3.2.1 Binding curves.....	37
3.2.2 Experimental yield of binding events .....	39



3.2.3 Force distribution.....	40
<b>3.3 Conclusion.....</b>	<b>44</b>
<b>Chapter 4: SG inhibitor toxicity and the effects on A<math>\beta</math> toxicity .....</b>	<b>45</b>
<b>4.1 Methods.....</b>	<b>45</b>
4.1.1 Cell culture models .....	45
4.1.2 Drug and A $\beta$ preparations.....	46
4.1.3 MTT assay.....	46
4.1.4 Statistical analysis .....	48
<b>4.2 Results &amp; Discussion .....</b>	<b>49</b>
4.2.1 SG inhibitor toxicity on mHT22 cells.....	49
4.2.2 Effect of inhibitors on A $\beta$ oligomer toxicity .....	50
4.2.3 Aggregation dependent effects of SGA1 .....	53
<b>4.3 Conclusion.....</b>	<b>54</b>
<b>Chapter 5: Comments and Future Directions.....</b>	<b>56</b>
<b>Chapter 6: Conclusion.....</b>	<b>59</b>
<b>References .....</b>	<b>60</b>
<b>Appendix A: Supplemental Material .....</b>	<b>75</b>
<b>Appendix B: Additional Research Projects.....</b>	<b>77</b>

## List of Figures

### Chapter 1

Figure 1: Amyloid- $\beta$ production and toxicity. ....	5
Figure 2: A $\beta$ aggregation schematic.....	5
Figure 3: Alzheimer’s disease pathology progression. ....	14

### Chapter 2

Figure 4: A $\beta$ aggregation and toxicity with time.....	16
Figure 5: Most probable structural conformations for A $\beta$ 13-23, SGA1 and its complex. ....	26
Figure 6: Most probably SG inhibitor structures. ....	28

### Chapter 3

Figure 7: AFM schematic.....	32
Figure 8: Schematic of A $\beta$ SMFS set-up. ....	34
Figure 9: Amine modification for SMFS. ....	36
Figure 10: Binding and non-binding force curves. ....	38
Figure 11: Multiple unbinding curve.....	39
Figure 12: Experimental yield of A $\beta$ binding with SG inhibitor. ....	40
Figure 13: The A $\beta$ force distribution for SG inhibitors.....	43

### Chapter 4

Figure 14: MTT metabolism. ....	47
Figure 15: SG inhibitor toxicity to HT-22 cells.....	50
Figure 16: SG inhibitor rescue of HT-22 cells from A $\beta$ .....	51
Figure 17: Aggregation dependence of SGA1 on A $\beta$ toxicity.....	54

### Appendix B

Figure 18: A $\beta$ force distribution with single peak fit. ....	75
Figure 19: Cell viability of HT-22 cells to A $\beta$ prepared at 37° C for 2 hours. ....	76

**List of Tables**

Table 1: Edge specific and homodimer dissociation energy.....	27
Table 2: SG inhibitor sequences.....	28

## List of Abbreviations

3-(4,5-Dimethylthiazol-2-yl)-2,5-Diphenyltetrazolium Bromide (MTT)

Alzheimer's disease (AD)

Amyloid- $\beta$  (A $\beta$ )

Amyloid precursor protein (APP)

Analysis of variance (ANOVA)

Antimicrobial peptide (AMP)

Atomic force microscopy (AFM)

Atomic force spectroscopy (AFS)

Blood-brain barrier (BBB)

Computer aided drug design (CADD)

Cell penetrating peptide (CPP)

Central nervous system (CNS)

Cerebral spinal fluid (CSF)

Dimethyl sulfoxide (DMSO)

Fetal bovine serum (FBS)

Least Significant Difference (LSD)

Low-density lipoprotein related protein 1 (LRP1)

Maleimide (Mal)

Molecular dynamics (MD)

Molecular weight (MW)

Monoclonal antibody (mAb)

Myristic acid (Myr)

Neurofibrillary tangles (NFT)

N-hydroxysuccinimide (NHS)

P-glycoprotein (P-gp)

Polyethyleneglycol (PEG)

Presenilin (PSEN)

Receptor for advanced glycation end products (RAGE)

Retro-inverso (RI)

Single molecule force spectroscopy (SMFS)

Thioflavin T (ThT)

Transactivator of transcription (TAT)

True control (TC)

## Chapter 1: Introduction

### 1.1 *Alzheimer's disease*

Alzheimer's disease (AD) is the leading cause of dementia worldwide, with an estimated 36 million cases as of 2010 with that number expected to double every 20 years, for a projected 120 million cases by 2050 <sup>1</sup>. In 1906, Dr. Alois Alzheimer first characterized a neurodegenerative disease in a 50 year old patient with symptoms of dementia, rapid cognitive decline and progressive memory loss, eventually resulting in death. Post-mortem autopsy of the brain tissue from this patient revealed severe cortical and hippocampal atrophy and the deposition of what is now known to be amyloid- $\beta$  ( $A\beta$ ) plaques and accumulation of intracellular neurofibrillary tangles (NFT) comprised of hyperphosphorylated tau. These pathological hallmarks led to formulation of two corresponding hypotheses regarding the aetiology of AD. In addition to a third hypothesis involving faulty cholinergic signalling these hypotheses have formed the basis of drug development in AD research for the past three decades, unfortunately, with no major clinical successes.

A common feature of neurodegenerative diseases is the accumulation of endogenous misfolded protein as in Huntington's disease, prion diseases and AD. In AD the amyloid cascade hypothesis suggests that increased  $A\beta$  accumulation in the brain results in misfolding and the formation of toxic  $A\beta$  aggregates <sup>2</sup>. The cause of  $A\beta$  accumulation in late onset AD is not precisely known but many factors have been implicated, including but not limited to: injury, inflammation and faulty lipid metabolism <sup>3-5</sup>.  $A\beta$  is a short endogenous (39 to 43 residue) protein produced from the cleavage of amyloid precursor protein (APP) to form the amyloidogenic species. The normal physiological function of APP/ $A\beta$  is not known for certain and the research in this area is highly speculative with most well established research on the associated pathology. Regardless,  $A\beta$  is neurotoxic and prone to causing the formation of reactive oxygen species (ROS) resulting in direct and indirect downstream dysfunction, such as: impaired calcium regulation, oxidative stress and hyperphosphorylation of the microtubule associated protein, tau. These combined neurotoxic insults interfere with neuronal processes, recruit and activate local immune cells triggering neuroinflammatory environment which

results in neuronal stress and eventually cell death. The neurotoxicity of A $\beta$  is expected to largely depend on the concentration of free soluble oligomers which are the most toxic species.

Current treatment options for AD in the clinic are limited to brief symptomatic relief in cognitive decline for up to a year with five pharmacological interventions approved by the FDA and with lifestyle and social interventions that can provide benefits to the quality of life of AD patients<sup>6</sup>. There are four acetylcholinesterase inhibitors which act by increasing the amount of acetylcholine in the brain, a neurotransmitter important for learning and memory that is depleted in AD patients<sup>7</sup>. The fifth approved AD drug, memantine, blocks NMDA receptors and the associated glutamatergic excitotoxicity observed in AD<sup>8,9</sup>. Both types have been shown to provide an improvement in the symptoms of memory loss and cognitive function, albeit for only a short periods of 6 to 12 months and with no effect on the trajectory of the disease<sup>7,8,10,11</sup>. Some evidence indicates that certain natural antioxidant supplements like vitamin E and melatonin have some benefit but the clinical evidence is not strong, nor is the benefit drastic, extended clinical trials are necessary in this area<sup>12,13</sup>. Non-steroidal anti-inflammatories are another class of drug that has some potential benefit in delaying the age of onset of AD as demonstrated by epidemiological studies but clinical trials remain inconclusive<sup>14</sup>. Clinical trials of advanced biological therapeutics designed to target underlying pathologies have not yielded any candidates in over 25 years of study and no treatments are available that modify disease trajectory<sup>15</sup>. The lack in mechanistic understanding of AD has made drug development slow and rationally designed next generation drug candidates that address the short-comings of the predecessor therapeutics are required in the drug development pipeline.

One strategy to prevent A $\beta$  toxicity in AD is to delay the formation of toxic oligomers thus giving the body more time to process and remove A $\beta$ . For this purpose, a class of pseudopeptide inhibitors has been proposed by Dr. Arvi Rauk's group at the University of Calgary. These "SG" inhibitors have been screened using molecular dynamics (MD) simulations wherein lead candidates are selected for maximal binding between the SG inhibitor and the target A $\beta$  self-recognition sequence<sup>16-18</sup>. This thesis aims to evaluate select lead candidates for experimental verification of their potential to target A $\beta$  and protect neurons from A $\beta$  toxicity providing important feedback for SG inhibitor design and informing future studies..

The remainder of the introduction will be focused on discussions surrounding the underlying A $\beta$  pathology and a brief review of strategies that target this pathology. In chapter 2 a more detailed look at design strategies for peptide inhibitors will be discussed including a look at challenges associated with central nervous system (CNS) delivery across the blood-brain barrier (BBB) and some literature surrounding SG inhibitor development. Chapters 3 and 4 will report the findings of the original research of this thesis project, first a nanoscale biophysics study of the effects that SG inhibitors have on A $\beta$ -A $\beta$  interactions using a single-molecule force spectroscopy biosensor, and then second, *in vitro* cell viability studies that assess SG inhibitor toxicity and the effects of SG inhibitors on A $\beta$  toxicity using HT-22 cells. Chapter 5 and 6 will discuss future directions and conclusions in turn.

## 1.2 Amyloid- $\beta$ pathology

The identification of A $\beta$  as the key constituent of senile plaques in AD patients and of its genetic origin, via the APP gene, led to the development of the amyloid cascade hypothesis<sup>2</sup>. It was hypothesized that clearance/production imbalance of A $\beta$  results in the accumulation of toxic aggregates, as A $\beta$  has strong self-assembly characteristics and has demonstrated neurotoxic activity<sup>2,19</sup>. Although the exact mechanism of A $\beta$  neurotoxicity is not precisely known, many pathways have been implicated, both apoptotic<sup>20,21</sup>, and to a lesser extent necrotic cell death has also been observed<sup>22</sup>. It is therefore the likely case that A $\beta$  neurotoxicity results from several parallel and compounding pathways, this becomes especially apparent when you consider the long list of effects that A $\beta$  has been associated with, including: excitotoxicity<sup>9</sup>, synaptotoxicity<sup>23</sup>, calcium dysregulation<sup>24,25</sup>, mitochondrial stress<sup>25,26</sup>, inflammation and oxidative stress<sup>20,22</sup>, and hyperphosphorylated tau<sup>27</sup>. There is a lack of clarity in the A $\beta$  pathology of AD, such as: the mechanisms which contribute to neuronal sensitivity and resistance to A $\beta$ , the extent to which receptor and non-specific membrane interactions contribute to toxicity, and the events upstream of A $\beta$  production which result in its deposition.

The pathology of A $\beta$  begins with its production (shown in Figure 1 below) which involves the processing of amyloid precursor protein (APP), a transmembrane protein with little known physiological functionality<sup>28</sup>. APP is cleaved sequentially by  $\beta$ - and  $\gamma$ -secretases predominantly inside the cell to form A $\beta$  monomers ranging from 39 to 42 amino acids in length<sup>29-31</sup>. In



additional there is an off amyloidogenic pathway that occurs primarily at the outer cell membrane wherein  $\alpha$ -secretase cleaves within the A $\beta$  sequence<sup>32</sup>. Once cleaved from APP, the A $\beta$  monomer is expected to take on an ensemble of structures, random coil, alpha helix or hairpin  $\beta$ -sheet, with  $\beta$ -sheet secondary structure increasing during the aggregation process (shown in figure 2 below)<sup>33-36</sup>. A $\beta$  oligomerization is initially driven by hydrophobic interactions<sup>35</sup>, with strong sequence specific interactions between the central regions playing a major role in  $\beta$ -sheet formation<sup>37,38</sup>. For this reason A $\beta_{42}$  aggregation rates are higher than the shorter A $\beta$  peptides as it contains additional strongly hydrophobic residues and higher aggregation rates are associated with greater toxicity<sup>35,39</sup>. The most toxic A $\beta$  species appear to be low weight disorganized oligomers that have low  $\beta$ -sheet structure<sup>35,39</sup>. As oligomers grow, transitioning from disordered oligomers into  $\beta$ -sheet oligomers, the A $\beta$  monomers misfold into hairpin structures with anti-parallel intramolecular  $\beta$ -sheet secondary structure<sup>35,40</sup>. Intermolecular interactions between adjacent A $\beta$  monomers are dependent on the central recognition region (A $\beta_{16-23}$ ) with side chain interactions stabilizing  $\beta$ -sheets which continue to grow, eventually forming fibrils then plaques<sup>34,37,41</sup>. Many studies indicate that A $\beta$  fibrils and plaques are less toxic than oligomers, with the smallest oligomers being most toxic<sup>39,41-44</sup>, although fibrils and plaques may be a source of free soluble oligomers<sup>45,46</sup>. The process of A $\beta$  aggregation is a complex equilibrium process that is sensitive to the environmental conditions such as pH, ionic strength, the presence of impurities and even traces of metal contaminants, especially iron and copper ions<sup>47-50</sup>. There are more layers of complexity due to multiple polymorphisms of oligomers and fibrils which have unique antibody binding characteristics and a correspondingly diverse immune response<sup>51</sup>.

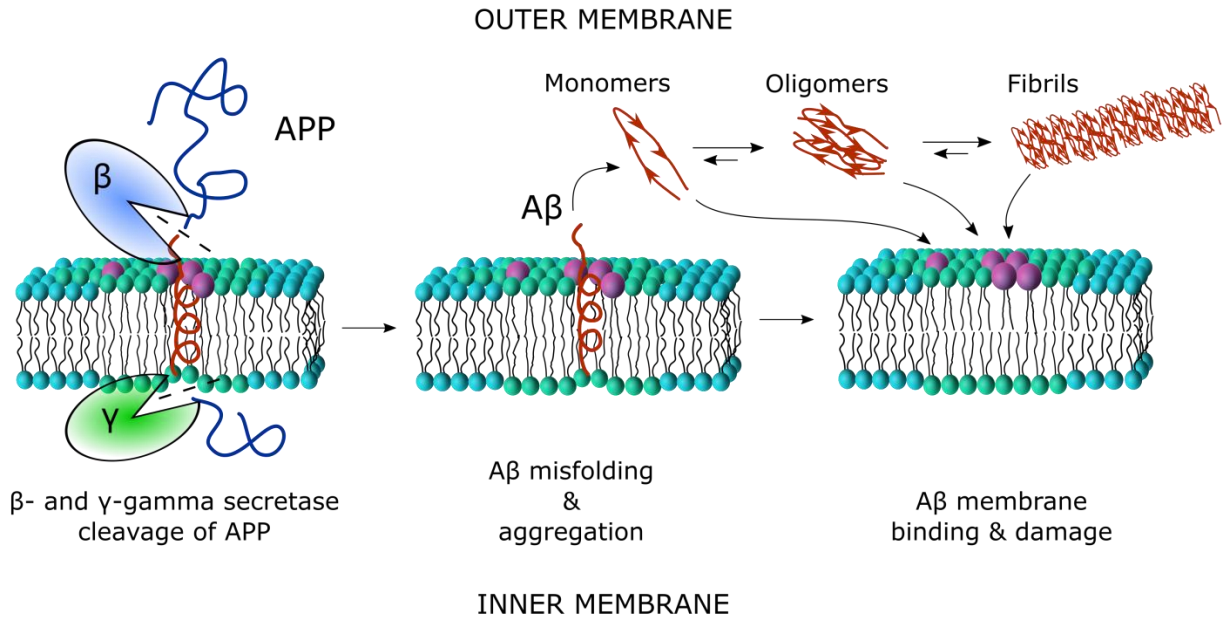


**Figure 1: Amyloid-β production and toxicity.** Transmembrane protein APP is predominantly found in cholesterol/sphingolipid rich membrane microdomains where it is cleaved by β- and γ- secretase in a sequential fashion to produce Aβ fragment that is free to aggregate into toxic oligomers and fibrils, which bind to and damage the neuronal membrane.

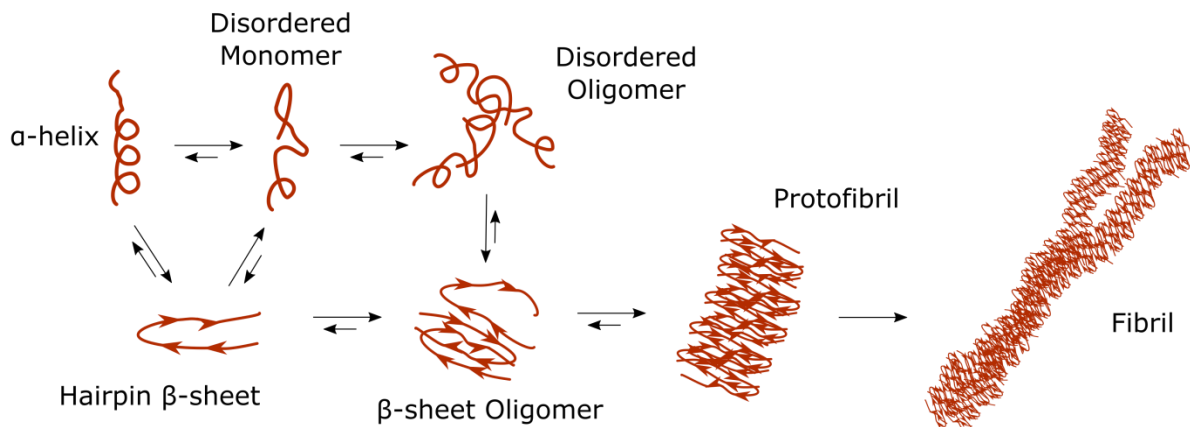


**Figure 2: Aβ aggregation schematic.** Once released from APP, Aβ takes on an ensemble of structures depending on environmental conditions; Aβ monomers alone are largely non-toxic. The α-helix is stabilized by the lipid membrane, the disordered monomer is favourable in bulk solution and the hairpin turn is most favourable as aggregation proceeds. Low molecule weight oligomers are the most toxic species that transition into higher β-sheet secondary structure acting as seeds for fibril growth, eventually forming less toxic insoluble fibrils.

Aβ toxicity is not only defined by its structure but is also related to the cell membrane with which it interacts strongly. Aβ oligomers bind to the lipid membrane triggering disruption of neuronal function through many mechanisms, eventually resulting in cell death. Lipid membrane composition<sup>52-55</sup> and the resulting lipid raft and membrane microdomain structure has been implicated in Aβ toxicity<sup>56-58</sup>. This strong dependence on the cell membrane is likely a

result of A $\beta$  aggregation occurring at the cell surface since it provides a hydrophobic interface for interaction<sup>59</sup>. A $\beta$  interactions with the lipid bilayer results in direct damage induced by permeabilization, perforation and depolarization of the cell membrane also interfering with receptor trafficking, ultimately affecting a broad spectrum of signalling pathways in neurons and glial cells within the brain<sup>43,60,61</sup>. The hydrophobicity and electrostatic surface potential of A $\beta$  with both positive and negative moieties make it capable of interacting with nanoscale electrostatic and topographical features of the cell membrane, which can act as nucleation sites for amyloid growth<sup>54,60</sup>. A $\beta$  induced depolarization of the cell membrane causes calcium dysregulation which results in a plethora of intracellular signalling changes, as well as mitochondrial stress via the Ca<sup>2+</sup> mediated opening of mitochondrial permeability transition; this dramatically impairs cellular metabolism and energy utilization<sup>25,26</sup>. A $\beta$  is primarily produced from intracellular APP, as such membrane bound organelles in the cytosol are also highly susceptible to disruption, especially the mitochondrial membrane<sup>26,62</sup>. A $\beta$  has also been shown to induce excess ROS production that damages proteins and especially unsaturated lipid causing oxidative stress which again has dramatic consequences on cellular function in general. These excess ROS cause increase saturated lipid content and is expected to trigger hyperphosphorylation of a structural microtubule protein, tau, which has been shown to occur upstream of – and to be mediated by – A $\beta$ <sup>63,64</sup>. There is an interesting and long discussion that could be had surrounding the role of the cell membrane in A $\beta$  toxicity and how neurons may be sensitized to A $\beta$  toxicity due to age-related changes to lipid metabolism and resulting changes in membrane composition and structure<sup>54</sup>, unfortunately that will be forgone for the time being for the sake of brevity.

Curiously, certain brain regions in AD are more susceptible to neurodegeneration than others, for instance the hippocampus and frontal cortex as compared to the cerebellum<sup>65</sup>. Even more curious A $\beta$  pathology has been observed in elderly individuals without the appearance of any AD symptoms<sup>66</sup>. Along with A $\beta$  pathology, neuroinflammation, oxidative stress, hyperphosphorylated tau, and cholinergic dysfunction are also observed in AD patients<sup>67–70</sup>. These inconsistencies, the diversity of molecular pathologies across AD populations and the continuing failure of A $\beta$  specific therapeutics has led some suggest that A $\beta$  accumulation is a

secondary event and not central to AD <sup>71</sup>. Regardless of whether or not it is the primary cause or a secondary downstream event, it is undoubtedly toxic and thus may be a necessary target for the effective treatment and/or prevention of AD.

### 1.3 *A $\beta$ physiology and aetiology of AD*

The body of this thesis is dedicated to a class of potential therapeutics which are designed to directly target the A $\beta$  aggregation pathway however there seems to be an opportunity to digress briefly and discuss the bigger picture and speculate as to the aetiology of AD, which remains elusive. Several key basic features of human physiology keep emerging in different areas of AD research in connection to A $\beta$  pathology, specifically: autophagy, immune function, and lipid trafficking and metabolism. The connections between immunity and lipids in A $\beta$  production and regulation that have been observed in basic pathology, genetic and epidemiological studies may hint at a potential physiological role for APP/A $\beta$  <sup>3,72-75</sup>. Any description of AD aetiology must explain the A $\beta$  production/clearance imbalance as it is the definitive molecular feature of AD. The exact mechanisms behind this imbalance are very complex and not well understood although some contributing factors have been identified <sup>76-79</sup>.

There is an important distinction between the pathology associated with aggressive familial forms of AD and late onset (or sporadic) AD, originally called senile dementia. These two diseases have similar symptoms and pathologies; although familial AD and sporadic AD are different in terms of disease onset and progression they are nonetheless considered two forms of the same disease, sharing common underlying disease pathology. Familial AD accounts for approximately 5% of AD patients and has a clear heritable cause from mutations in the genes that encode APP and the subunits of  $\gamma$ -secretase, presenilin-1 (PSEN1) and presenilin 2 (PSEN2). The identification of APP provided the early genetic evidence for the critical role of A $\beta$  in AD pathology <sup>80</sup>. In contrast sporadic age-related late onset AD has been associated with over two dozen different genes with a variety of expected roles in immune function, lipid metabolism/trafficking, autophagy and endosome formation, including: APOE, CLU, PICALM to name but a few <sup>74,81-83</sup>. In addition to these genetic risk factors and aside from age – the number one risk factor for AD – epidemiological studies point to lifestyle factors such as poor diet, lack of exercise, high stress and insulin resistance as contributing factors in AD progression

and age of onset<sup>74,75</sup>. Owing to the multifaceted and broad impact of these genetic and lifestyle factors on overall health, and brain health in particular, it should not be surprising that the precise mechanisms have eluded researchers so far and that much controversy remains in terms of AD aetiology<sup>84</sup>.

Despite no clear mechanism of late onset AD pathology, genome wide association studies and epidemiological data seem to correlate, broadly speaking, with genetic and lifestyle factors that strongly influence immune function and lipid homeostasis<sup>74</sup>. This should not be too surprising as lipid homeostasis plays an important role in immune system and inflammatory regulation, both through lipid mediators – like prostaglandins – but also from changes in the lipid membrane – which directs trafficking of immune receptors<sup>4,85,86</sup>. Epidemiological studies indicate that injury is a strong predictor of increased A $\beta$  pathology and thus AD, for instance traumatic brain injury, systemic infection and chronic inflammatory conditions such as type II diabetes<sup>5,87,88</sup>. After injury, during the proinflammatory response, significant amounts of lipids are required for tissue remodelling thus their metabolism and trafficking are incredibly important. Cholesterol in the brain is synthesized almost entirely *de novo* and only very small amounts of circulating cholesterol is transported across the BBB; this means slight perturbations in cholesterol homeostasis within the brain may have dramatic consequences, especially over chronic timescales<sup>89</sup>. Long thought to be immune privileged the brain in fact is highly impacted by the immune system and reciprocates to aid in regulating the peripheral immune system, largely through the limbic and neuroendocrine systems, in particular by producing stress hormones which are typically built from sterols, a form of lipid<sup>90,91</sup>.

Lipids are largely insoluble as such they must form complexes with other lipids and proteins for trafficking; APP/A $\beta$  may be such a protein. APP is constantly trafficked between membrane bound organelles and the cell membrane spending little time at the outer membrane, being rapidly internalized or excreted<sup>92</sup>. Studies in neuroblastoma cells overexpressing APP indicate that in the steady state only 10% of APP is found at the cell membrane, with 30% being excreted and the rest distributed within the Golgi-endosomal network<sup>92,93</sup>. APP that is located within cholesterol and sphingomyelin enriched microdomains of intracellular organelles undergoes proteolytic processing by  $\beta$ - and  $\gamma$ - secretases to form A $\beta$ ,

whereas APP in the cell membrane is predominantly processed by  $\alpha$ -secretase – off the amyloidogenic pathway<sup>92–95</sup>. It has been shown that reductions in cholesterol cause a reduction in A $\beta$  production, which may suggest reduced trafficking of APP to the cholesterol enriched microdomains<sup>96</sup>. In addition, membrane cholesterol appears to play a key role in  $\beta$ - and  $\gamma$ - secretase activity, again possibly through trafficking of these complexes to membrane microdomains containing APP<sup>31,97</sup>. In a separate study it was observed that A $\beta$ <sub>40</sub> and A $\beta$ <sub>42</sub> decreased cholesterol and sphingomyelin levels, respectively, by modulating their metabolism<sup>98,99</sup>. This suggests a negative feedback mechanism between cholesterol and sphingomyelin with APP/A $\beta$  production. There is evidence for the role of APP, not only in lipid metabolism through A $\beta$  intermediate but, in lipid and cholesterol trafficking as APP has been observed to mediate cholesterol uptake at the intestinal epithelium<sup>99–101</sup>. Interestingly APP has a strong effect on the migration of neurons to the cortical plate during brain development in utero<sup>28</sup>. It should not be surprising to find regulators of lipid homeostasis expressed to a large extent within the brain where synaptic plasticity and pruning constantly requires a high level of neuron, and thus neuronal lipid membrane, reorganization<sup>102</sup>.

In addition to the role that APP and A $\beta$  play in regulating cholesterol and sphingomyelin, it has also been suggested that A $\beta$  may serve a physiological function as an anti-microbial peptide (AMPs)<sup>103–106</sup>. A $\beta$  contains many of the hallmark features of AMPs, including: high hydrophobicity, net positive charge, native  $\alpha$ -helical secondary structure, and the propensity to aggregate on – and perforate – cell membranes<sup>106</sup>. This is supported by a recent report that showed transgenic mice over-expressing APP were more resilient to bacterial infection than their wild-type litter mates<sup>105</sup>. The antimicrobial activity was visualized quite nicely using SEM imaging wherein bacteria were observed trapped by amyloid fibres, limiting their motility<sup>105</sup>. Another recent study looked at the effect of gut bacteria on AD transgenic mice and found that germ-free AD mice produced less A $\beta$  pathology, further highlighting the link between anti-microbial activity and A $\beta$ <sup>104</sup>. Further evidence for the role of A $\beta$  as a tool of the innate immune system comes from epidemiological studies which indicate a strong correlation between systemic infection and the risk of developing AD later in life<sup>87,107</sup>. AMPs represent one of the

oldest conserved evolutionarily adapted host defense systems; as such it is possible that A $\beta$  is a remnant of an ancient innate immune system.

There are many pathways for the degradation and clearance of A $\beta$ . First and foremost autophagy within neurons should degrade overproduced A $\beta$ <sup>108,109</sup>, which explains the link between impaired autophagy and AD. Soluble extracellular A $\beta$  oligomers and fibrils uniquely activate microglial cells, but ultimately trigger phagocytic endocytosis of A $\beta$ <sup>110</sup>. A $\beta$  can also be cleared from the brain across the blood-brain barrier (BBB) and the blood-cerebral spinal fluid (CSF) barrier<sup>111</sup>. All of these pathways have been shown to be impeded by A $\beta$  itself which could make A $\beta$  production snowball in a positive feedback loop. The importance of PSEN1 for efficient autophagy may explain why mutations in these genes result in familial AD<sup>112,113</sup>, while genome-wide screening has indicated that other autophagy regulating genes are differentially regulated in normal and AD cell models and that A $\beta$  directly interferes with autophagy<sup>109</sup>. Microglial clearance of A $\beta$  oligomers and fibrils may be accomplished through binding of A $\beta$  to cell surface receptors where it signals endosome mediated proteolytic degradation; this also causes microglial activation and subsequently triggers neuroinflammation<sup>114–116</sup>. This neuroinflammatory response uniquely depends on the aggregation state of A $\beta$ <sup>51,110</sup>. A $\beta$  production is strongly associated with microglial activation and inflammation, since increased levels of LPS and pro-inflammatory cytokines are associated with greater A $\beta$  deposition, in part by interfering with Toll-like receptor mediated phagocytosis of A $\beta$ <sup>67,117,118</sup>. Clearance of A $\beta$  across the BBB is regulated efflux transporters and receptors expressed at the endothelium such as P-glycoprotein (P-gp), multidrug resistance protein (MRP), receptor for advanced glycation end products (RAGE) and especially low-density lipoprotein receptor protein 1 (LRP1)<sup>111,119–121</sup>. Neurovascular clearance mechanisms have also been shown to be impaired in AD, where LRP1 and P-gp have been shown to be down-regulated in the cerebral vasculature near amyloid deposits<sup>120,121</sup>. If A $\beta$  cannot be cleared the formation of large A $\beta$  plaques may be neuroprotective as they appear to be largely inert.

It is therefore possible that APP/A $\beta$  serve a basic physiological role in brain lipid homeostasis and neuroimmunity, not only for host defense– but also for microglial activation and trafficking of lipids for tissue remodelling. This brief overview of APP/A $\beta$  regulation is but a

small sample of the literature in this area and many complex overlapping feedback loops appear to be involved. Unintended consequences represent a large limitation to drug effectiveness. Without a consensus on the physiological function of A $\beta$ , the unintended consequences of therapeutics directed at A $\beta$  pathology will be harder to predict and mitigate.

#### 1.4 Therapeutics targeting A $\beta$

Several different strategies that target the A $\beta$  production/clearance pathway are being explored in preclinical and clinical trials. General strategies to prevent the accumulation of A $\beta$  and its associated pathology have been developed which directly target A $\beta$  preventing toxicity and/or promoting clearance from the brain, or indirectly by preventing production of toxic A $\beta$  <sup>29,30,122</sup>. Active & passive immunotherapies in the form of vaccines and monoclonal antibodies (mAbs), respectively, promote immunogenic clearance of A $\beta$ . Small molecules and peptides have been explored as options for preventing aggregation and thus its associated toxicity. In addition, strategies which target upstream processing of APP into A $\beta$  by secretases using mAbs, as well as small molecule inhibitors and modulators have been explored <sup>29,30</sup>. Aside from compounds which affect A $\beta$  pathology many other strategies are being explored which target tau pathology, cholinergic signalling or a combination of pathological features found in AD.

Synthetic and naturally occurring small molecules have been explored for the potential treatment of AD, including: small molecule aggregation inhibitors, anti-inflammatory drugs, anti-oxidants and drugs which affect signalling pathways important for learning and memory <sup>30,123–127</sup>. Thioflavin T (ThT) and curcumin are small hydrophobic molecules which have been shown bind A $\beta$  and help to maintain protein folding homeostasis in worm models of AD, greatly expanding lifespan and reducing the paralytic effect of A $\beta$  on the nematode models <sup>125</sup>. In addition curcumin has an abundance of other properties which may make it useful for the treatment or prevention not only AD, but a variety of other diseases as it induces neurogenesis, and has anti-inflammatory, anti-oxidant, anti-microbial and anti-tumorigenic properties <sup>128,129</sup>. Melatonin is a pineal hormone which has demonstrated protective effects against A $\beta$  toxicity through receptor independent mechanisms <sup>130</sup>. Melatonin's protective effects are likely multi-faceted as they have been shown to reduce A $\beta$  aggregation, prevent oxidative stress, restore



mitochondrial function and directly protect the cell membrane from A $\beta$  by modifying its biophysical properties<sup>21,126,131–133</sup>. Multifunctional synthetic small molecules that operate on several aspects of AD pathology (A $\beta$  aggregation and cholinergic signalling) are currently in development and represent an interesting direction in therapeutic interventions<sup>134–136</sup>. Tramiprosate is a synthetic small molecule shown to bind A $\beta$  and inhibit neurotoxic aggregation which previously showed promise *in vitro* and *in vivo* but ultimately failed to meet primary endpoints in phase III clinical trials for mild AD<sup>123,137</sup>. Ultimately, small molecules directed toward A $\beta$  pathology are limited by their small size, and consequent lack of specificity, while their low molecular weight does not guarantee target engage or the ability to circumvent the delivery challenges imposed by the BBB, which will be discussed in more detail in the next chapter.

Immunotherapies that make use of the host immune system to stimulate removal of A $\beta$  have demonstrated potential in AD animal models, in particular high specificity mAbs that bind various species of A $\beta$  have been shown to reduce aggregation and promote immunogenic clearance of various A $\beta$  species from the brain<sup>138–140</sup>. Three non-mutually exclusive pathways for the immunogenic clearance mechanisms have been suggested however all may act in parallel<sup>141</sup>. First, mAbs are expected to directly trigger an immune response against A $\beta$  deposits in the brain, increasing microglial uptake<sup>138</sup>. Second, mAbs can also prevent aggregation of and disaggregate fibrils and plaques through dynamic competitive equilibrium processes as was supported by an early AFM study<sup>142</sup>. Finally, mAbs do not cross the BBB efficiently and have been suggested to improve cognition by removing amyloid burden through a proposed “sink” mechanism where the reduction of free soluble A $\beta$  in the periphery causes a shift in amyloid equilibrium to favour efflux from the brain<sup>143,144</sup>. In AD, BBB integrity is compromised with significantly high amounts of neuroinflammation and microglial activation which should be considering in developing potential therapeutics<sup>145</sup>. It should not be surprising that dangerous risks have been associated with A $\beta$  immunotherapies, including: cerebral amyloid angiopathy and cerebral micro-haemorrhage from both vaccines and mAbs<sup>145–147</sup>. Attempts to engineer safer vaccines and mAbs with reduced effector response and improved BBB permeation are currently being explored<sup>138,148,149</sup>. Passive immunotherapy has been largely successful in many

preclinical AD mouse models at reducing A $\beta$  burden and improving behavioural deficits<sup>143,150,151</sup>, unfortunately in humans it has been unsuccessful at meeting the primary outcomes in many AD clinical trials<sup>152-154</sup>.

Solanezumab is the humanized IgG1 mAb, m266.2, which recognizes the central A $\beta$ <sub>13-28</sub> region and binds soluble A $\beta$  species preferentially compared to plaques<sup>142,155</sup>. Solanezumab was shown to have no significant effect on the primary outcome measures of patients in two phase III clinical trials, though no adverse events were associated with it<sup>152</sup>. A more detailed subgroup analysis yielded mildly encouraging results for a population of prodromal (pre-dementia) and mild AD patients<sup>156,157</sup>, ultimately the effect was not efficacious enough to justify continuation of the trial. Bapineuzumab is another mAb which binds the N-terminal of A $\beta$ , preferentially associating with fibrils and plaques where the central region is inaccessible. Bapineuzumab was shown to have no significant effect on improving cognition of patients in two phase 3 clinical trials and safety concerns raised by MRI imaging showed abnormalities associated with vasogenic edema in some patients<sup>153</sup>. These setbacks have led experts to a shift in expectations for A $\beta$  intervention therapies and suggest that immunotherapy may not be effective after the onset of symptoms due to the significant amount neuron loss already present in the AD brain<sup>154,158</sup>. Recently, clinical trials have shifted to preventative studies, with the newcomer Crenezumab beginning a five-year preventative trial in 2012<sup>148</sup>. Crenezumab was engineered with an IGg4 backbone which elicits a less potent immune response yet still binds with high affinity to A $\beta$  monomers, oligomers and fibrils demonstrating a neuroprotective benefit and increased uptake of A $\beta$  by microglial cells in AD mouse models<sup>150</sup>. Gantenerumab is yet another mAb which binds both the N-terminus and mid-region of A $\beta$  but predominantly fibril species and is still being tested in phase III trials with prodromal and mild AD patients<sup>159</sup>. Aducanumab is also being tested in phase I clinical trial indicating A $\beta$  target engagement and reduction of A $\beta$  plaques<sup>160</sup>. The results of these and other preventive trials are long awaited in AD drug development research, with further engineered mAbs and other peptide inhibitors of amyloidosis in the pipeline that may also delay progression and age of onset.

### Alzheimer's Disease Pathology Progression

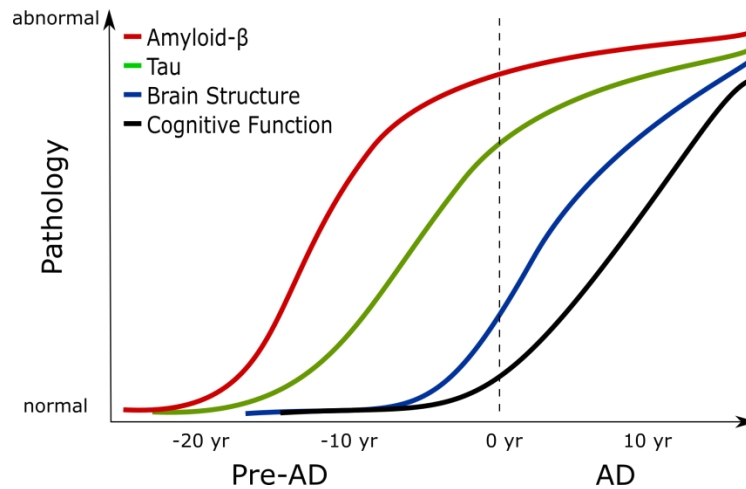


**Figure 3: Alzheimer's disease pathology progression.** A representative plot shows the progression of AD pathology and symptoms with clinical disease stage. A $\beta$  accumulation occurs 10-20 years before the onset of symptoms and before hyperphosphorylated tau and gross structural changes to the brain<sup>161</sup>.

The recent and continuing failure of several A $\beta$  directed therapeutics in clinical trials of patients with mild to moderate AD has left much to be sceptical of regarding the current paradigms in AD drug development<sup>71,154,162</sup>. A $\beta$  insult may occur as early as 20 years prior to the onset of clinical symptoms (see figure 3 above)<sup>161,163</sup>, thus the reversal of AD may not be possible by targeting A $\beta$  for removal from the brain in moderate and late stage AD. That being said it may be possible to modify disease trajectory if A $\beta$  treatments are applied sufficiently early in the amyloid cascade, preventing or delaying disease onset<sup>158</sup>. Some speculate that A $\beta$  is not the primary cause of neural degradation and AD progression but is instead a necessary mediator of brain homeostasis<sup>162</sup> or a secondary downstream event<sup>164</sup>, with others suggesting that prevention of amyloidosis earlier on in the disease progression may be necessary<sup>158</sup>. Indeed, a single molecular mechanism has not emerged as a clear candidate for the initiation of AD and there are many factors involved in AD pathology which may need to be addressed when trying to delay disease onset, including: A $\beta$  production and clearance mechanisms<sup>77,120</sup>, inflammation<sup>87,88,165</sup>, oxidative stress<sup>68</sup>, abnormal metabolism and mitochondrial dysfunction<sup>26,164,166</sup>, neurovascular mechanisms<sup>121,167</sup>, and tau pathophysiology<sup>69</sup>. Further testing of A $\beta$  targeted therapeutics in the pre-dementia population is needed to verify the amyloid cascade hypothesis, unfortunately this is limited by a lack of early clinical diagnostic

tools. Despite decades of progress much more work is needed on understanding and treating A $\beta$  pathology in AD.

## Chapter 2: Rational design of A $\beta$ aggregation inhibitors

The rationale for using aggregation inhibitors to prevent the formation of toxic A $\beta$  oligomers, the most toxic species of amyloid identified in AD, and drive aggregation equilibrium in favour of the least toxic monomeric form of A $\beta$ . A representative toxicity curve showing the time/aggregation dependence of A $\beta$  in solution, and the corresponding representative time dependent distribution of amyloid species, is shown in figure 4 below. To reduce A $\beta$  toxicity associated with low MW oligomers can be accomplished by either driving A $\beta$  equilibrium toward the monomer state or accelerating aggregation into fibrils. Since monomeric A $\beta$  is considerably less toxic than fibrils it may be preferred to stabilize the monomer and prevent toxic oligomerization to begin with. Biological candidates for potential inhibitors include: small molecules, peptides, and even mAbs have been shown to inhibit fibrillization. In this chapter a review of several seminal and more recent peptide A $\beta$  aggregation inhibitor design strategies will be discussed, including a brief discussion on challenges of delivery imposed by the blood-brain barrier (BBB), and finally a description of the design process for the SG inhibitors.

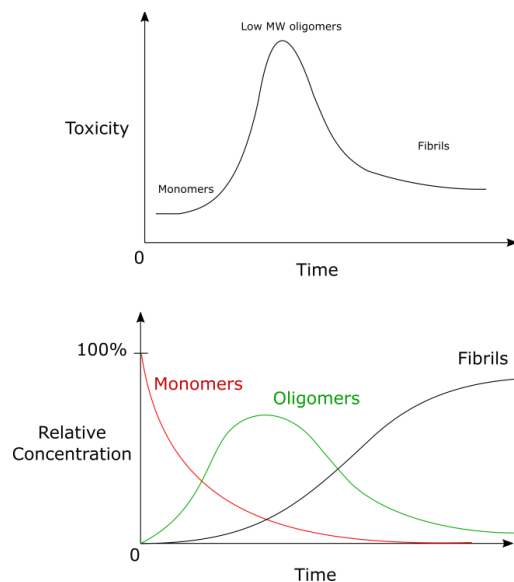


**Figure 4: A $\beta$  aggregation and toxicity with time.** Simplified representative plot shows the time/aggregation dependence on toxicity and the relative concentration of each species per unit of time.

### 2.1 Testing A $\beta$ aggregation inhibitors

Methods to detect A $\beta$  aggregation typically rely on detecting and quantifying changes in secondary structure such as nuclear magnetic resonance, circular dichroism and Thioflavin T

(ThT) fluorescence assays<sup>33,168–170</sup>. The size and gross morphological structure of amyloid aggregates can be assessed using electrophoresis such as SDS-PAGE, and electron and atomic force microscopy (AFM)<sup>171,172</sup>. These assays are limited to providing structural information of thermodynamic ensembles of A $\beta$  in solution with temporal and spatial limitations which underscore their physiological relevance. That being said these aggregation assays provide necessary information pertaining to drug-A $\beta$  interactions and how drugs modify A $\beta$  aggregation, which combined with A $\beta$  toxicity studies *in vitro* provide important structure-toxicity relationships<sup>173,174</sup>.

Cell viability assays in neuronal cell models and primary neurons are used to measure A $\beta$  toxicity of A $\beta$  prepared with and without aggregation modifying compounds. These *in vitro* assays require super-physiological concentrations of A $\beta$  – 100-fold greater than physiological conditions – to achieve significant toxicity over short time periods; as such they lack some physiological relevance but are nonetheless important for proof of principle. Compounds that demonstrate potential to reduce A $\beta$  toxicity *in vitro* are applied to AD animal models where physiological and behavioural effects can be measured<sup>175</sup>. Many different AD models have been developed, with the simplest to induce A $\beta$  toxicity directly by injection into the brain. More sophisticated animal models require genetically modified transgenic animals that endogenously overexpress familial AD genes: APP, PSEN1 and PSEN2<sup>175</sup>. The typical scheme for preclinical tests of A $\beta$  aggregation inhibitors first involves characterization of the inhibitory effect on A $\beta$  aggregation; these structural changes can then be related to the effects on A $\beta$  toxicity *in vitro*, and finally cognitive behavioural deficits *in vivo* AD models. Unfortunately, no clinical trials of peptide based inhibitors have been performed despite significant evidence of their potential in preclinical trials.

## 2.2 Peptide inhibitors

In 1996, Tjernberg et al. reported the use of amyloid peptide fragment KLVFF as an aggregation inhibitor and showed peptide-based ligands built from the sequence of A $\beta$  itself can be used to modify aggregation rates<sup>37</sup>. Although aggregation was still seen, a noticeable decrease in fibrillization suggests that these peptides bind and modify the dynamics of aggregation of A $\beta$ <sup>37</sup>. This study systematically tested 31 decamer A $\beta$  fragments using surface

plasmon resonance (SPR) to measure the binding of the fragments to intact A $\beta$ . These experiments allowed for identification of the key self-recognition binding region of A $\beta$  and how various portions of the molecule contribute to A $\beta$  dimerization, including the hydrophobic C terminus. After they selected the decapeptide with highest A $\beta$  affinity, it was truncated to determine the minimum sequence for A $\beta$  binding, KLVFF (A $\beta_{16-20}$ )<sup>37</sup>. It was later determined that shuffling the KLVFF amino acid sequence results in comparable inhibition of A $\beta$  fibril formation with nearly identical binding characteristics implying that overall hydrophobicity of the peptide inhibitor is critical<sup>176</sup>.

Also in a 1996 report, Ghanta et al. demonstrated that A $\beta_{15-25}$  attached to a repeated oligolysine disrupter element could reduce A $\beta$  toxicity, *in vitro*, on neuron differentiated PC12 cells<sup>38</sup>. Although this peptide inhibitor did not block  $\beta$ -sheet interactions or fibril formation, it did cause changes in aggregation kinetics and higher order structural changes in fibrils, shortening the length of the fibrils and increasing the amount of fibril entanglement<sup>38</sup>. In this case a more densely packed fibril may cause a reduction in the A $\beta$  dissociation and less few soluble species, highlighting the importance of how the aggregated structure of A $\beta$  can affect cytotoxicity. In subsequent studies published shortly later, Soto et al. modified the recognition sequence LVFFA by adding or substituting proline residues at various positions, for instance LPFFD (called iA $\beta$ -5)<sup>177,178</sup>. Proline is a well-known  $\beta$ -sheet breaker peptide to disrupt  $\beta$ -sheet interactions preventing aggregation and even causing disassembly of preformed fibrils when incorporated at certain positions<sup>179</sup>. Further modifications can improve peptide properties such as the addition of terminal charge to increase solubility and incorporation of D-amino acids for proteolytic stability; these were then tested in a non-Tg AD rat model demonstrating decreased A $\beta$  deposition<sup>178</sup> and later positive behavioural changes<sup>180</sup>. Standard L-amino acid peptides are susceptible to proteolytic degradation and may have low BBB permeation and bioavailability as a result. These early preliminary studies have paved the way for the design of next generation peptide inhibitors.

With a foundation of knowledge built from early A $\beta$  inhibitor studies, and advances made in protein and peptide therapeutics it may be possible to design effective amyloid aggregation inhibitors with suitable drug-like properties including: stability, solubility, target

affinity, immune system evasion, and cell membrane and BBB permeability. Small peptides with less than nine residues that contain synthetic amino acids (N-methylated, dextrorotary) improve immune system evasion, proteolytic stability, and A $\beta$  binding<sup>181-183</sup>. More recently, a peptide inhibitor was designed starting from the KLVFF sequence, modified with a single glycine spacer between charged amino acid residues at the N and C terminuses, called OR2<sup>184</sup>. These charged residues are expected to improve aqueous solubility and disrupt fibril formation with the glycine providing peptide flexibility. OR2 was shown to modify early aggregation of A $\beta$  and protect the SH-SY5Y neuroblastoma cell line from A $\beta$  cytotoxicity<sup>184</sup>. Later, increased proteolytic stability and reduced immune response was achieved by substitution of various amino acids with their corresponding D-enantiomer<sup>185</sup>. To maintain the A $\beta$  binding activity of the original peptide a simple swap is insufficient and reversal of the peptide bond is also required<sup>182,185</sup>. This “retro-inverso” (RI) version of the peptide, RI-OR2, was shown to be effective at inhibiting oligomerization and improving the survival of SH-SY5Y cells against A $\beta$  toxicity, while also remaining stable in human blood serum and brain extract for at least 24 hours<sup>185</sup>. The increase in stability afforded by the addition of a few retro inverted D amino acids will also help to overcome the challenges associated delivery to the brain and bioavailability.

Peptide based inhibitors are an alternative preventative strategy to mAb therapies that may be intrinsically safer due to a lower immunological profile. Antibody fragments and engineered mAbs with lower immune signalling profiles are designed to be safer alternatives to traditional immunotherapies but may not offer significant advantages over peptide based inhibitors. Peptide inhibitors are also easily modified for superior BBB permeation through the addition of targeting ligands and shuttling molecules<sup>186-189</sup>. It must be mentioned that mAbs can also be improved by making them bi-specific, able to bind A $\beta$  and some feature of the BBB for improved brain delivery<sup>190-192</sup>. Immunogenic clearance of A $\beta$  has been the focus of most clinical research; however as paradigms in AD treatment shift to prevention, inhibition of A $\beta$  aggregation may be suitable to allow natural clearing of the monomer without detrimental immune response. The success of peptide inhibitors will rely on delivery to the brain parenchyma across the BBB and stands as a major obstacle for drug development of any CNS disease.



### 2.3 *Delivery challenges due to the blood-brain barrier*

The lack of therapeutics for the treatment of Alzheimer's and other CNS diseases is not due to the lack of effective drugs, but their inability to cross into the brain across the BBB. The BBB is a highly selective, regulated and efficient barrier that protects the brain from unwanted molecules and pathogens. The BBB is the single largest hurdle that needs to be overcome in order to deliver potential therapeutic and diagnostic agents to the brain, with only 2% of drugs on the market able to effectively cross it<sup>193,194</sup>. Typically, these molecules are small (less than 400 Da), lipophilic, neutral molecules capable of passive diffusion into the cell membrane, like alcohols and steroidal hormones. This is a concentration dependent route into the brain and by itself cannot support delivery of larger macromolecule therapeutics such as peptides and mAbs for targeting A $\beta$ .

In the human brain there is approximately 100 billion capillaries with a BBB surface area of 20 m<sup>2</sup>, as compared to 0.021 m<sup>2</sup> for the blood-CSF barrier, thus the BBB regulates most of the traffic between the peripheral system and the brain<sup>195</sup>. The BBB is an interface separated by brain endothelial cells on the blood side with pericytes and astrocytes on the brain side which polarize and communicate with the endothelial cells to regulate protein expression and cell membrane composition, locally adjusting BBB properties as needed<sup>195,196</sup>. The endothelial cells of the BBB are bound together with occludins, claudins and adherin molecules which form the tight junctions (TJs) between cells and adherent junctions to the basement membrane<sup>195</sup>. The BBB has an extremely high resistivity to ionic flow as measured using transendothelial electrical resistance (TEER) of between 1500 – 2000  $\Omega$ /m<sup>2</sup>, an order of magnitude higher than a typical epithelial barriers in the body<sup>195–197</sup>. This resistance prevents access to most charged moieties so that only small, neutral and water-soluble molecules can pass through undisrupted paracellular TJs between endothelial cells<sup>196</sup>.

The BBB is essential for regulation of brain homeostasis where influx and efflux of nutrients and metabolites, as well as humoral signalling molecules, takes place. The extremely restrictive nature of the TJs between cells forces the transport of molecules across, mostly specific, transcellular routes into the brain parenchyma. Cells at the BBB not only prevent the entry of unwanted molecules but actively remove them from the brain. The diverse processes

governing the influx of necessary molecules for brain homeostasis provide a variety of options that can be hijacked to improve the delivery of therapeutics and diagnostics into the brain<sup>193,194,198</sup>. The means by which BBB delivery is engineered must be carefully considered for safety and efficacy, moreover any effects of the disease state on the BBB should also be considered in this regard<sup>193</sup>. In AD, BBB integrity can often be compromised which in principle may make delivery easier but should discourage further disruption<sup>145</sup>.

Several high capacity transporter proteins are expressed that move nutrients and other small molecules for metabolism and signalling, including: glucose, amino acids, fatty acids, and cationic-organic small molecules. The latter moves small cationic molecules like currently used AD drugs (memantine and cholinesterase inhibitors) across the BBB<sup>199,200</sup>. These transporter proteins are too small to deliver larger macromolecules like mAbs, however carrier-mediated transport of small (<10 amino acid) polypeptides across the BBB has been observed, for instance the opioid heptapeptide, deltorphin<sup>201,202</sup>. These high capacity transporter proteins could potentially be used to transport peptide inhibitors to the brain parenchyma provided they fit the recognition motif on the extracellular transporter protein.

Alternatively, receptor proteins for endosome assisted transcytosis, or receptor-mediated transcytosis (RMT) can transport larger proteins, such as insulin and transferrin, into and out of the brain. RMT of large therapeutic proteins and small nanoparticles can be accomplished by high jacking the receptors for insulin, transferrin, lipoproteins, and diphtheria toxin among a few other receptors<sup>193,194</sup>. The high specificity of RMT provides a great potential for brain specific targeting of drug delivery systems and therapeutics. In designing ligands for RMT high affinity does not predict high efficiency transcytosis, in fact high affinity anti-transferrin receptor antibody was shown to promote lower levels of transcytosis compared to lower affinity versions<sup>191</sup>. This implies that there is an ideal affinity for RMT that will achieve a balance between selectivity and transport capacity. Small peptide ligands for peptide and nanoparticle delivery, as well as chimeric or bi-specific antibodies, have been developed and tested in preclinical studies for AD treatment applications<sup>192,203-205</sup>.

With the ever growing literature surrounding BBB physiology in various CNS diseases informed designs can be made to optimize targeted delivery to the diseased brain, and perhaps

even to specific diseased brain regions, in such a way as to improve both safety and efficacy. Insulin receptors are commonly explored for RMT unfortunately insulin and glucose homeostasis is impaired in AD as A $\beta$  binds and readily competes with insulin for its own receptor<sup>206,207</sup>, as such insulin receptors may not be an ideal candidate for drug delivery in AD. Transferrin is a protein chaperone that collects and traffics free iron in the blood for transport into organs and its receptor has a high density at the BBB<sup>193</sup>. Using transferrin itself as the ligand may not be ideal since transferrin receptors are fully saturated by native transferrin in circulation, nonetheless it has been shown to enhance nanoparticle uptake into the brain<sup>194,208,209</sup>. The targeting ligand can be directed against other epitopes of the receptor which do not compete with binding of the native substrate to overcome any potential competition<sup>204,210</sup>. Even if competition has been minimized there is a strong possibility for the drug delivery system to modulate receptor trafficking and activity which should be considered to ensure no negative consequences<sup>211</sup>.

Efflux pumps are a family of transporter proteins and receptors expressed in the brain parenchyma to move unwanted molecules out of the brain. It is known that A $\beta$  binds various efflux and influx pumps<sup>111,119</sup>. To prevent efflux from the brain a carefully designed drug will not bind P-gp and other efflux pumps. If that is not possible it may be beneficial to utilize efflux pump inhibitors. This will increase concentrations of the drug in the brain by limiting binding of the drug to the efflux pump. In an AD mouse model it was shown that P-gp deficiency resulted in an increase in A $\beta$  deposition so this particular strategy in many cases may interfere with the natural protection offered by the efflux pumps and may not be suitable for use in treating AD or other chronic CNS diseases.

Native positively charged proteins and macromolecules such as protamine and human serum albumin are capable of endosome mediated transcytosis across the BBB through electrostatic interactions with the negatively charged endothelial cell membrane, a process called absorptive-mediated transcytosis (AMT)<sup>212</sup>. Drug delivery systems that induce or improve AMT have the potential to greatly increase the permeation of many drugs at the BBB by encapsulating the drug in cationic liposomes or polymeric nanoparticles<sup>193,213</sup>. AMT has a higher capacity for improving BBB permeation as compared to RMT, since it does not rely on

binding to specific receptors, however this comes at the expense of specificity<sup>213</sup>. As a result low specificity endocytosis of the drug delivery system will cause uptake in other tissues in the body, especially the liver and kidney, which leads to less brain uptake. This challenge is not insurmountable as it is known that polyethylene glycol (PEG) coated nanoparticles have decreased liver uptake and increased blood circulation time<sup>214</sup>. Combining AMT favourable surface enhancements with RMT may improve transport efficient for high capacity and specificity drug delivery across the BBB for the treatment of various CNS diseases.

Cell-penetrating peptides (CPPs) are an interesting class of peptides that have been used to improve transcytosis of nanoparticles and individual peptides and proteins for CNS delivery<sup>213,215,216</sup>. CPPs are class of short (less than 30 residues) peptides capable of improving penetration into cells. The exact mechanisms governing CPPs are currently in debate with evidence to support different pathways. CPPs may involve cationic endocytosis as in AMT<sup>186,217</sup>, while molecular dynamics simulations indicate local disruption of the cell membrane and the formation of a transient water tunnel or pore through which CPPs translocate without endosome formation<sup>218,219</sup>. Regardless of whether CPP delivery is endosome dependent, it is nonetheless limited by lack of specificity to the target organ, as they readily cross all biological membranes.

The conjugation of a CPP derived from the HIV transactivator of transcription (TAT) to the previously mentioned RI-OR2 inhibitor showed remarkable results in a transgenic AD model<sup>188</sup>. This TAT-RI-OR2 peptide was able to cross the BBB and bind A $\beta$  plaques. After 21 days of intraperitoneal injections transgenic mice had 25% reduction in cerebral cortex A $\beta$ , 32 % reduction in plaque count, 44% reduction in activated microglial cells, 25% reduction in oxidative damage and 210% increased neuron count in the dentate gyrus<sup>188</sup>. These results indicate that oxidative damage, reduced neurogenesis and inflammation are results of A $\beta$  aggregation and can be reduced with the use of peptide inhibitors provided they can be delivered to the brain. Despite this success no clinical trials have been performed of peptide A $\beta$  aggregation inhibitors most likely due to historical challenges associated with peptide based therapeutics, such as: proteolytic stability, immune response, deliverability, and production

costs<sup>220</sup>. These challenges are now easily overcome and with the growth of peptide inhibitors in the market costs associated with their production will only decrease.

#### 2.4 SG inhibitors

The SG inhibitor structures were proposed based on previous studies mentioned above then screened for target affinity *in silico* using molecular dynamics (MD) simulations. This computer aided drug design (CADD) method is a rapid and cost-effective technique for screening most suitable drug candidates, for example by optimizing the binding between the drug and target, prior to expensive experimental trials<sup>18</sup>. For predicted SG inhibitors the predicted affinity to A $\beta$  is calculated using ligand-receptor docking simulations where the 11-residue region containing the self-recognition region (R) of the peptide, A $\beta$ <sub>13-23</sub> (**HHQKLVFFAED** – red indicates positive and blue negative charge, respectively) is considered the receptor and the SG inhibitor as the ligand. The CADD process used to screen SG inhibitors evaluated the binding affinity with the 11 residue self-recognition segment of A $\beta$ ; as such important interactions have not been accounted for, especially hydrophobic interactions with the C terminus. Unlike traditional receptors such as G-coupled protein receptors and receptor tyrosine kinases, the A $\beta$  “receptor” has less well defined higher order structure and is quite flexible making traditional CADD much more complicated. There are four classes of inhibitors categorized based on their predicted binding orientation with A $\beta$  and by the type of amino acid backbone they possess: SGA contains an L-amino acid backbone, SGB contains a D-amino acid backbone but both bind in anti-parallel  $\beta$ -sheet orientation to A $\beta$ , while SGC and SGD are L- and D- amino acids, respectively, that bind in parallel  $\beta$ -sheets<sup>18</sup>. A large library of hypothetical SG inhibitor candidates was developed for computational screening from which lead candidates were synthesized for experimental studies.

The entries in the SG inhibitor library was constructed around the A $\beta$  recognition sequence containing the hydrophobic core sequence: KLVFF, LVFFAE or KLVFFAE, as identified and utilized in earlier studies as a base ligand for A $\beta$ <sup>18,37,176,177</sup>. This library of SG inhibitors was screened for lead candidates based on a series of molecular docking simulations to the recognition region, R<sup>18</sup>. There are four orientations for binding to R, forming parallel or antiparallel  $\beta$ -sheets with either the top or bottom face<sup>17,18,221</sup>, as such inhibitors need to bind

both edges to completely inhibit A $\beta$  aggregation. The highest predicted conformational stability of R indicates a very flexible chain which has a hairpin turn between Val<sub>18</sub> and Phe<sub>19</sub> and contains an intramolecular  $\beta$ -sheet (Figure 4a). Within the recognition sequence a salt bridge between K<sub>16</sub> and E<sub>22</sub> is expected to drive the formation of the hairpin turn<sup>16,18,221</sup>. Various modifications and substitutions to the base ligand are made to maximize affinity for R, such as  $\gamma$ -diaminobutyric acid on the *N*-terminus, which is suspected to improve interactions with D<sub>23</sub> on A $\beta$ , or substitution of lysine with the synthetic amino acid ornithine to improve electrostatic side chain interactions with E<sub>22</sub> on A $\beta$ <sup>16,18</sup>. Other improvements to peptide inhibitors can be made by substituting various lipophilic aromatic residues, which may optimize hydrophobic interactions between the drug and A $\beta$  target, as this has been shown to be important for A $\beta$  recognition<sup>222,223</sup>.

The core design principle behind the SG inhibitors involves not only A $\beta$  binding but also inhibition of A $\beta$ -A $\beta$  binding. To that end, all SG inhibitors contain alternating amino acids in the peptide backbone that are *N*-methylated. Theoretically upon binding to A $\beta$  these methyl groups will appear on one face of the drug-A $\beta$  complex preventing the growth of A $\beta$  oligomers, as this blocks hydrogen bonding between adjacent  $\beta$ -sheets on the SG side of the complex<sup>17,18,224</sup>. In addition the *N*-methylation increases the hydrophobicity of the peptide and may improve permeability of the membrane<sup>224</sup>. Proline residues can disrupt the  $\beta$ -sheets formed between intra- or inter-molecular hydrogen bonds of A $\beta$  as previously mentioned, therefore some entries in the SG library contain proline residues<sup>189</sup>. Upon binding to the complex *N*-methyl and proline residues should inhibit A $\beta$  interactions.

Delivery of SG inhibitors across the BBB is addressed by the addition of a myristic acid tail to the *N*-terminus which should improve cellular uptake<sup>18,225,226</sup>. The attachment of a lipid to proteins (or lipidation) is a common post-translational modification which can localize the protein near the membrane, direct binding, insertion and trafficking into the lipid bilayer<sup>227,228</sup>. Lipidation for drug delivery could make use of both nonspecific absorption similar to CPPs and/or involve fatty acid protein transporters that will improve uptake<sup>213,225,226</sup>. Unlike cholesterol, the brain produces only low levels of fatty acids and thus depends on influx from the periphery which has been shown to involve protein transporters<sup>229</sup>. Since the brain has a

high metabolic demand it likely has a high capacity for fatty acid transport and a corresponding distribution of transporter proteins. Therefore myristylation may be suitable for improving delivery of SG inhibitors to the brain, these inhibitors are referred to with the 'Myr-' prefix.

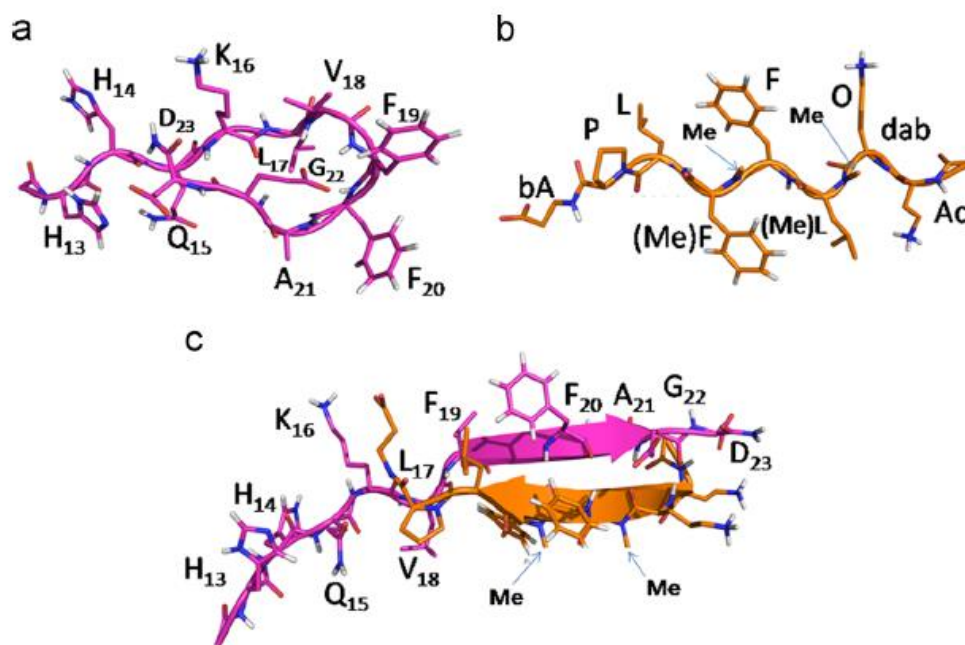


**Figure 5: Most probable structural conformations for A $\beta$ <sub>13-23</sub>, SGA1 and its complex.** a) A $\beta$  13-23 most stable conformation shows hairpin turn stabilized by intramolecular hydrogen bonds, b) SGA1 most probable conformation is a rigid chain, c) SG-R complex – From Hane et al. (2014). *Biosensors and Bioelectronics*. 54: 492-298<sup>230</sup>.

Lead candidates from the docking simulations have been analyzed further in more detailed MD simulations between SG and R to study site and edge specificity by calculating the dissociation energy for the inhibitor to the top ( $R^T$ ) and bottom ( $R^B$ ) binding configurations<sup>17</sup>. It is necessary to block these two different A $\beta$  binding sites to completely inhibit oligomer formation, thus the edge specificity is highly important. In addition, to the specific binding orientation it is important to know the inhibitor self-affinity. The homodimer stability, as measured by its dissociation energy, must be minimal to prevent competition to itself for A $\beta$  binding thus reducing its capacity to inhibit oligomerization. Both the edge specific and homodimer dissociation energies for several SGA series inhibitors are shown in Table 1 below. It is most desirable for the dissociation energy of R – SG to be greater and that of SG – SG to be minimal. Three SGA inhibitors were shown to demonstrate interesting and unique predicted edge specificity and homodimer binding. SGA1 is predicted to have preferential specificity for  $R^T$  over  $R^B$  as indicated by the higher dissociation energy and had relatively low homodimer

dissociation energy<sup>17</sup>. SGA4 had the opposite specificity with slightly higher homodimer stability judging by the higher homodimer dissociation energy<sup>17</sup>. SGA3, interestingly, had little difference in edge specificity with very high dissociation energies to both R<sup>T</sup> and R<sup>B</sup> but had a much higher SG – SG stability<sup>17</sup>. Based on these dissociation energies excess molar concentrations of SGA3 alone or excess of SGA1 and SGA4 in combination would have the highest potential for completely inhibiting A $\beta$  aggregation<sup>17</sup>.

**Table 1: Edge specific and homodimer dissociation energy.** The edge specific and homodimer dissociation energies of SGA inhibitors to the recognition region, R, and itself<sup>17</sup>.

	R <sup>T</sup> – SG	R <sup>B</sup> – SG	SG – SG homodimer
<b>SGA1</b>	43 ± 3 kJ/mol	28 ± 2 kJ/mol	21 ± 4 kJ/mol
<b>SGA3</b>	56 ± 3 kJ/mol	47 ± 2 kJ/mol	46 ± 4 kJ/mol
<b>SGA4</b>	28 ± 3 kJ/mol	44 ± 3 kJ/mol	37 ± 3 kJ/mol

Initial computational studies of SGA1 demonstrated a very rigid amino acid chain, most likely due to the N-methyl amino acids (Figure 5b) and indicate that the SGA1-R complex (Figure 5c) adopts a fairly rigid structure as compared to R alone (Figure 5a). The predicted dissociation energy for the SGA1 – R complex was calculated to be 51 kJ/mol, as compared to 62 kJ/mol for the R – R complex, and 24 kJ/mol for the SGA1 – SGA1 homodimer, where the lower dissociation energy corresponds to lower binding affinity. This indicates a strong potential for SGA1 to bind the A $\beta$  recognition region, with minimal self-dimerization. When the SGA1 ligand is in excess of A $\beta$  the SGA1-R complex should dominate inhibiting oligomerization and to be safe a 2-fold excess should be sufficient at low concentration. SGA1 was then tested for its ability to block the formation of high  $\beta$ -sheet content aggregates using the ThT fluorescence assay, western blot and circular dichroism where favourable correlations between MD simulations were found<sup>18</sup>. Furthermore, it was confirmed previously by our lab using single molecule force spectroscopy (SMFS) that SGA1 was able to reduce binding events between single A $\beta$  monomers, and atomic force microscopy (AFM) imaging studies indicated a decrease in fibrillization, albeit at the expense of producing a higher oligomer to fibril ratio<sup>230,231</sup>.



The aim of this thesis project was to evaluate several more inhibitors on the single molecule level using SMFS to identify how structural identity affected A $\beta$  dimerization and then to test the potential neuroprotective benefit of inhibitors *in vitro* using an AD neuronal cell culture model. In the first part (chapter 3), a SMFS study of three inhibitors (Myr-SGA1, SGA3 and SGC1) was performed to add to the previous data on SGA1 acquired previously<sup>230</sup>. In the second part (chapter 4), five inhibitors (SGA1, Myr-SGA1, SGA3, Myr-SGA3 and SGC1 – sequences in Table 2 below) were tested in cell viability assays to verify inhibitors are non-toxic and protect neurons from A $\beta$  toxicity. The most probable structures for SGA1, SGA3, Myr-SGA1 and SGC1 are shown in Figure 6 below, in all cases the amino acid chain is fairly rigid, compared to A $\beta_{13-23}$ , while the Myr- group has a tendency to fold back on the amino acid backbone due to hydrophobic effects.

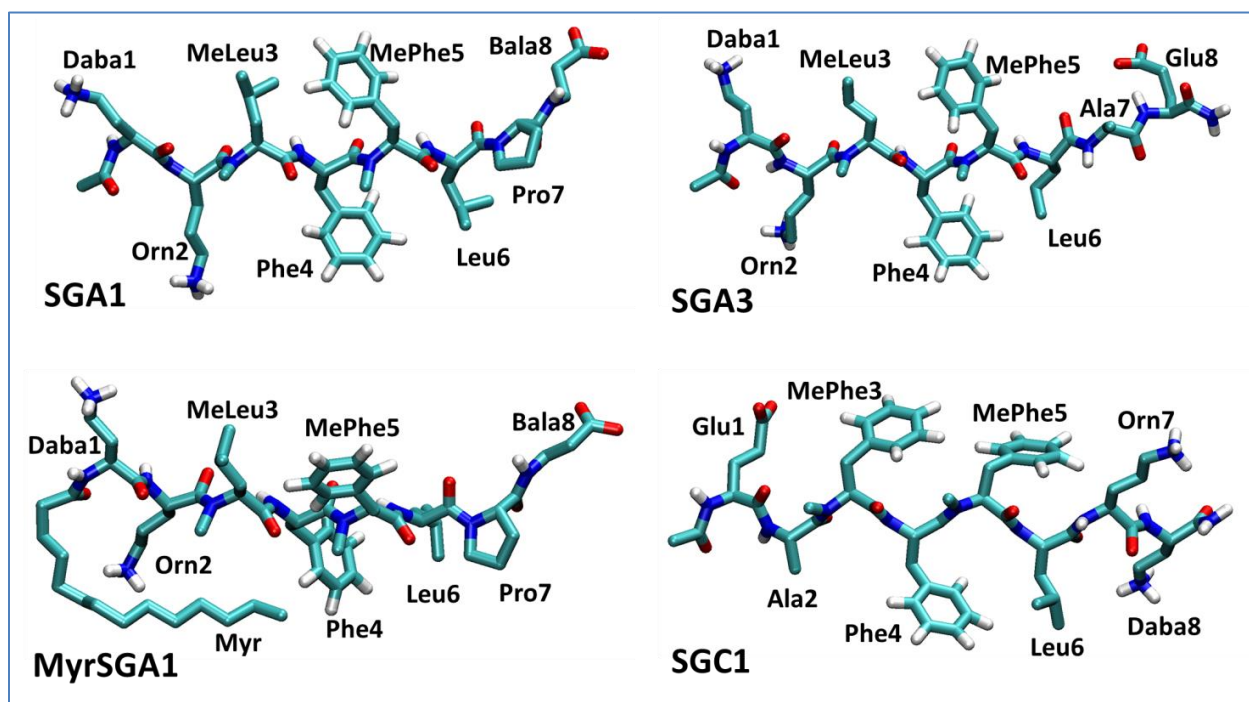


**Figure 6: Most probably SG inhibitor structures.** Schematic representation of several SG inhibitors studied in this thesis. From Robinson et al. (2017). BBA: proteins and proteomics – accepted in press<sup>232</sup>.

**Table 2** The amino acid sequences of SG inhibitors that were studied and reported on in this thesis.

SG Inhibitor	Inhibitor Sequence
<b>SGA1</b>	Daba-Orn-(Me)Leu-Phe-(Me)Phe-Leu-Pro-Bala
<b>Myr-SGA1</b>	Myr-Daba-Orn-(Me)Leu-Phe-(Me)Phe-Leu-Pro-Bala
<b>SGA3</b>	Daba-Orn-(Me)Leu-Phe-(Me)Phe-Leu-Ala-Glu
<b>Myr-SGA3</b>	Myr-Daba-Orn-(Me)Leu-Phe-(Me)Phe-Leu-Ala-Glu

---

**SGC1**

Glu-Ala-(Me)Phe-Phe-(Me)Phe-Leu-Orn-Daba

---

## Chapter 3: Single molecule biophysical study of A $\beta$ dimerization

Atomic Force Microscopy (AFM) is a high resolution imaging technique, which can operate in Atomic Force Spectroscopy (AFS) mode to directly measure unbinding forces between single biomolecules<sup>48,233–235</sup>. Here AFS is used to obtain experimental evidence that SG pseudo-peptide inhibitors, optimized by MD simulations, prevent the binding of A $\beta$  monomers, therefore inhibiting the first step of toxic A $\beta$  oligomer formation. A $\beta$  aggregation is must be studied in solution to perform structural and size analysis, typically with biochemical and biophysical methods as: NMR, circular dichroism, ThT, SDS-PAGE, and nanoscale imaging with AFM and electron microscopy. The assessment of inhibitors in these types of assays are limited in terms of their resolution as they are evaluating a large thermodynamic ensemble of molecules and can only resolve changes in higher order structures of larger aggregates (oligomers verse fibrils) and cannot easily assess small oligomer and monomer structure. The advantage of single molecule approaches is that a direct measure of interactions between two individual monomers can obtained, and thus how inhibitors affect dimerization, the first step in oligomerization can be assessed.

### 3.1 Methods

#### 3.1.1 Atomic Force Microscopy

The Atomic Force Microscope (AFM) is a mechanical microscope that works by scanning an atomically sharp probe tip over a sample; by measuring the forces between the tip and the sample a nanoscale topographical map of the surface can be generated<sup>233</sup>. The AFM is capable of characterizing topographical nanoscale features of organic and inorganic sample surfaces, many variations have been developed to measure other surface properties such as electrostatic surface potential, and adhesive properties. The AFM is an important tool for measuring structural information of biological systems, such as DNA, proteins, and lipid membranes, in either air or liquid environments with incredibly high nanometer resolution. This technique is widely utilized for studying the effect of different environmental conditions and relevant molecules on A $\beta$  aggregation, especially fibrillization and the effect of A $\beta$  on lipid membranes.

The AFM generates high resolution topographical images by feeling the surface schematic shown in Figure 7 below. It requires an atomically sharp tip mounted on to the end of a cantilever bar which bends according to the force it experiences from the surface. A laser-photodiode detection system is typically used to measure cantilever bending which is directly proportional to the force on the tip times the cantilever stiffness. The tip is brought into close proximity with the surface through the use of an extremely precise piezoelectric actuator more casually called the “piezo tube”. A piezoelectric device has a well-defined mechanical response to an applied electric field and the opposite, an electric field in response to mechanical stress. The piezo tube allows for sub-nanometer z control of the tip above the surface which is under control of a feedback system to limit the amount of force between the tip and sample. The set point, as defined by the user, determines how much force is allowed to be exerted between the tip and the sample before the piezo tube must adjust to reduce the force, in this way a stable image can be maintained.

There are several imaging modes that can be employed. In contact mode - the simplest mode of operation - the tip sample force is kept constant in the repulsive force region by means of the feedback system. As the tip moves across the changing topology any change in cantilever bending (usually measured by means of laser-photodiode) is compensated for by adjusting the cantilever height in such a way as to maintain a constant force according to Hooke's law,  $F = -kx$ . The cantilever height is adjusted by applying a voltage to the z control of the piezo tube. The voltage applied to the piezo needed to maintain a constant cantilever deflection can then be converted into a height profile as the voltage displacement relation for the piezo tube is known, that is, the amount of mV applied to the piezo to produce a given height displacement. The imaging rate depends heavily on the refresh rate of the feedback system and typically is only good enough to provide very low temporal resolution, as imaging requires timescales on the order of tens of minutes.

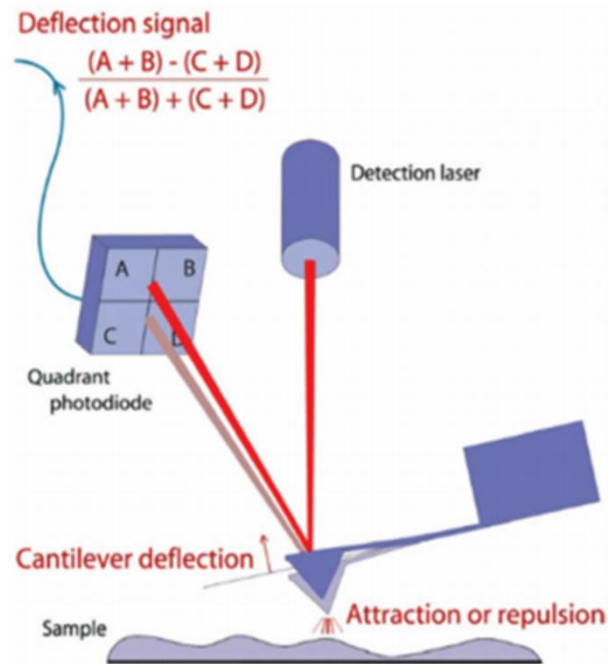


**Figure 7: AFM schematic.** Cartoon representation of a basic AFM set-up, probe, cantilever, laser detection system measures deflection of the cantilever and using a feedback loop to minimize the deflection allows for determining the topography of a sample. Image courtesy of JPK.

### 3.1.2 Single Molecular Force Spectroscopy

An operational mode of the AFM called atomic force spectroscopy (AFS) can be used to measure the force of interaction between the AFM probe and a sample surface. This can be used to provide mechanical information relating to the material, such as stress/strain analysis of nanoscale features, which can be tested through indentation of the surface from inorganic materials to biological systems including whole cells. If enough force is applied to a thin film or other layered sample, and the probe is sufficiently strong, a breakthrough event will occur which can provide not only maximum force the film layer can withstand but also estimate the thickness of the thin film. In addition to measuring forces induced by pressing on a sample, AFS can also be used for measuring adhesion to a sample surface. To measure adhesion the probe is brought into contact with the surface where it pauses for a user-defined amount of time allowing the tip to interact with the surface, it is then retracted and the force of adhesion can be measured. This is usefully for measuring cellular adhesion and studying cell-cell interactions.

A variation of AFS called single molecule force spectroscopy (SMFS) is useful for measuring single interactions between individual biomolecules for studying receptor-ligand,

antigen-antibody, and more generally, protein-protein, nucleic acid-protein and lipid-protein interactions. In a typical SMFS experiment, the tip and surface are chemically modified with the ligand and receptor of interest. The chemically modified tip containing the ligand is brought into contact with the chemically modified surface and allowed to interact. The tip is then retracted from the surface and if there is a binding event the attractive forces on the tip can be measured. If an unfolding or unbinding event occurs a rupture on the force plot can be easily identified and the rupture or unfolding force measured (see figure 8 and 10 below). This can be used to quantify binding forces, and can be correlated with the binding affinity using a suitable model. SMFS experiments of single molecules must be carefully designed and the surface chemistry carefully considered for isolating the desired interaction so that it is not obscured by non-specific tip-sample interactions. Several thousand force curves must be acquired to have enough specific binding events for a statistically sound data set, as not every force curve will contain a binding event. The number of binding events in a given experiment is referred to as the experimental yield. A detailed analysis of this yield can be done by calculating the specific unbinding forces for estimating the binding affinity. This highly sensitive nanoscale technique can measure unbinding forces between single molecules on the order of pico-Newtons.

A SMFS system has been developed to analyse whether or not SG inhibitors engage A $\beta$  and block A $\beta$  dimerization, shown in figure 8 below. Previous work with this system has demonstrated that metal ions increase the interaction energy between A $\beta$  monomers which correlates well with molecular dynamics simulation and other aggregation studies that report copper and iron increase fibrillization<sup>48</sup>. The inhibitor SGA1 was also evaluated in SMFS previously; Hane et al. was able to show that SGA1 prevented the dimerization of A $\beta$  as indicated by significant reduction in the experimental yield of A $\beta$  dimerization in the presence of SGA1<sup>230</sup>. There was an inverse exponential relationship between the yield and concentration and the rupture force increased linearly with concentration, which implies diminishing returns with increased SGA1 inhibitor. These studies set the stage for the work presented here, wherein three more SG inhibitors, Myr-SGA1, SGA3 and SGC1 are evaluated.

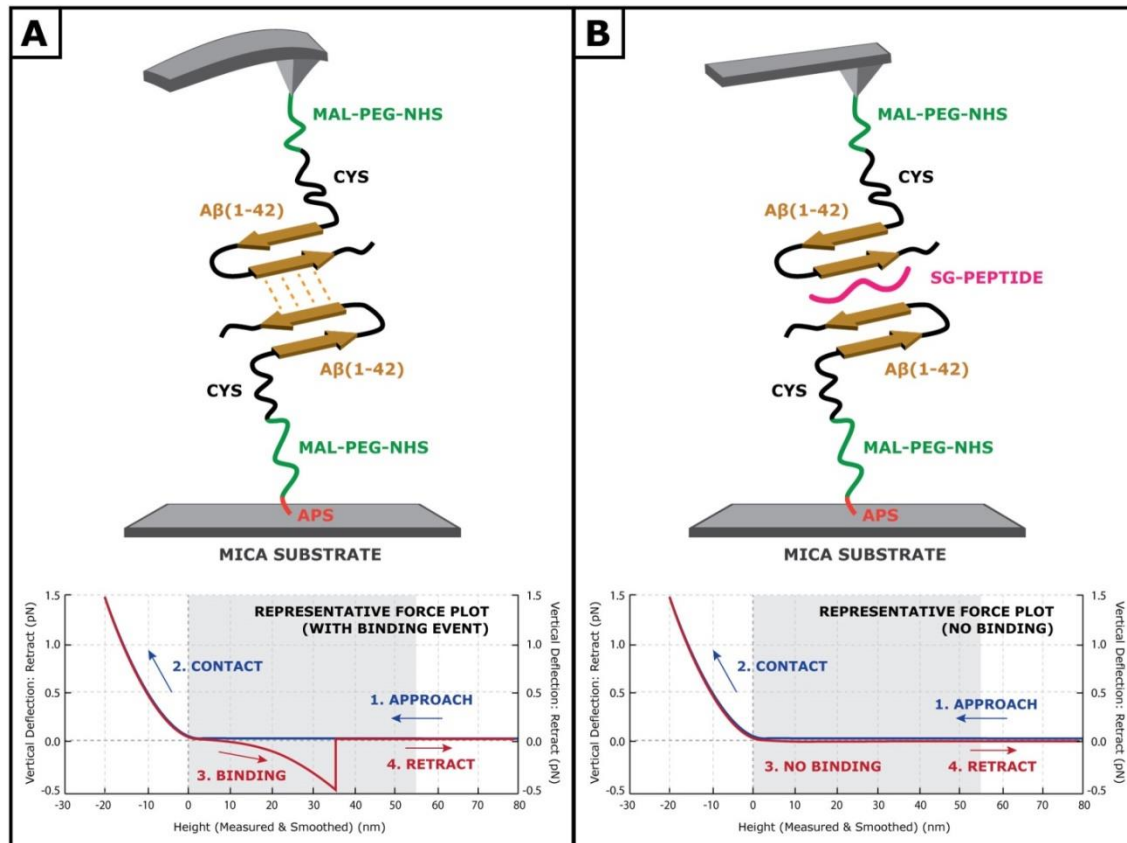


**Figure 8: Schematic of Aβ SMFS set-up.** Covalently, attached Aβ via PEG linker allow for the identification of specific interactions between individual amyloid monomers. In the presence of potential drugs or other environmental conditions their effects on dimerization can be measured directly. From Robinson et al. (2017). BBA: proteins and proteomics – accepted in press<sup>232</sup>.

### 3.1.3 Surface Modification for SMFS

To study protein and nucleic acid binding with SMFS requires chemical modification of a support surface and the AFM tip, covalently attaching one molecule of interest to the tip and the other on a supporting substrate, typically mica. There are several types of chemistry for the covalent attachment of the molecules depending on the type of molecule and the surface. Sulfhydryl crosslinking chemistry using maleimide (Mal) combined with amino N-hydroxysuccinimide (NHS) ester is most commonly done. First, the surfaces are modified by attaching free amines: gold coated surfaces can be modified using thiol chemistry and hydrophilic surfaces which contain free hydroxyl groups such as silicon nitride and mica can be easily silanized (Figure 9). Once the surface is covalently covered in free amines a flexible linker is attached to prevent non-specific interactions from obscuring the single molecule binding event as mentioned above. Polyethylene glycol (PEG) terminated with an NHS ester on one end

and maleimide on the other (Mal-PEG-NHS) can react with free amines on the modified surfaces and can crosslink to sulfhydryl terminated oligonucleotides and proteins containing cysteine. To attach A $\beta$  monomers for SMFS experiments here, a custom synthesized N-terminal cysteine modified A $\beta$  is used. Briefly the steps for surface chemistry are outlined below:

Surface chemistry for SMFS:

1. Clean MLCT cantilever probes and mica substrates, first soak in pure ethanol bath for 10 min to degrease followed by 20 min in UV-ozone cleaner which should oxidize any remaining contaminants and expose the hydroxyl surface underneath increasing the hydrophilicity of the silicon nitride tip and mica surface.
2. Silanization of the probe and mica substrates by incubating clean probes and mica in a solution of 167mM aminopropyl silatrane (APS) for 30 minutes, see figure 9. Rinse in ethanol followed by ultrapure water.
3. Probes and surfaces are incubated in 167mM Mal-PEG-NHS for 3 hours, followed by rinses in ethanol and water. The heterobifunctional Mal-PEG-NHS polymer will serve as a linker with one terminal maleimide and one terminal NHS ester. The NHS group reacts with free amine on the silanized surface. The maleimide group on the other end of the linker is free to react with sulfhydryl (-SH) groups, such as in cysteine.
4. The tip is incubated in 0.22 nM N-terminal cysteine modified A $\beta$  (1-42) for 30 minutes, followed by rinse in DMSO and ethanol.
5. Any unreacted maleimide are then quenched with  $\beta$ -mercaptoethanol to prevent any polymerization with free maleimide during the experiment.



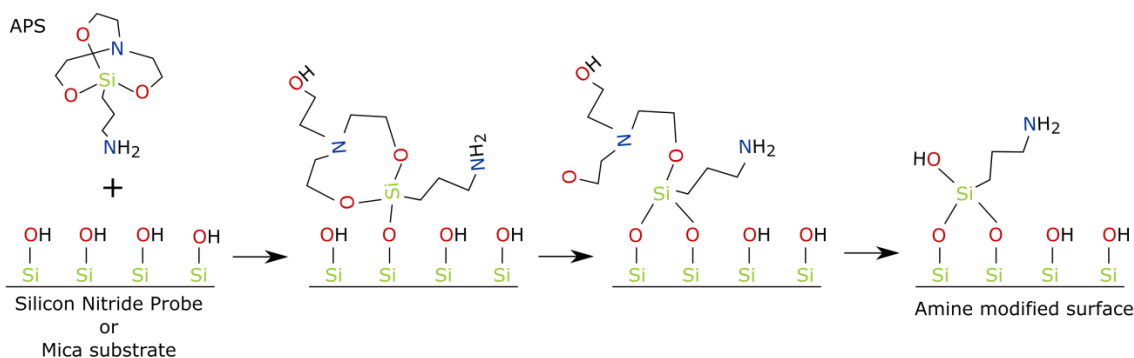


**Figure 9: Amine modification for SMFS.** Aminopropyl silatrane (APS) incubation with mica and silicon nitride AFM cantilever surfaces to produce an amine modified surface <sup>236</sup>.

### 3.1.4 Data acquisition and statistical analysis

Following surface chemistry modifications, the force plots are acquired in buffer conditions (HEPES 20nM, 140mM NaCl, pH 7.4) at room temperature. Using, JPK data acquisition software, the probe is programmed to approach the surface at a set velocity, pause for 0.5 seconds at the surface and then retract at the same velocity. For each probe sample set the force scans are calibrated for sensitivity by first acquiring a force curve and measuring the slope of the contact region, which corresponds to the negative slope below 0nm (see figure 8 above or 10 below). Several thousand force single molecule curves over N=6 trials were obtained (625 – 900 per trial condition – control and inhibitor each) for proper statistical analysis. First a set of force curves are acquired in buffer to serve as control. Next, SG inhibitor solutions prepared in same buffer is substituted for control conditions and another –set of curves are then acquired, using identical approach and retract settings. The experimental yield, a ratio of single molecule unbinding events to the total force scans is computed. Comparing the experiment yield between these two data sets (control, no drug, and with drug) provides empirical information as to the effectiveness of inhibitors at reducing A $\beta$  dimerization. The experimental yield was further analysed by calculating the unbinding forces and plotting the resulting histogram, this distribution of binding events was then analyzed further identifying the most probably unbinding forces between control and inhibitor.

Statistical analysis of experimental yields was performed using GraphPad Prism software. The experimental yields for control and inhibitor group were averaged and compared using paired T-test, for each control/inhibitor pair data set. Analysis of variance (ANOVA,  $p < 0.05$ ) was applied to the means of the difference in experimental yields of each inhibitor. Unbinding forces were calculated using JPK Data Processing software by fitting curves each unbinding curve to a WLC model with significance set to  $p < 0.05$ . This histogram of unbinding forces was then further analyzed by fitting multiple Gaussian peaks to the distribution of forces using OriginPro software. The peak fit will provide the most probably binding force with the extent calculated from the fit providing the significance; this is then compared between control and inhibitor.

## **3.2 Results and Discussion**

### *3.2.1 Binding Curves*

In a force spectroscopy experiment, or force measurement, the AFM probe is repeatedly moved towards and away from the sample and the interaction force between the probe and the sample surface is measured as a function of probe-sample separation. The distance dependence of attractive and repulsive forces is obtained. When the molecules of interest are attached to the AFM probe and the sample surface the specific interaction between single molecules can be measured. The analysis of the interaction forces and fitting the experimental curves to theoretical models provides valuable information about the interactions between biomolecules at a single molecule level. In the SMFS experiment, the A $\beta$  peptide was attached to the AFM probe and to the mica substrate, schematic representation shown in Figure 8. When the AFM probe was brought to the surface (approach curve shown in blue on Figures 8, 10 and 11) the binding between two A $\beta$  monomers can occur. When the probe is moved away from the surface monomers dissociate (probe retraction indicated in red, Figure 8, 10 and 11) resulting in adhesion peak in the force plot, (Figure 8A, 10A). When no binding occurs, the adhesion peak in the force plot is absent, (Figure 8B, 10B). A PEG linker is used to separate the amyloid molecule from the surface to allow for differentiating the adhesion peak from non-

specific tip-substrate interactions as indicated by the negative vertical deflection between 0 and 10 nm above the surface (Figure 10 A and B).

The surface modifications to the tip and mica surface are carefully designed to isolate individual amyloid-amyloid binding forces sufficiently high above the surface to differentiate from non-specific binding of the tip with the mica substrate that may otherwise obscure A $\beta$  interactions. Non-specific binding, as indicated by the small adhesion peak (negative vertical deflection) between 0 and 10 nm above the surface, results from non-specific tip interaction with mica surface (see figure 10 A and B below). The presence of PEG linker allows us to separate non-specific binding from A $\beta$ -A $\beta$  binding. The PEG linker has an average expected length of about 20 nm – calculated from the molecular weight – but experimentally has been shown to be 35 nm, as observed in previous force spectroscopy experiments<sup>48,230</sup>. Therefore, we expect the unbinding events to occur starting at 40 nm above the surface but have been observed to occur between 35 and 80 nm above the surface due to variance in polymer length. Only single molecule interactions are considered so that only curves with one distinct adhesion peak are used (Figure 10A below). When the density of A $\beta$  on the surface or tip is too high the number of force plots with multiple unbinding increases, example shown in Figure 10. Trials where the number of force plots with multiple peaks exceeds 5% of the total binding curves were omitted.

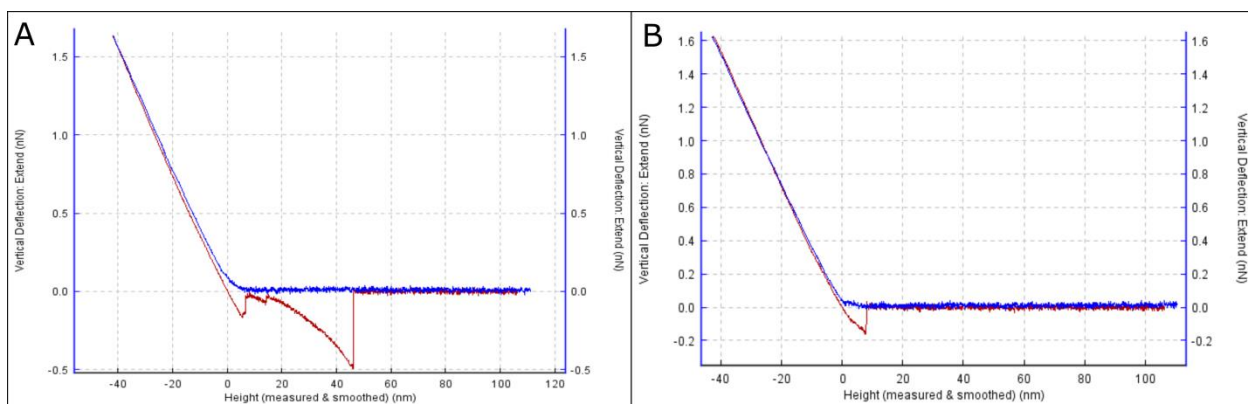


**Figure 10: Binding and non-binding force curves.** A force curve showing the unbinding of two A $\beta$  proteins at 45 nm above the surface, approach (red) and retraction (blue) of the probe. Contact occurs at  $x = 0$ .

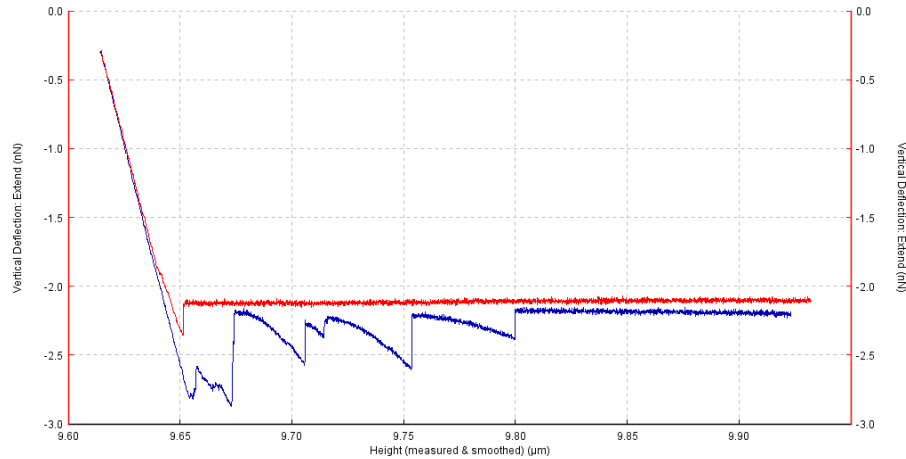


**Figure 11: Multiple unbinding curve.** A force curve showing multiple unbinding of A $\beta$  proteins, approach (red) and retraction (blue) of the probe.

### 3.2.2 Experimental Yield of Binding Events

The percent yield was generated as the ratio of unbinding events by the total number of force curves taken; results from each SG inhibitor are shown in Figure 12A. We then compared the number of binding events with and without inhibitor to get a reduction in experimental yield shown in Figure 12B. As the inhibitors are designed to block the self-recognition region of the A $\beta$  peptide and prevent dimerization detailed analysis of the specific unbinding forces yields no differences between control and inhibitor<sup>230</sup>. We previously explored the concentration dependent effects of SGA1 using this assay and found an inverse exponentially decreasing relationship between the experimental yield and concentration with an apparent asymptotic limit of the inhibitor to block dimerization events<sup>230</sup>. As such all inhibitors were tested at the low concentration of 40nM (corresponding to 1:2 ratio of A $\beta$  to inhibitor) where each inhibitor is expected to be monomeric and previously found good A $\beta$ -A $\beta$  inhibition activity<sup>230</sup>.

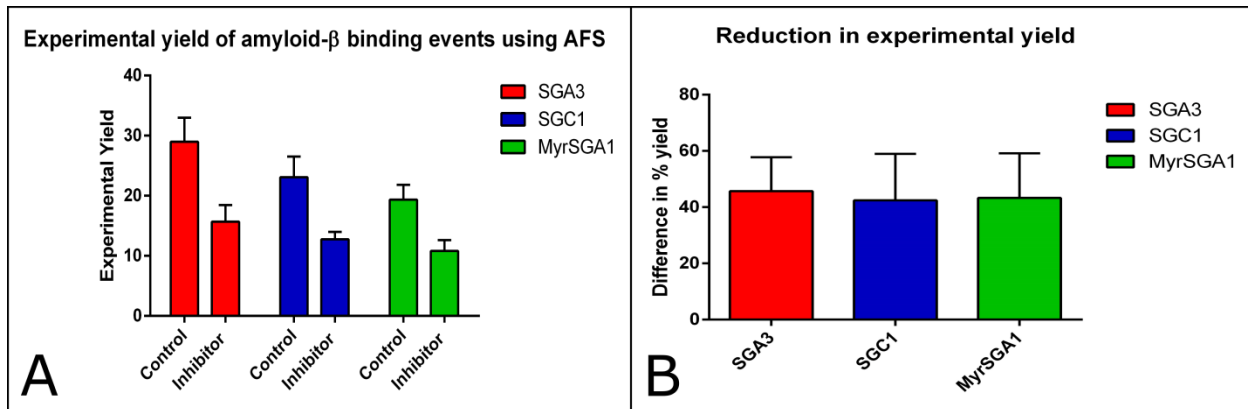


**Figure 12: Experimental yield of A $\beta$  binding with SG inhibitor.** A) Experimental yield of A $\beta$  unbinding events (N=3) for SGA3, SGC1 and M-SGA1 plotted with SEM. All inhibitors significantly reduced binding/unbinding of A $\beta$  ( $P < 0.05$ ), (B) Reduction in experimental yield of unbinding events plotted with SEM. From Robinson et al. (2017). BBA: proteins and proteomics – accepted in press.

It can be seen that effective inhibition of A $\beta$  dimerization is observed with all three inhibitor molecules (paired T-test –  $P < 0.05$ ; Figure 12A). Experimental data show no significant difference in the ability of each SG inhibitor to prevent dimerization between inhibitors using analysis of variance (ANOVA,  $P < 0.05$ ; Figure 12B). Although the three inhibitors were shown to have slightly different binding affinities and edge specificity towards the A $\beta_{13-23}$  fragment, as shown by MD data<sup>16,17,232</sup>, they all effectively prevent A $\beta$ -A $\beta$  binding as shown by SMFS experiments with no discernable distinction.

### 3.2.3 Distribution of Forces

The histograms below show the distribution of the unbinding forces between A $\beta$  monomers with and without the inhibitor compounds (Figure 13). It can be seen from the force distributions below that all inhibitors reduce the total number of binding events. It is difficult to make any concrete conclusions about how the inhibitors interfere with the process of A $\beta$  dimerization however there may be some grounds to suggest the inhibitors not only block dimerization but each may cause different contributions to the strength of A $\beta$ -A $\beta$  forces that are allowable, by preferentially allowing certain types of interactions in a structurally dependent way. All mean A $\beta$  – A $\beta$  unbinding forces were calculated using JPK data processing software and then plotted as a histogram and analysed further using Origin Pro multiple peak Gaussian fitting. A two peak fit to the force distribution the control force distribution shows one

peak centered at  $99 \pm 6$  pN and the other about  $217 \pm 26$  pN (mean  $\pm$  SD over all 3 control data sets, Figure 13), with the first peak being narrower than the second.

In looking at the force distributions, it appears that SGC1 does not appreciably change the position of the first peak but drastically reduces its extent, while the position of the second peak was shifted significantly to a higher binding force of  $280 \pm 20$  pN (Figure 13A). It can be seen from the plot of SGC1 that two additional peaks, each with lower probably but higher unbinding forces can be seen. These unbinding events may correspond to a multiple unbinding event occurring at the same rupture length, and is thus indistinguishable from a single molecule event. SGC1 caused an average A $\beta$ -A $\beta$  unbinding force of  $105 \pm 4$  pN (Appendix A: supplemental material, Figure 18). In computational studies, SGC1 was found to bind to each face of the A $\beta$  recognition region without bias, meaning its predicted binding energy was the same for each side<sup>232</sup>.

The control force histogram for the SGA3 data set poorly fit a normal distribution ( $R^2=0.55373$ , Appendix A - supplemental material, Figure 18). Unfortunately, the control unbinding forces for SGA3 did not follow as closely to the distribution as expected. When comparing to the force distribution across all control trials (peak 1 =  $99 \pm 6$  pN and peak 2 =  $217 \pm 26$  pN), it appears as though SGA3 does not have a significant effect on the position of the peaks (peak 1 =  $106 \pm 2$  pN and peak 2 =  $210 \pm 17$  pN, Figure 13B). This indicates SGA3 more uniformly blocked binding events as compared to SGC1 which caused a shift in the second binding peak to a higher probable unbinding force.

Myr-SGA1 it was found to strongly prevent higher energy binding configurations, which were barely populated, with few unbinding events larger than 300pN (Figure 13C). That being said it had very limited effect at preventing lower energy binding configurations of the monomers, while reducing the lowest mean A $\beta$ -A $\beta$  unbinding force, from  $99 \pm 6$  pN to  $89 \pm 1$  pN. This may be due to the terminal myristic acid group on the pseudopeptide which increases its hydrophobicity. The inhibitor has strong binding characteristics to the recognition region of the peptide preventing higher energy hydrogen bonding between monomers but may not prevent the lower energy hydrophobic interactions. The interaction between the myristic acid attached to the SG inhibitor to the strongly hydrophobic C-terminal of the A $\beta$  monomers would

not be able to prevent an A $\beta$  dimer complex. In terms of the larger therapeutic implications this may be problematic as it may stabilize the oligomer state, as mentioned previously low MW oligomers are largely held together by hydrophobic interactions and not  $\beta$ -sheets<sup>35</sup>. Therefore inhibitors that have high hydrophobicity with the ability to block  $\beta$ -sheets may stabilize disordered low MW oligomers which are most toxic.

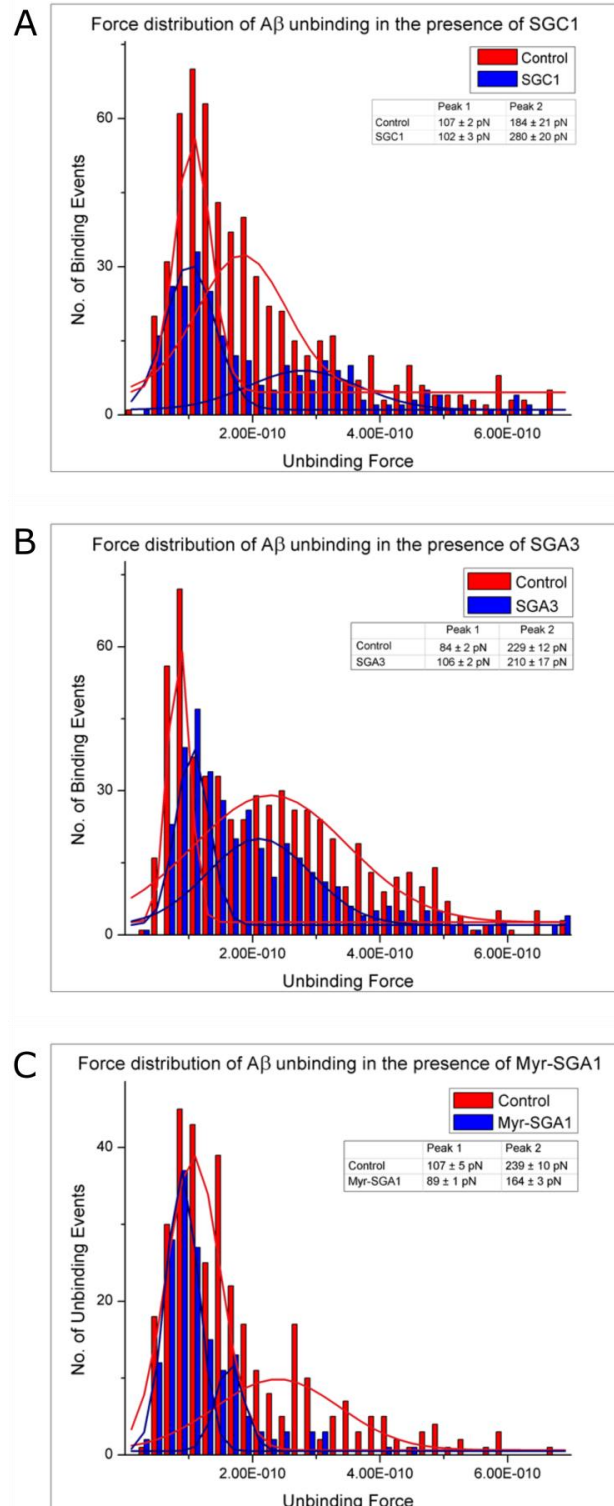


**Figure 13: The A $\beta$  force distribution for SG inhibitors.** For each inhibitor with corresponding control unbinding forces. A dual Gaussian fit was applied to each distribution – SGC1, SGA3 and Myr-SGA1. The distribution for SGC1 (A) contained a shift in the second peak towards higher energy binding, while the distribution for SGA3 (B) was unchanged and finally, Myr-SGA1 (C) caused an extremely significant shift in the force distribution towards the lower energy binding forces, blocking nearly all higher energy binding configurations. From Robinson et al. (2017). BBA: proteins and proteomics – accepted in press



### 3.3 Conclusion

These results show that all three inhibitors effectively prevent amyloid-amyloid binding due to strong binding to amyloid- $\beta$  peptide and also that SG inhibitors cause changes in the distribution of amyloid-amyloid unbinding events in a structurally unique fashion, providing some insight into how the inhibitors mediate A $\beta$  dimerization. The biophysical properties (especially hydrophobicity) and structure of inhibitors appears to be important for modifying A $\beta$  dimerization. SGC1 demonstrated a fairly uniform reduction in binding events across a range of forces but did shift the higher energy binding peak to a higher probably unbinding force, which may indicate limited effectiveness to block oligomer formation. SGA3 had little effect on the force distribution more evenly reducing binding events across the histogram. The myristylated inhibitor (Myr-SGA1) drastically reduced the number of higher energy binding events and lowered the most probable unbinding force. The low energy binding events most likely correspond to hydrophobic interactions alone with the higher energy forces likely involving contributions from both hydrophobic interactions and hydrogen bonding between A $\beta$  monomers.

## Chapter 4: SG inhibitor toxicity and the effects on A $\beta$ toxicity

Cell viability studies evaluating drug toxicity and the effect of the drug on A $\beta$  toxicity is essential for early proof of principle preclinical trials. In this chapter SG inhibitor toxicity and SG inhibitor neuroprotection against A $\beta$  toxicity of several lead candidates are reported. A murine hippocampal-derived immortalized cell line, designated HT-22, was used to assess cellular viability to A $\beta$  toxicity. HT-22 cells exhibit glutamate excitotoxicity<sup>237</sup>, neuronal cholinergic markers<sup>238</sup>, and importantly are sensitive to A $\beta$  toxicity<sup>239,240</sup>. A previous reports in HT-22 based AD models have demonstrated dose dependant A $\beta$  toxicity that can be ameliorated by activation of nicotinic acetylcholine receptors<sup>240</sup>. These neuronal characteristics make HT-22 cells suitable for evaluating the effects of A $\beta$  on cell viability as cholinergic dysfunction and neuronal excitotoxicity are involved in A $\beta$  pathology and AD. These models are however limited by the high proliferation rate of the immortalized HT-22 cells and require a super-physiological concentration of A $\beta$  to induce cytotoxicity. These two features, high proliferation rate and high concentration of A $\beta$ , are not physiological and should be considered in the interpretation of results.

### 4.1 Methods

#### 4.1.1 Cell Culture Models

HT-22 cells were grown in 10 cm<sup>2</sup> tissue culture treated dishes in full growth media comprised of DMEM/F12, 10% fetal bovine serum (FBS) and 1% penicillin/streptomycin in a humidified environment at 37° C and 5% CO<sub>2</sub>. The cellular viability of HT-22 cells exposed to A $\beta$  as assessed using the metabolic MTT assay. To mimic AD in vitro, super-physiological concentrations of 5 $\mu$ M A $\beta$  prepared in various states (monomers, oligomers and fibrils) are applied to the cells and incubated for 24 hours – these treatment groups will be labelled the A $\beta$  control. The true control (TC) is simply untreated cells. In this particular model A $\beta$  oligomers should reduce cellular viability to 50  $\pm$  10% of TC. Next, the concentration dependant effects of SG inhibitors on A $\beta$  toxicity are then compared to the A $\beta$  control. DMSO is used in suspending A $\beta$  into media for treatment and thus an additional control containing an equivalent amount of DMSO added to media was performed to ensure the effect of DMSO on cell viability is within

10% of the TC. Finally, the effects of SG inhibitors on A $\beta$  prepared in various aggregation states will be evaluated.

#### *4.1.2 Inhibitor and A $\beta$ preparations*

Stock solutions of SG inhibitors were prepared at 100  $\mu$ M in ultrapure water and stored at -80 C and thawed immediately prior to use. Stock solutions were kept up to 6 months. To prepare treatments stock solutions were further diluted in DMEM/F12 to the final concentration 10  $\mu$ M, 5  $\mu$ M and 2.5  $\mu$ M. On the day of treatment, full growth media in the 96 well plates (described above), was fully removed and replaced with inhibitor dissolved in DMEM/F12.

Several different preparations of A $\beta$  were used. A $\beta$  monomers, oligomers and fibrils were prepared following adapted Stine's protocols <sup>47</sup>. 1 mg of A $\beta$  (1-42) (< 97 % pure, HFIP, purchased from rPeptide) was dissolved in HFIP to a concentration of 1mg/ml and 70  $\mu$ L aliquots of this solution are pipetted into microcentrifuge tubes, placed inside a desiccator in the fume hood and allowed to evaporate in low humidity environment for 24 hours leaving behind a thin film of A $\beta$  monomers. These stock aliquots of 70  $\mu$ g A $\beta$  were then stored at -20° C in glass jar containing desiccant for up to 1 year. Immediately prior to use 70  $\mu$ g A $\beta$  was resuspended in DMSO at a concentration of 5 mM, vortexed for 30 seconds, pulse centrifuged for 30 seconds and then sonicated for 10 minutes. The 5 mM A $\beta$  solution prepared in DMSO was then diluted to 100  $\mu$ M in cold DMEM/F12 media, this solution represents the 0 hour time point and can be said to be monomeric although it will immediately begin aggregating at rates dependant on concentration and temperature. The 100  $\mu$ M solution was then further diluted to 5 or 33  $\mu$ M in fresh DMEM/F12 or DMEM/F12 containing SG inhibitor at various concentrations corresponding to a final ratio of A $\beta$  to SG of 5:1, 2:1, 1:1 and 1:2. For monomeric A $\beta$  the 5  $\mu$ M solution was used immediately, to produce oligomers the 5 or 33  $\mu$ M solution was placed in 4°C fridge for 24 hours, and finally to produce fibrils a 33 $\mu$ M solution was incubated at 37°C for 24 hours. The 33  $\mu$ M solutions of A $\beta$  were then diluted to a final concentration of 5  $\mu$ M for treatment.

#### *4.1.3 MTT Assay*

The cytotoxicity of compounds can be measured by counting live and dead cells differentiated by their ability to take up particular dye into the cell, such as trypan blue. This is time consuming without automated cell counters; as such other high throughput biochemical methods that assess cellular viability have been established. This is most routinely accomplished through the use of colorimetric assays which gauge cellular metabolism. Here a molecule that undergoes a color change following metabolism is used, the amount of coloured metabolite is related to the metabolic capacity of the culture and acts as a proxy measure of the cultures health. It is then straight forward to simply quantify the strength of signal at a particular wavelength associated with the metabolite and compare to untreated cells for a relative measure of cellular viability. In the MTT assay 3-(4,5-Dimethylthiazol-2-yl)-2,5-Diphenyltetrazolium (MTT) Bromide, a yellow salt, is metabolized via an NADH dependent pathway to a purple metabolite, formazan, which has an absorbance peak at 570 nm (Figure 14).

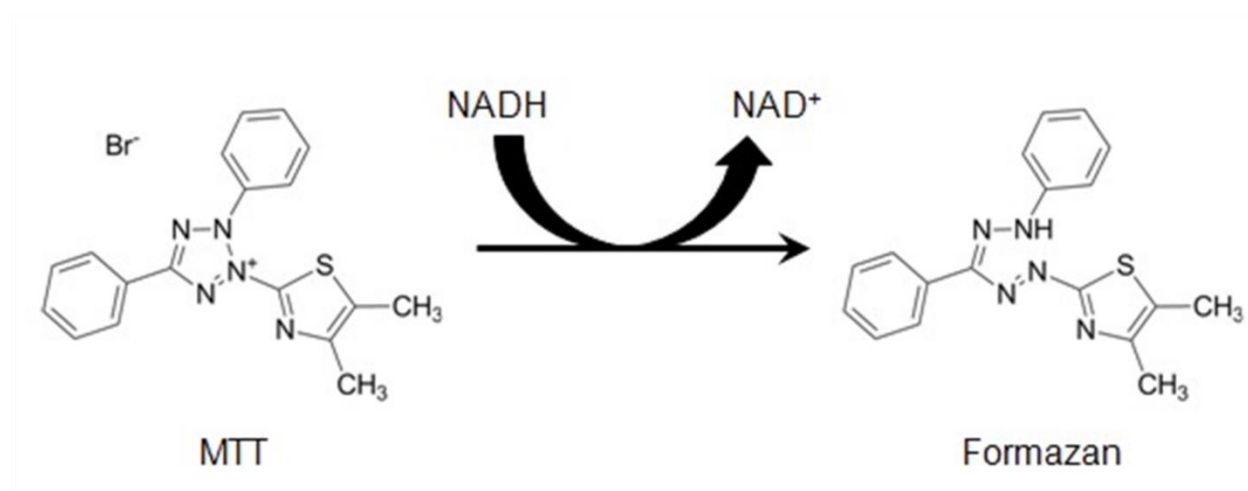


**Figure 14: MTT metabolism** to formazan is NADH dependent changing from yellow to a purple. This can be easily quantified using absorbance spectroscopy with the absorbance peak set to 570 nm<sup>241</sup>.

The MTT assay was used to evaluate the viability of HT22 cells exposed to solutions of either inhibitor alone (for drug toxicity) or mixtures of inhibitor with full length A $\beta$ , prepared as described above. HT-22 cells were plated into 96-well cell culture plates with a cell density of 10,000 cells/well, and then grown in full growth media at 37 C, 5% CO<sub>2</sub> for until 80 % confluent (20 - 24 hours) at which point treatments were applied. Full growth media was exchanged for treatment media, and then returned to incubator for 24 hours, allowing treatments to affect

cell viability. After, the media was exchanged for phenol red-free DMEM/F12 with 10% MTT solution. The cells were returned to the incubator to metabolize the MTT for 3.5 hours. The cells are then solubilized in a buffer solution of isopropanol with 10 % Triton X-100 and 0.1 M HCl by manual pipetting. After solubilisation each well of the plate was read in Molecular Dynamics plate reader at 570 nm and 690 nm. The signal at 690 nm is subtracted from the value at 570 nm for each well to account for background. Media controls (wells containing no cells) were averaged to calculate the background signal from MTT that has not be metabolised and then subtracted from each of the wells containing cells. All treatment groups were then expressed as a ratio to the TC for each plate.

#### *4.1.4 Statistical Analysis*

Inhibitor toxicity to HT-22 cells was assessed in triplicates after exposure to each individual inhibitor (SGA1, Myr-SGA1, SGA3, Myr-SGA3 and SGC1) at concentrations of 2.5, 5.0 and 10.0  $\mu\text{M}$  for 24 hours. A total of N=4 independent trials were performed for all inhibitors at 2.5, 5.0 and 10 $\mu\text{M}$  for HT-22 cells between passage number 3 and 15. A two-way ANOVA with multiple comparisons was performed to establish any significant differences between all groups with a null hypothesis that the inhibitors would have no effect on cellular viability. Multiple comparisons between individual inhibitors, at each concentration, with the TC were performed during the two-way ANOVA using Fisher's least significant difference (LSD) test where significance was assigned when  $p < 0.05$ . The Fisher's LSD is identical to performing individual T-tests between each inhibitor at a specific concentration with control A $\beta$  as it does not perform any correction to the p-value for multiple comparisons. This is suitable as the variance between each inhibitor cannot be assumed to be the same. Without correction the risk of false positive is greater but the chances of false negatives are minimized.

In assessing the effects of the SG inhibitors on A $\beta$  toxicity HT-22 cells were exposed to 5  $\mu\text{M}$  A $\beta$  or 5  $\mu\text{M}$  A $\beta$  with inhibitor at a concentration of 1.0, 2.5, 5.0 or 10  $\mu\text{M}$  in triplicate for each treatment group per trial for N=3 independent trials. Only trials where A $\beta$  control exhibited a reduction in cell viability by at least 35% were considered, two standard deviations from the target of 50%. Again two-way ANOVA with multiple comparisons using Fisher's LSD

was performed. All comparisons were between the A $\beta$  control and each inhibitor at a particular concentration, significance is assigned when  $p < 0.05$ .

## 4.2 Results and Discussion

### 4.2.1 SG inhibitor toxicity on HT-22 cells

First the toxicity of the SG inhibitor was evaluated on HT22 neurons cultured according to the methodology above. SG inhibitor was prepared at 2.5, 5.0 and 10.0  $\mu\text{M}$  in DMEM/F12 media, applied to cells and incubated for 24 hours prior to treating with MTT. From the graph below (Figure 15) it can be seen that SGA1 and SGA3 are not toxic, with no significant difference in viability as compared to TC, while SGC1 did not significantly affect cell viability at but followed a trend toward dose dependent toxicity. Myristic acid modified inhibitors (Myr-SGA1 and Myr-SGA3) showed a strong dose dependent toxicity (Figure 15). The toxicity associated with these inhibitors could be for a variety of non-mutually exclusive reasons. The first is that myristic acid itself is likely lipotoxic toward neuronal cells; some evidence for this comes from two reports indicating caspase-1 mediated lipotoxicity<sup>242</sup>, as well as AD-like tau hyperphosphorylation<sup>63</sup>, associated with stearic and palmitic acids - which differ from myristic acid by 2 and 4 carbons on the fatty acid tail, respectively. These two reports suggest a potential mechanism for saturated fatty acid induced cell death from myristylated inhibitors. In addition to these mechanisms computational studies indicate high Myr-SGA1 self-association, as indicated by the high stability of Myr-SGA1 homodimer, which could indicate aggregation or detergent like toxic<sup>232</sup>.

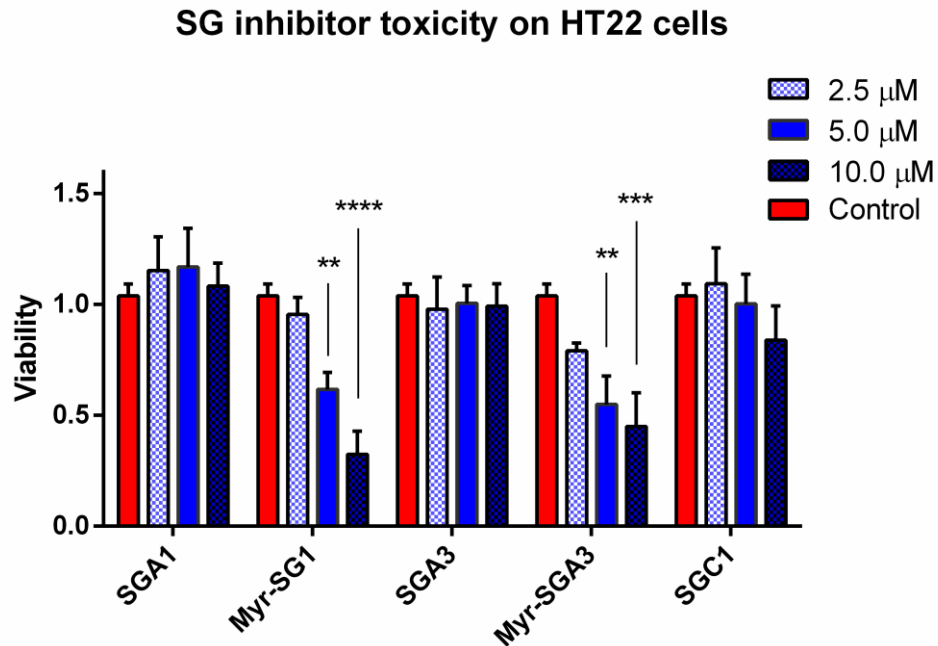


**Figure 15: SG inhibitor toxicity to HT-22 cells.** MTT cell viability assays indicate that myristic acid modified SG inhibitors (designated “Myr-”) show a dose dependent toxicity, while non-myristylated inhibitors are not toxic to mHT22 cells. Triplicate measures, N = 4, mean  $\pm$  SEM, Fisher’s LSD ( $p < 0.01$ \*\*,  $p < 0.001$ \*\*\* and  $p < 0.0001$ \*\*\*\*).

#### 4.2.2 Effect of inhibitors on A $\beta$ oligomers

The A $\beta$  treatment prepared according to modified Stine’s protocols with no inhibitor reliably produces oligomers with which to compare against A $\beta$  – SG inhibitor mixtures<sup>47</sup>. A slight modification to the protocol for these studies was to incubate A $\beta$  at 5 $\mu$ M as opposed to 100  $\mu$ M. This was done to accommodate the SG inhibitor and ensure the monomeric form was dominant in solution as SG inhibitors have a low self-affinity that can cause the formation of homodimers at sufficiently high concentrations<sup>17</sup>. The SG inhibitors proposed are predicted to bind to R, the self-recognition region of A $\beta$ , stabilizing the monomer and driving equilibrium toward the low toxicity species, ideally containing a higher proportion of monomers to oligomers and thus reducing toxicity.

### Cell Viability of HT22 - A $\beta$ with SG Inhibitor

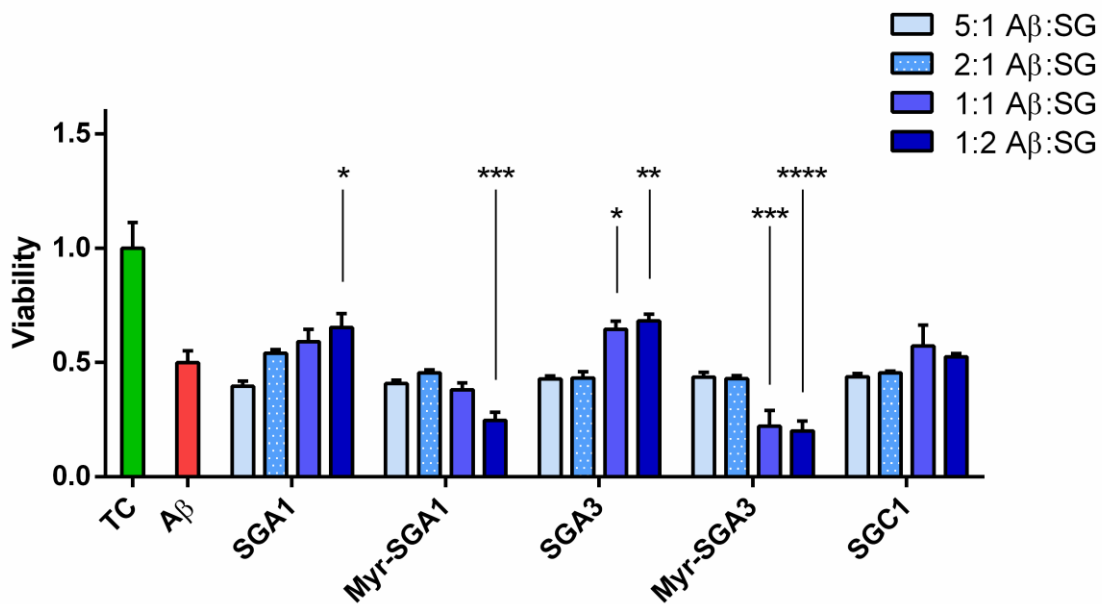


**Figure 16: SG inhibitor rescue of HT-22 cells from A $\beta$ .** Cell viability after exposure to A $\beta$  without (mean + SEM, N=6) and with SG inhibitor at 5:1, 2:1, 1:1 and 1:2 ratio of A $\beta$  to SG (mean + SEM, N=3). SGA1 and SGA3 demonstrate a dose dependent effect on toxicity, improving cellular viability by 15 and 18 % at a 1:2 ratio, respectively. Toxicity of myristylated inhibitors is compounded with the presence of A $\beta$  oligomers in a dose dependent fashion (triplicate measures, two-way ANOVA with Fisher's LSD ( $p < 0.05^*$ ,  $p < 0.01^{**}$ ,  $p < 0.001^{***}$  and  $p < 0.0001^{****}$ )).

It can be seen from Figure 16 above that the HT-22 cell viability after A $\beta$  treatment alone was approximately  $50 \pm 5$  %. Only two of the five inhibitors demonstrated protective effects against A $\beta$  toxicity as reflected by the percent viability. SGA1 was shown to provide mild protection compared to A $\beta$ , with the SGA1-A $\beta$  treatment at 1:2 improving the survival to  $65 \pm 6$  % ( $p < 0.05^*$ ), which corresponds to a relative increase over A $\beta$  treatment by approximately  $30 \pm 14$  %. SGA3 performed even better with the 1:1 and 1:2 A $\beta$ :SG treatment groups improving cell viability compared to A $\beta$  treatment to  $64 \pm 3$  % and  $68 \pm 3$  % for a relative increase of  $30 \pm 12$  and  $38 \pm 12$ %, over A $\beta$  respectively ( $p < 0.05^*$  and  $p < 0.01^{**}$ ). Although the statistical test showed significance the neuroprotection of SGA1 and SGA3 was modest.

Further studies of SG inhibitors on A $\beta$  toxicity were performed in less controlled circumstances at 37° C to try and improve SG – A $\beta$  interactions. The results from these experiments were inconclusive (shown Appendix B: supplement material – Figure 18) most likely due to the large variability in A $\beta$  toxicity. No significant effect was observed which could



be due to the lower inhibitor to A $\beta$  ratio (1:1) or the higher temperature which would promote aggregation.

The toxicity of Myr-SG inhibitors appeared to enhance A $\beta$  toxicity (Figure 15,  $p < 0.001^{***}$  and  $p < 0.0001^{****}$ ). This increase in toxicity could be due to combined A $\beta$  and lipotoxicity related to fatty acid exposure. As demonstrated in the previous chapter using SMFS, Myr-SGA1 had the capacity to block A $\beta$  dimerization and dramatically changed the distribution of binding forces between A $\beta$  monomers favouring lower energy binding configurations that may correspond to hydrophobic association. It is highly likely that Myr-SG inhibitors would impact the aggregation state of A $\beta$ , owing to its high affinity to the recognition region of A $\beta$ . The hydrophobicity of the myristic acid tail should promote SG-A $\beta$  interactions despite a high homodimer stability<sup>232</sup>. It may be the case that Myr-SG inhibitors do in fact engage A $\beta$  but promote and include themselves in the formation of A $\beta$  oligomers due to strong hydrophobic interactions that drive early oligomer formation. With the N-methyl backbone of the peptide it would prevent  $\beta$ -sheet interactions and indeed could stabilize the small molecular weight A $\beta$  species while delaying fibril formation, enhancing A $\beta$  cytotoxicity.

These modest increases in survival for SGA1 and SGA3 at the highest ratio of A $\beta$  to SG are promising especially considering the super-physiological concentrations of A $\beta$  used in this assays. In AD, interstitial brain fluid and CSF levels of free soluble A $\beta$  are estimated to be on the order of  $10^{-9}$  M, 1000-fold lower than what was used in this assay. In addition this assay does not take into account any A $\beta$  clearance and degradation pathways. Although HT-22 cells mimic several important neuronal characteristics in AD, this *in vitro* AD model is an artificial environment which does not accurately represent physiological levels of A $\beta$  or the progressive accumulation of A $\beta$ . Even worse, A $\beta$  is produced predominantly in the intracellular compartment before being excreted into the brain parenchyma and intracellular A $\beta$  accumulation appears to be most critical in the early disease as it greatly affects cellular viability prior to extracellular deposits<sup>243,244</sup>. It is most likely that the earliest neuronal stress induced by A $\beta$  occurs from the inside out rather than the outside in. This style of *in vitro* model like the one used in this report most accurately represents the extreme of advanced AD where extracellular soluble A $\beta$  is in high concentration. That being said SG inhibitors are expected to

perform better with a smaller ratio of SG to A $\beta$  more indicative of the early or prodromal phase of AD. The use of these types of assays appear more well suited to studying pharmacological interventions that provide indirect A $\beta$  protection through mechanisms which do not specifically involve A $\beta$  aggregation, such as activation of growth factors or neuroprotective receptors<sup>240</sup>.

#### 4.2.3 Aggregation dependence

The effect of SG inhibitors on the formation of various A $\beta$  species may provide hints as to effects on earlier and later stages of Alzheimer's disease. SGA1 demonstrated anti-cytotoxic effects against A $\beta$  oligomers prepared at 5  $\mu$ M and thus was chosen for further testing. A $\beta$  in various aggregation states were prepared according to the methods described above. One day before treatment, solutions of 33  $\mu$ M monomers, oligomers and fibrils with and without SGA1 at a concentration ratio of 1:2 A $\beta$  to SG were placed in -80° C, 4° C and 37° C, respectively. Monomeric solutions were thawed under sonication to maintain its monomeric form. Immediately prior to treatment each group was diluted to a final concentration of 5  $\mu$ M and applied to cells. A $\beta$  fibrils demonstrated lower toxicity than oligomers (Figure 17 below, Student's T-test –  $p < 0.05$ ); although the difference between oligomers and monomers was insignificant it trended towards lower monomer toxicity as expected (Figure 17). Since the HT-22 cells were exposed to A $\beta$  species for 24 hours monomeric A $\beta$  would have ample time to aggregate such that A $\beta$  prepared in monomeric form would quickly form oligomers after being applied to cells. Sampling the health of the cell culture as a function of time may show important differences in viability that were lost after a complete 24 hour cycle.

In HT-22 cells SGA1 appeared to have no significant effect on A $\beta$  toxicity when co-incubated in conditions where monomers or preformed oligomers are the dominant molecular species (Figure 17). This is in contrast to the previous section wherein SGA1 demonstrated a mild reduction in A $\beta$  oligomer toxicity (Figure 16 above). This may be explained by the higher concentration of SGA1 and A $\beta$  used in this set of experiments (33  $\mu$ M as compared to 5  $\mu$ M). At higher concentration SGA1 forms semi-stable homodimers and the rates of A $\beta$  aggregation are much higher. This may lower the interaction probability between SGA1 and A $\beta$ . SGA1 enhanced the cytotoxicity of A $\beta$  when prepared under fibril forming conditions, 33 $\mu$ M at 37° C (Figure 17, Student's T test –  $p < 0.05$ ). This increase in toxicity is likely due to SGA1 stabilization of

oligomer structure where the inhibition caused by SG inhibitors is sufficient to delay fibril formation but not sufficient to drive the equilibrium to favour monomeric A $\beta$ . This is in agreement with previous result by Hane et al. where it was demonstrated by AFM imaging that SGA1 caused dramatically higher oligomer to fibril ratio compared to A $\beta$  alone<sup>230</sup>.

### Aggregation Dependence on Cell Viability of HT22

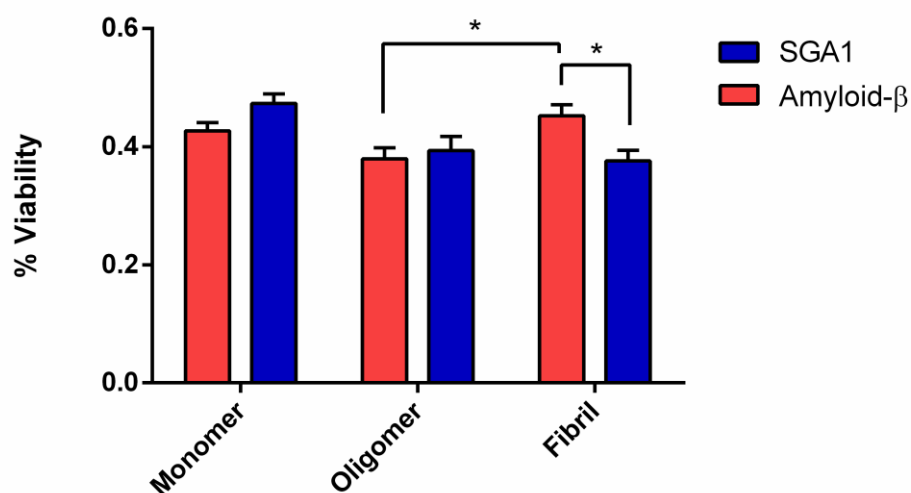


**Figure 17: Aggregation dependence of SGA1 on A $\beta$  toxicity** evaluated at 2:1 ratio of inhibitor to A $\beta$ . No significant differences in toxicity are observed for monomers and oligomers; however enhanced toxicity is observed when SG inhibitors are present during the preparation of fibrils (N=4, quadruplicate measures, Student's T-test ( $p < 0.05^*$ )).

### 4.3 Conclusion

SG inhibitors are largely non-toxic up to 10 $\mu$ M, with the exception of the myristic acid modified SG inhibitors which caused dose dependent toxicity to cells. Unfortunately a different design strategy for delivery of the SG inhibitors across the BBB barrier will be necessary.

The effects of SG inhibitors on A $\beta$  oligomer toxicity as assessed with HT-22 cells were small but promising. Two of the three inhibitors (SGA1\* and SGA3\*\*) caused approximately a one third improvement in cellular viability from A $\beta$  toxicity ( $p < 0.05^*$  and  $p < 0.001^{**}$ , respectively). SGA1 caused increased toxicity of A $\beta$  solutions prepared in fibril forming conditions ( $p < 0.05^*$ ), potentially shifting equilibrium in favour of toxic oligomers. It was demonstrated previously<sup>230</sup> and in Chapter 3 above that SG inhibitors do not fully block A $\beta$  dimerization, and based on MD simulations will form SG homodimers at sufficiently high concentrations and therefore must dissociate before engaging A $\beta$ <sup>17,18</sup>. The complicated equilibrium between SG-SG, SG-A $\beta$  and A $\beta$ -A $\beta$  in solution may discourage formation of

oligomers at the onset but that after some time  $A\beta$  interactions may dominate promoting longer lag in fibril growth, thus SG peptides may increase the effective lifetime of toxic oligomers. Previous reports have demonstrated that lipids can effectively solubilize otherwise insoluble inert  $A\beta$  fibrils into toxic proto-fibrils<sup>45</sup>, further studies will need to determine if SG inhibitors also induce reversal of fibrils to more toxic state.

## Chapter 5: Future Directions

The SMFS study presented above provides information pertaining to the effect of SG inhibitors on A $\beta$  dimerization that can be compared with cell viability studies. The experimental yield of A $\beta$  events was significantly reduced in the presence of all SG inhibitors however with no difference between the inhibitors. Detailed analyses of the unbinding forces demonstrate significant structure dependent effects on the force distribution. SGA3 had no significant effects on the distribution of forces compared to the mean control distribution but showed some effectiveness at protecting against A $\beta$  toxicity. SGC1 appeared to cause an increase in higher energy binding events, increasing the second most probable unbinding force and could be related to the lack of effect on A $\beta$  toxicity. Myr-SGA1 caused a drastic decrease in high energy binding events but unfortunately, demonstrated an inherent A $\beta$  independent neurotoxicity that compounded in the presence of A $\beta$ .

Studies where super-physiological concentrations of A $\beta$  are applied to induce toxicity have obvious shortcomings and their physiological relevance to human AD is limited, as discussed in Chapter 4. These types of studies may be more relevant to drug candidates whose pharmacological interventions involve receptor-mediated drug protection to ameliorate, rather than prevent, aggregation associated A $\beta$  toxicity<sup>240</sup>. The positive neuroprotective effect on HT-22 cells justifies further evaluation of SGA1 and SGA3 *in vitro* with primary neurons which are more physiologically relevant. It should be a high priority to repeat the studies presented here, as well as in primary neurons, for the B and D class SG inhibitors – as they incorporate D-amino acids which should be expected to perform better than the L-amino analogues tested here<sup>245</sup>. Provided experiments on primary neurons confirm the results presented in this thesis, future studies *in vivo* using AD animal models would be justified.

Alternatively, it may be important to use a cell culture model that progressively accumulates A $\beta$  over time which would be more physiological, albeit more resource intensive. Advances in tissue engineering and 3D cell culture models have demonstrated more physiological cell culture models that are more representative of the progressive nature of AD and A $\beta$  accumulation in particular<sup>27,246</sup>. In these models genetically modified human neuroprogenitor cells that overexpress the AD protein, APP, are seeded into Matrigel

nanoscaffolding<sup>27,246</sup>. The deposition of extracellular A $\beta$ , a major hallmark of AD, develops within 6 weeks of culturing, followed at 14 weeks by the appearance hyperphosphorylated tau protein, a major secondary downstream event in A $\beta$  pathology<sup>27,246</sup>. Since these models rely on changing the media every few days to sustain the culture this would in a fashion simulate the CSF flushing that occurs *in vivo*, another important physiological process. In these models prevention could be more accurately determined by assessing the cell culture at few time points, measuring various pathological hallmarks, such as A $\beta$ , ROS and even changes in cellular signalling pathways.

Structural characterization of the fraction of A $\beta$  species produced when incubated with the SG inhibitors would provide a better understanding of structure-toxicity relationship. Fractionation techniques based on size exclusion have become much more efficient in recent years. Symmetric flow-field flow fractionation may be the most accurate method for determining ratios of A $\beta$  fractions in a sample and has been used to identify with higher precision the nature of A $\beta$  toxicity in relation to prion diseases, but could be very useful for realizing aggregation dependent effects<sup>247,248</sup>. Correlating the various fractions of A $\beta$  species produced with and without inhibitor will help to better understand the toxicity-structure studies presented in this thesis.

The myristic acid delivery system intended for CNS uptake of SG inhibitors will have to be rethought as demonstrated by the compounding toxicity of the Myr-SG inhibitors in conjunction with A $\beta$ . The TAT CPP has already been shown to be a suitable candidate for enhanced CNS delivery for A $\beta$  targeted inhibitors<sup>188</sup>, so this is an option. Alternatively, the pseudo-peptide SG inhibitor itself could potentially be turned into a CPP by optimizing electrostatic and hydrophobic/hydrophilic character. That being said an improvement in BBB uptake could also be achieved using receptor-mediated delivery with the addition of specific BBB ligands, for instance, a 12-residue peptide ligand for transferrin receptor has been shown to improve uptake of gold nanoparticles into the brain<sup>204</sup>. As well, the 29-residue rabies virus glycoprotein fragment which binds nicotinic acetylcholine receptors has also been demonstrated to safely transport peptides across the BBB<sup>205</sup>.

Despite over 100 years of research and shifting paradigms, the aetiology of A $\beta$  pathology and AD is not definitively known, while it may be the case that AD is too broadly classified and that several subtypes of AD should be defined and clarified. The strategy of inhibiting A $\beta$  aggregation as a preventative treatment for AD has not been sufficiently studied to close the subject for good. SG peptide inhibitors could stand to be a useful preventative measure in pre-dementia patients, perhaps alongside mAbs or other treatments designed to increase A $\beta$  clearance.

## Chapter 6: Conclusion

The studies presented in this thesis present experimental evidence in molecular and cellular studies that demonstrate the potential of theoretically proposed SG inhibitors as A $\beta$  targeted AD treatments. We show that A $\beta$  aggregation inhibitors can be tested with single-molecule biophysics approaches. In addition, the work presented here provides verification that HT-22 cells are useful as a cell culture model for testing A $\beta$  toxicity, *in vitro*. In this study it was demonstrated that all SG inhibitors have been shown to engage A $\beta$  and inhibit amyloid-amyloid binding at the single molecule level. These SG class inhibitors prevent dimerization in structurally unique ways and, importantly two SG inhibitors were shown to mitigate A $\beta$  oligomer toxicity in cell viability studies. A new SG inhibitor delivery system is certainly required moving forward, due to the associated toxicity of the myristic acid modification to neurons. The protection of the non-myristoylated SG inhibitors to super-physiological concentrations of A $\beta$  oligomer toxicity was minimal and the propensity of inhibitor to increase neurotoxic activity when mixed with A $\beta$  under conditions to promote fibrils is a concern. Although the protective effect was minimal the cell culture models used here more accurately reflect late stage AD, as such SG inhibitors should behave more efficiently in preventative models of AD, both *in vitro* and *in vivo*. SGA1 and SGA3 should be tested further *in vitro*, with primary hippocampal neurons. The two studies presented in this thesis provide motivation and justification for further preclinical studies of theoretically designed novel amyloid inhibitors.



## References

1. Prince, M. *et al.* World Alzheimer Report 2015: The Global Impact of Dementia - An analysis of prevalence, incidence, cost and trends. *Alzheimer's Dis. Int.* **84** (2015). doi:10.1111/j.0963-7214.2004.00293.x
2. Hardy, J. A. & Higgins, G. A. Alzheimer's disease: the amyloid cascade hypothesis. *Science* **256**, 184–5 (1992).
3. Jones, L., Harold, D. & Williams, J. Genetic evidence for the involvement of lipid metabolism in Alzheimer's disease. *Biochim. Biophys. Acta* **1801**, 754–761 (2010).
4. Heppner, F. L., Ransohoff, R. M. & Becher, B. Immune attack: the role of inflammation in Alzheimer disease. *Nat Rev Neurosci* **16**, 358–372 (2015).
5. Sivanandam, T. M. & Thakur, M. K. Traumatic brain injury: A risk factor for Alzheimer's disease. *Neuroscience and Biobehavioral Reviews* **36**, 1376–1381 (2012).
6. Hane, F. T. *et al.* Recent Progress in Alzheimer's Disease Research, Part 3: Diagnosis and Treatment. *J. Alzheimer's Dis.* **57**, 645–665 (2017).
7. Lee, N. Y., Choi, H. O. & Kang, Y. S. The acetylcholinesterase inhibitors competitively inhibited an acetyl L-carnitine transport through the blood-brain barrier. *Neurochem. Res.* **37**, 1499–1507 (2012).
8. Schneider, L. S. Lack of Evidence for the Efficacy of Memantine in Mild Alzheimer Disease. *Arch. Neurol.* **68**, 991 (2011).
9. Ong, W. Y., Tanaka, K., Dawe, G. S., Ittner, L. M. & Farooqui, A. A. Slow excitotoxicity in alzheimer's disease. *Journal of Alzheimer's Disease* **35**, 643–668 (2013).
10. Raina, P. *et al.* Effectiveness of cholinesterase inhibitors and memantine for treating dementia: evidence review for a clinical practice guideline (Structured abstract). *Ann. Intern. Med.* **148**, 379–397 (2008).
11. Howard, R. *et al.* Donepezil and Memantine for moderate-to-severe Alzheimer's disease. *N. Engl. J. Med.* **366**, 893–903 (2012).
12. Dysken, M. W. *et al.* Effect of vitamin E and memantine on functional decline in Alzheimer disease: the TEAM-AD VA cooperative randomized trial. *Jama* **311**, 33–44 (2014).
13. Pohanka, M. Alzheimer's disease and related neurodegenerative disorders: implication and counteracting of melatonin. *J. Appl. Biomed.* **9**, 185–196 (2011).
14. Wang, J. *et al.* Anti-Inflammatory Drugs and Risk of Alzheimer's Disease: An Updated Systematic Review and Meta-Analysis. *J. Alzheimers Dis.* **44**, 385–396 (2015).
15. Karran, E., Mercken, M. & Strooper, B. De. The amyloid cascade hypothesis for Alzheimer's disease: an appraisal for the development of therapeutics. *Nat. Rev. Drug Discov.* **10**, 698–712 (2011).
16. Mothana, B., Roy, S. & Rauk, A. Molecular dynamics study of the interaction of A $\beta$  (13-23) with  $\beta$ -sheet inhibitors. *Arkivoc* **2009**, 116–134 (2009).
17. Mehrazma, B., Petoyan, A., Opare, S. K. A. & Rauk, A. Interaction of the N -AcA $\beta$  (13 – 23) NH 2 segment of the beta amyloid peptide with beta-sheet-blocking peptides : site and edge specificity. *Can. J. Chem.* **10**, 1–

- 10 (2016).
18. Roy, S. PhD dissertation: Designing Novel Peptidic Inhibitors of Beta Amyloid Oligomerization. (University of Calgary, 2010).
  19. Hardy, J. & Selkoe, D. J. The amyloid hypothesis of Alzheimer's disease: progress and problems on the road to therapeutics. *Science* **297**, 353–356 (2002).
  20. Loo, D. T. *et al.* Apoptosis is induced by beta-amyloid in cultured central nervous system neurons. *Proc. Natl. Acad. Sci. U. S. A.* **90**, 7951–5 (1993).
  21. Feng, Z. & Zhang, J. T. Protective effect of melatonin on  $\beta$ -amyloid-induced apoptosis in rat astrogloma c6 cells and its mechanism. *Free Radic. Biol. Med.* **37**, 1790–1801 (2004).
  22. Behl, C., Davis, J. B., Klier, F. G. & Schubert, D. Amyloid beta peptide induces necrosis rather than apoptosis. *Brain Res.* **645**, 253–264 (1994).
  23. Sepulveda, F. J., Parodi, J., Peoples, R. W., Opazo, C. & Aguayo, L. G. Synaptotoxicity of Alzheimer beta amyloid can be explained by its membrane perforating property. *PLoS One* **5**, 1–9 (2010).
  24. Demuro, A. *et al.* Calcium dysregulation and membrane disruption as a ubiquitous neurotoxic mechanism of soluble amyloid oligomers. *J. Biol. Chem.* **280**, 17294–17300 (2005).
  25. Pivovarova, N. B. & Andrews, S. B. Calcium-dependent mitochondrial function and dysfunction in neurons. *FEBS J.* **277**, 3622–36 (2010).
  26. Abramov, A. Y., Canevari, L. & Duchen, M. R.  $\beta$ -Amyloid Peptides Induce Mitochondrial Dysfunction and Oxidative Stress in Astrocytes and Death of Neurons through Activation of NADPH Oxidase. *J. Neurosci.* **24**, 565–575 (2004).
  27. Kim, Y. H. *et al.* A 3D human neural cell culture system for modeling Alzheimer's disease. *Nat. Protoc.* **10**, 985–1006 (2015).
  28. Young-Pearse, T. L. *et al.* A Critical Function for  $\beta$ -Amyloid Precursor Protein in Neuronal Migration Revealed by In Utero RNA Interference. *J. Neurosci.* **27**, 14459–14469 (2007).
  29. Evin, G. & Hince, C. BACE1 as a therapeutic target in alzheimer's disease: Rationale and current status. *Drugs and Aging* **30**, 755–764 (2013).
  30. Mitani, Y. *et al.* Differential effects between  $\gamma$ -secretase inhibitors and modulators on cognitive function in amyloid precursor protein-transgenic and nontransgenic mice. *J. Neurosci.* **32**, 2037–50 (2012).
  31. Riddell, D. R., Christie, G., Hussain, I. & Dingwall, C. Compartmentalization of  $\beta$ -secretase (Asp2) into low-buoyant density, noncaveolar lipid rafts. *Curr. Biol.* **11**, 1288–1293 (2001).
  32. Bodovitz, S. & Klein, W. L. Cholesterol modulates alpha-secretase cleavage of amyloid precursor protein. *J. Biol. Chem.* **271**, 4436–4440 (1996).
  33. Tycko, R. Insights into the amyloid folding problem from solid-state NMR. *Biochemistry* **42**, 3151–3159 (2003).
  34. Petkova, A. T. *et al.* A structural model for Alzheimer's beta  $\beta$ -amyloid fibrils based on experimental

- constraints from solid state NMR. *Proc. Natl. Acad. Sci. U. S. A.* **99**, 16742–16747 (2002).
35. Ahmed, M. *et al.* Structural conversion of neurotoxic amyloid- $\beta$ 1–42 oligomers to fibrils. *Nat. Struct. Mol. Biol.* **17**, 561–567 (2010).
  36. Hamley, I. W. *et al.* Influence of the solvent on the self-assembly of a modified amyloid beta peptide fragment. II. NMR and computer simulation investigation. *J. Phys. Chem. B* **114**, 940–951 (2010).
  37. Tjernberg, L. O. *et al.* Arrest of  $\beta$ -amyloid fibril formation by a pentapeptide ligand. *J. Biol. Chem.* **271**, 8545–8548 (1996).
  38. Ghanta, J., Shen, C. L., Kiessling, L. L. & Murphy, R. M. A strategy for designing inhibitors of  $\beta$ -amyloid toxicity. *J. Biol. Chem.* **271**, 29525–29528 (1996).
  39. Hung, L. W. *et al.* Amyloid- $\beta$  Peptide (A $\beta$ ) Neurotoxicity Is Modulated by the Rate of Peptide Aggregation: A Dimers and Trimers Correlate with Neurotoxicity. *J. Neurosci.* **28**, 11950–11958 (2008).
  40. Sciarretta, K. L., Gordon, D. J., Petkova, A. T., Tycko, R. & Meredith, S. C. A $\beta$ 40-lactam(D23/K28) models a conformation highly favorable for nucleation of amyloid. *Biochemistry* **44**, 6003–6014 (2005).
  41. Sakono, M. & Zako, T. Amyloid oligomers: Formation and toxicity of A $\beta$  oligomers. *FEBS Journal* **277**, 1348–1358 (2010).
  42. Klein, W. L., Krafft, G. A. & Finch, C. E. Targeting small A $\beta$  oligomers: The solution to an Alzheimer's disease conundrum? *Trends in Neurosciences* **24**, 219–224 (2001).
  43. Williams, T. L. *et al.* A $\beta$ 42 oligomers, but not fibrils, simultaneously bind to and cause damage to ganglioside-containing lipid membranes. *Biochem. J.* **439**, 67–77 (2011).
  44. Dahlgren, K. N. *et al.* Oligomeric and fibrillar species of amyloid- $\beta$  peptides differentially affect neuronal viability. *J. Biol. Chem.* **277**, 32046–32053 (2002).
  45. Martins, I. C. *et al.* Lipids revert inert A $\beta$  amyloid fibrils to neurotoxic protofibrils that affect learning in mice. *EMBO J.* **27**, 224–233 (2008).
  46. Upadhaya, A. R., Lungrin, I., Yamaguchi, H., Fändrich, M. & Thal, D. R. High-molecular weight A $\beta$  oligomers and protofibrils are the predominant A $\beta$  species in the native soluble protein fraction of the AD brain. *J. Cell. Mol. Med.* **16**, 287–295 (2012).
  47. Stine, W. B., Jungbauer, L., Yu, C. & LaDu, M. J. Preparing synthetic A $\beta$  in different aggregation states. *Methods Mol. Biol.* **670**, 13–32 (2011).
  48. Hane, F., Tran, G., Attwood, S. J. & Leonenko, Z. Cu<sup>2+</sup> Affects Amyloid- $\beta$  (1-42) Aggregation by Increasing Peptide-Peptide Binding Forces. *PLoS One* **8**, p.e59005 (2013).
  49. Hane, F. & Leonenko, Z. Effect of Metals on Kinetic Pathways of Amyloid- $\beta$  Aggregation. *Biomolecules* **4**, 101–16 (2014).
  50. Jun, S. & Saxena, S. The aggregated state of amyloid- $\beta$  peptide in vitro depends on Cu<sup>2+</sup> ion concentration. *Angew. Chemie - Int. Ed.* **46**, 3959–3961 (2007).
  51. Hatami, A., Albay, R., Monjazebe, S., Milton, S. & Glabe, C. Monoclonal antibodies against A $\beta$ 42 fibrils

- distinguish multiple aggregation state polymorphisms in vitro and in Alzheimer disease brain. *J. Biol. Chem.* **289**, 32131–32143 (2014).
52. Nicholson, A. M. & Ferreira, A. Increased membrane cholesterol might render mature hippocampal neurons more susceptible to beta-amyloid-induced calpain activation and tau toxicity. *J. Neurosci.* **29**, 4640–51 (2009).
  53. Bucciantini, M. *et al.* Toxic effects of amyloid fibrils on cell membranes: the importance of ganglioside GM1. *FASEB J.* **26**, 818–831 (2012).
  54. Drolle, E., Negoda, A., Hammond, K., Pavlov, E. & Leonenko, Z. Changes in lipid membranes may trigger amyloid toxicity in Alzheimer's disease. *PLoS One* **In Press**, arXiv: 1704.08394 (2017).
  55. Abramov, A. Y., Ionov, M., Pavlov, E. & Duchon, M. R. Membrane cholesterol content plays a key role in the neurotoxicity of ??-amyloid: Implications for Alzheimer's disease. *Aging Cell* **10**, 595–603 (2011).
  56. Zampagni, M. *et al.* Lipid rafts are primary mediators of amyloid oxidative attack on plasma membrane. *J. Mol. Med.* **88**, 597–608 (2010).
  57. Evangelisti, E. *et al.* Lipid rafts mediate amyloid-induced calcium dyshomeostasis and oxidative stress in Alzheimer's disease. *Curr. Alzheimer Res.* **10**, 143–53 (2013).
  58. Cordy, J. M., Hooper, N. M. & Turner, A. J. The involvement of lipid rafts in Alzheimer's disease. *Mol. Membr. Biol.* **23**, 111–122 (2006).
  59. Cecchi, C. & Stefani, M. The amyloid-cell membrane system. The interplay between the biophysical features of oligomers/fibrils and cell membrane defines amyloid toxicity. *Biophys. Chem.* **182**, 30–43 (2013).
  60. Drolle, E., Gaikwad, R. M. & Leonenko, Z. Nanoscale electrostatic domains in cholesterol-laden lipid membranes create a target for amyloid binding. *Biophys. J.* **103**, (2012).
  61. Miñano-Molina, A. J. *et al.* Soluble oligomers of amyloid- $\beta$  peptide disrupt membrane trafficking of  $\beta$ -amino-3-hydroxy-5-methylisoxazole-4-propionic acid receptor contributing to early synapse dysfunction. *J. Biol. Chem.* **286**, 27311–27321 (2011).
  62. Rosales-Corral, S. *et al.* Accumulation of exogenous amyloid- $\beta$  peptide in hippocampal mitochondria causes their dysfunction: A protective role for melatonin. *Oxid. Med. Cell. Longev.* **2012**, (2012).
  63. Patil, S. & Chan, C. Palmitic and stearic fatty acids induce Alzheimer-like hyperphosphorylation of tau in primary rat cortical neurons. *Neurosci. Lett.* **384**, 288–293 (2005).
  64. Ryan, S. D. *et al.* Amyloid-beta<sub>42</sub> signals tau hyperphosphorylation and compromises neuronal viability by disrupting alkylacylglycerophosphocholine metabolism. *Proc. Natl. Acad. Sci.* **106**, 20936–20941 (2009).
  65. Wang, X., Michaelis, M. L. & Michaelis, E. K. Functional genomics of brain aging and Alzheimer's disease: Focus on selective neuronal vulnerability. *Curr. Genomics* **11**, 618–633 (2010).
  66. Iacono, D. *et al.* The Nun Study. *Neurology* **73**, 665–673 (2009).
  67. Combs, C. K., Johnson, D. E., Karlo, J. C., Cannady, S. B. & Landreth, G. E. Inflammatory mechanisms in

- Alzheimer's disease: inhibition of beta-amyloid-stimulated proinflammatory responses and neurotoxicity by PPARgamma agonists. *J. Neurosci.* **20**, 558–67 (2000).
68. Cai, Z., Zhao, B. & Ratka, A. Oxidative stress and  $\beta$ -amyloid protein in Alzheimer's disease. *NeuroMolecular Medicine* **13**, 223–250 (2011).
  69. Maccioni, R. B., Farías, G., Morales, I. & Navarrete, L. The Revitalized Tau Hypothesis on Alzheimer's Disease. *Arch. Med. Res.* **41**, 226–231 (2010).
  70. Craig, L. A., Hong, N. S. & McDonald, R. J. Revisiting the cholinergic hypothesis in the development of Alzheimer's disease. *Neuroscience and Biobehavioral Reviews* **35**, 1397–1409 (2011).
  71. Panza, F., Solfrizzi, V., Imbimbo, B. P. & Logroscino, G. Amyloid-directed monoclonal antibodies for the treatment of Alzheimer's disease: the point of no return? *Expert Opin. Biol. Ther.* **14**, 1465–76 (2014).
  72. Lambert, J. C. *et al.* Implication of the immune system in Alzheimer's disease: evidence from genome-wide pathway analysis. *J. Alzheimer's Dis.* **20**, 1107–1118 (2010).
  73. Lipinski, M. M. *et al.* Genome-wide analysis reveals mechanisms modulating autophagy in normal brain aging and in Alzheimer's disease. *Proc. Natl. Acad. Sci. U. S. A.* **107**, 14164–14169 (2010).
  74. Robinson, M., Lee, B. Y. & Hane, F. T. Recent Progress in Alzheimer's Disease Research Part 2 - Genetics and Epidemiology. *J. Alzheimer's Dis.* **57**, 317–330 (2017).
  75. Qiu, C., Kivipelto, M. & von Strauss, E. Epidemiology of Alzheimer's disease: occurrence, determinants, and strategies toward intervention. *Dialogues Clin. Neurosci.* **11**, 111–128 (2009).
  76. Kanekiyo, T. *et al.* Neuronal clearance of amyloid- $\beta$  by endocytic receptor LRP1. *J. Neurosci.* **33**, 19276–83 (2013).
  77. Wildsmith, K. R., Holley, M., Savage, J. C., Skerrett, R. & Landreth, G. E. Evidence for impaired amyloid- $\beta$  clearance in Alzheimer's disease. *Alzheimers. Res. Ther.* **5**, 33 (2013).
  78. Vetrivel, K. S. & Thinakaran, G. Membrane rafts in Alzheimer's disease beta-amyloid production. *Biochimica et Biophysica Acta - Molecular and Cell Biology of Lipids* **1801**, 860–867 (2010).
  79. Oda, A., Tamaoka, A. & Araki, W. Oxidative stress up-regulates presenilin 1 in lipid rafts in neuronal cells. *J. Neurosci. Res.* **88**, 1137–1145 (2010).
  80. Tanzi, R. E. & Bertram, L. Twenty years of the Alzheimer's disease amyloid hypothesis: A genetic perspective. *Cell* **120**, 545–555 (2005).
  81. Jones, L. *et al.* Genetic evidence implicates the immune system and cholesterol metabolism in the aetiology of Alzheimer's disease. *PLoS One* **5**, (2010).
  82. Harold, D. *et al.* Genome-wide association study identifies variants at CLU and PICALM associated with Alzheimer's disease. *Nat. Genet.* **41**, 1088–93 (2009).
  83. Lambert, J. C. *et al.* Meta-analysis of 74,046 individuals identifies 11 new susceptibility loci for Alzheimer's disease. *Nat. Genet.* **45**, 1452–8 (2013).
  84. Selkoe, D. J. Resolving controversies on the path to Alzheimer's therapeutics. *Nat. Med.* **17**, 1060–1065

- (2011).
85. Farooqui, A. A., Horrocks, L. A. & Farooqui, T. Modulation of inflammation in brain: A matter of fat. *J. Neurochem.* **101**, 577–599 (2007).
  86. Fessler, M. B. & Parks, J. S. Intracellular lipid flux and membrane microdomains as organizing principles in inflammatory cell signaling. *J. Immunol.* **187**, 1529–35 (2011).
  87. Lim, S. L., Rodriguez-Ortiz, C. J. & Kitazawa, M. Infection, systemic inflammation, and Alzheimer’s disease. *Microbes and Infection* **17**, 549–556 (2015).
  88. Akiyama, H. *et al.* Inflammation and Alzheimer’s disease. *Neurobiology of Aging* **21**, (2000).
  89. Arispe, N. & Doh, M. Plasma membrane cholesterol controls the cytotoxicity of Alzheimer’s disease AbetaP (1-40) and (1-42) peptides. *FASEB J.* **16**, 1526–1536 (2002).
  90. Swaab, D. F. *et al.* Increased Cortisol Levels in Aging and Alzheimer’s Disease in Postmortem Cerebrospinal Fluid. *J. Neuroendocrinol.* **6**, 681–687 (1994).
  91. Silverman, M. N. & Sternberg, E. M. Glucocorticoid regulation of inflammation and its functional correlates: From HPA axis to glucocorticoid receptor dysfunction. *Annals of the New York Academy of Sciences* **1261**, 55–63 (2012).
  92. Koo, E. H., Squazzo, S. L., Selkoe, D. J. & Koo, C. H. Trafficking of cell-surface amyloid beta-protein precursor. I. Secretion, endocytosis and recycling as detected by labeled monoclonal antibody. *J. Cell Sci.* **109**, 991–998 (1996).
  93. Thinakaran, G. & Koo, E. H. Amyloid precursor protein trafficking, processing, and function. *J. Biol. Chem.* **283**, 29615–29619 (2008).
  94. Sasahara, K., Morigaki, K. & Shinya, K. Effects of membrane interaction and aggregation of amyloid  $\beta$ -peptide on lipid mobility and membrane domain structure. *Phys. Chem. Chem. Phys.* **15**, 8929 (2013).
  95. Toh, W. H. *et al.* Dysregulation of intracellular trafficking and endosomal sorting in Alzheimer’s disease: controversies and unanswered questions. *Biochem. J.* **473**, 1977–93 (2016).
  96. Guardia-Laguarta, C. *et al.* Mild cholesterol depletion reduces amyloid- $\beta$  production by impairing APP trafficking to the cell surface. *J. Neurochem.* **110**, 220–230 (2009).
  97. Wahrle, S. *et al.* Cholesterol-Dependent  $\gamma$ -Secretase Activity in Buoyant Cholesterol-Rich Membrane Microdomains. *Neurobiol. Dis.* **9**, 11–23 (2002).
  98. Grimm, M. O. W. *et al.* Regulation of cholesterol and sphingomyelin metabolism by amyloid-beta and presenilin. *Nat. Cell Biol.* **7**, 1118–23 (2005).
  99. Zinser, E. G., Hartmann, T. & Grimm, M. O. W. Amyloid beta-protein and lipid metabolism. *Biochim. Biophys. Acta* **1768**, 1991–2001 (2007).
  100. Hicks, D. A., Nalivaeva, N. N. & Turner, A. J. Lipid rafts and Alzheimer’s disease: Protein-lipid interactions and perturbation of signaling. *Front. Physiol.* **3 JUN**, (2012).
  101. Puig, K. L., Manocha, G. D. & Combs, C. K. Amyloid Precursor Protein Mediated Changes in Intestinal

- Epithelial Phenotype In Vitro. *PLoS One* **10**, 1–16 (2015).
102. Ho, V. M., Lee, J.-A. & Martin, K. C. The cell biology of synaptic plasticity. *Science* **334**, 623–8 (2011).
  103. Matsuzaki, K. Peptide-membrane interactions in biological sciences: antimicrobial peptides and Alzheimer's beta-amyloid peptides as paradigms. *Pept. Sci.* **41st**, 87–88 (2005).
  104. T. Harach, N. Marungruang, N. Dutilleul, V. Cheatham, K. D. Mc Coy, J. J. Neher, M. Jucker, F. Fåk, T., L. and T. B. Reduction of Alzheimer's disease beta-amyloid pathology in the absence of gut microbiota. *n/a* (2015).
  105. Kumar, D. K. V. *et al.* Amyloid- peptide protects against microbial infection in mouse and worm models of Alzheimers disease. *Sci. Transl. Med.* **8**, 340ra72-340ra72 (2016).
  106. Soscia, S. J. *et al.* The Alzheimer's disease-associated amyloid ??-protein is an antimicrobial peptide. *PLoS One* **5**, (2010).
  107. Holmes, C. Systemic infection, interleukin 1beta, and cognitive decline in Alzheimer's disease. *J. Neurol. Neurosurg. Psychiatry* **74**, 788–789 (2003).
  108. Friedman, L. G., Qureshi, Y. H. & Yu, W. H. Promoting Autophagic Clearance: Viable Therapeutic Targets in Alzheimer's Disease. *Neurotherapeutics* **12**, 94–108 (2015).
  109. Lipinski, M. M. *et al.* Genome-wide analysis reveals mechanisms modulating autophagy in normal brain aging and in Alzheimer's disease. *Proc. Natl. Acad. Sci. U. S. A.* **107**, 14164–9 (2010).
  110. Lee, C. Y. D. & Landreth, G. E. The role of microglia in amyloid clearance from the AD brain. *J. Neural Transm.* **117**, 949–960 (2010).
  111. Deane, R., Wu, Z. & Zlokovic, B. V. RAGE (Yin) versus LRP (Yang) balance regulates Alzheimer amyloid ??-peptide clearance through transport across the blood-brain barrier. *Stroke* **35**, 2628–2631 (2004).
  112. Lee, J. H. *et al.* Lysosomal proteolysis and autophagy require presenilin 1 and are disrupted by Alzheimer-related PS1 mutations. *Cell* **141**, 1146–1158 (2010).
  113. Neely, K. M., Green, K. N. & LaFerla, F. M. Presenilin is necessary for efficient proteolysis through the autophagy-lysosome system in a  $\gamma$ -secretase-independent manner. *J. Neurosci.* **31**, 2781–2791 (2011).
  114. Hu, J., Akama, K. T., Krafft, G. a, Chromy, B. a & Van Eldik, L. J. Amyloid-beta peptide activates cultured astrocytes: morphological alterations, cytokine induction and nitric oxide release. *Brain Res.* **785**, 195–206 (1998).
  115. Origlia, N. *et al.* Microglial receptor for advanced glycation end product-dependent signal pathway drives beta-amyloid-induced synaptic depression and long-term depression impairment in entorhinal cortex. *J. Neurosci.* **30**, 11414–11425 (2010).
  116. Itagaki, S., McGeer, P. L., Akiyama, H., Zhu, S. & Selkoe, D. Relationship of microglia and astrocytes to amyloid deposits of Alzheimer disease. *J. Neuroimmunol.* **24**, 173–182 (1989).
  117. Qiao, X. X., Cummins, D. J. & Paul, S. M. Neuroinflammation-induced deposition in the APP(V717F) acceleration of amyloid transgenic mouse. *Eur. J. Neurosci.* **14**, 474–482 (2001).

118. Koenigsnecht-Talboo, J. Microglial Phagocytosis Induced by Fibrillar  $\beta$ -Amyloid and IgGs Are Differentially Regulated by Proinflammatory Cytokines. *J. Neurosci.* **25**, 8240–8249 (2005).
119. Cirrito, J. R. *et al.* P-glycoprotein deficiency at the blood-brain barrier increases amyloid- $\beta$  deposition in an Alzheimer disease mouse model. *J. Clin. Invest.* **115**, 3285–3290 (2005).
120. Sagare, A. P., Bell, R. D. & Zlokovic, B. V. Neurovascular defects and faulty amyloid- $\beta$  vascular clearance in Alzheimer's disease. *Adv. Alzheimer's Dis.* **3**, 87–100 (2012).
121. Nelson, A. R., Sweeney, M. D., Sagare, A. P. & Zlokovic, B. V. Neurovascular dysfunction and neurodegeneration in dementia and Alzheimer's disease. *Biochim. Biophys. Acta - Mol. Basis Dis.* **1862**, 887–900 (2016).
122. Karran, E., Mercken, M. & De Strooper, B. The amyloid cascade hypothesis for Alzheimer's disease: an appraisal for the development of therapeutics. *Nat. Rev. Drug Discov.* **10**, 698–712 (2011).
123. Aisen, P. S. *et al.* Tramiprosate in mild-to-moderate Alzheimer's disease - A randomized, double-blind, placebo-controlled, multi-centre study (the alphase study). *Arch. Med. Sci.* **7**, 102–111 (2011).
124. Karran, E. & Hardy, J. A critique of the drug discovery and phase 3 clinical programs targeting the amyloid hypothesis for Alzheimer disease. *Ann. Neurol.* **76**, 185–205 (2014).
125. Alavez, S., Vantipalli, M. C., Zucker, D. J. S., Klang, I. M. & Lithgow, G. J. Amyloid-binding compounds maintain protein homeostasis during ageing and extend lifespan. *Nature* **472**, 226–229 (2011).
126. Pappolla, M. a *et al.* Melatonin prevents death of neuroblastoma cells exposed to the Alzheimer amyloid peptide. *J. Neurosci.* **17**, 1683–1690 (1997).
127. Zolezzi, J. M. & Inestrosa, N. C. Peroxisome proliferator-activated receptors and alzheimer's disease: Hitting the blood-brain barrier. *Mol. Neurobiol.* **48**, 438–451 (2013).
128. Yallapu, M. M., Nagesh, P. K. B., Jaggi, M. & Chauhan, S. C. Therapeutic Applications of Curcumin Nanoformulations. *AAPS J.* **17**, 1341–56 (2015).
129. Tiwari, S. K. *et al.* Curcumin-loaded nanoparticles potently induce adult neurogenesis and reverse cognitive deficits in Alzheimer's disease model via canonical Wnt/ $\beta$ -catenin pathway. *ACS Nano* **8**, 76–103 (2014).
130. Pappolla, M. *et al.* The neuroprotective activities of melatonin against the Alzheimer beta-protein are not mediated by melatonin membrane receptors. *J. Pineal Res.* **32**, 135–142 (2002).
131. Matsubara, E. *et al.* Melatonin increases survival and inhibits oxidative and amyloid pathology in a transgenic model of Alzheimer's disease. *J. Neurochem.* **85**, 1101–1108 (2003).
132. Dragicevic, N. *et al.* Melatonin treatment restores mitochondrial function in Alzheimer's mice: A mitochondrial protective role of melatonin membrane receptor signaling. *J. Pineal Res.* **51**, 75–86 (2011).
133. Drolle, E. *et al.* Effect of melatonin and cholesterol on the structure of DOPC and DPPC membranes. *Biochim. Biophys. Acta - Biomembr.* **1828**, 2247–2254 (2013).
134. Mohamed, T. & Rao, P. P. N. 2,4-Disubstituted quinazolines as amyloid- $\beta$  aggregation inhibitors with dual cholinesterase inhibition and antioxidant properties: Development and structure-activity relationship (SAR)



- studies. *Eur. J. Med. Chem.* **126**, 823–843 (2017).
135. Osman, W. *et al.* Structure–activity relationship studies of benzyl-, phenethyl-, and pyridyl-substituted tetrahydroacridin-9-amines as multitargeting agents to treat Alzheimer’s disease. *Chem. Biol. Drug Des.* 710–723 (2016). doi:10.1111/cbdd.12800
  136. Bu, X. Le, Rao, P. P. N. & Wang, Y. J. Anti-amyloid Aggregation Activity of Natural Compounds: Implications for Alzheimer’s Drug Discovery. *Molecular Neurobiology* **53**, 3565–3575 (2016).
  137. Gervais, F. *et al.* Targeting soluble A $\beta$  peptide with Tramiprosate for the treatment of brain amyloidosis. *Neurobiol. Aging* **28**, 537–547 (2007).
  138. Robert, R. & Wark, K. L. Engineered antibody approaches for Alzheimer’s disease immunotherapy. *Archives of Biochemistry and Biophysics* **526**, 132–138 (2012).
  139. Lemere, C. A. Immunotherapy for Alzheimer’s disease: hoops and hurdles. *Mol. Neurodegener.* **8**, 36 (2013).
  140. Spencer, B. & Masliah, E. Immunotherapy for alzheimer’s disease: Past, present and future. *Front. Aging Neurosci.* **6**, 1–7 (2014).
  141. Morgan, D. Mechanisms of A $\beta$  plaque clearance following passive A $\beta$  immunization. *Neurodegener. Dis.* **2**, 261–266 (2006).
  142. Legleiter, J. *et al.* Effect of Different Anti-A $\beta$  Antibodies on A $\beta$  Fibrillogenesis as Assessed by Atomic Force Microscopy. *J. Mol. Biol.* **335**, 997–1006 (2004).
  143. DeMattos, R. B. *et al.* Peripheral anti-A $\beta$  antibody alters CNS and plasma A $\beta$  clearance and decreases brain A $\beta$  burden in a mouse model of Alzheimer’s disease. *Proc. Natl. Acad. Sci.* **98**, 8850–8855 (2001).
  144. Banks, W. A. *et al.* Passage of amyloid beta protein antibody across the blood-brain barrier in a mouse model of Alzheimer’s disease. *Peptides* **23**, 2223–2226 (2002).
  145. Banks, W. A. Drug delivery to the brain in Alzheimer’s disease: Consideration of the blood-brain barrier. *Advanced Drug Delivery Reviews* **64**, 629–639 (2012).
  146. Pfeifer, M. *et al.* Cerebral Hemorrhage After Passive Anti-A $\beta$  Immunotherapy. *Science* **298**, 1379 (2002).
  147. Racke, M. *et al.* Exacerbation of Cerebral Amyloid Angiopathy-Associated Microhemorrhage in Amyloid Precursor Protein Transgenic Mice by Immunotherapy Is Dependent on Antibody Recognition of Deposited Forms of Amyloid. *J. Neurosci.* **25**, 629–636 (2005).
  148. Garber, K. Genentech’s Alzheimer’s antibody trial to study disease prevention. *Nat. Biotechnol.* **30**, 731–732 (2012).
  149. Vidarsson, G., Dekkers, G. & Rispen, T. IgG subclasses and allotypes: From structure to effector functions. *Front. Immunol.* **5**, 1–17 (2014).
  150. Adolfsson, O. *et al.* An effector-reduced anti- $\beta$ -amyloid (A $\beta$ ) antibody with unique a $\beta$  binding properties promotes neuroprotection and glial engulfment of A $\beta$ . *J. Neurosci* **32**, 9677–9689 (2012).
  151. Wilcock, D. M. *et al.* Passive immunotherapy against A $\beta$  in aged APP-transgenic mice reverses cognitive

- deficits and depletes parenchymal amyloid deposits in spite of increased vascular amyloid and microhemorrhage. *J. Neuroinflammation* **1**, 24 (2004).
152. Doody, R. S. *et al.* Phase 3 trials of solanezumab for mild-to-moderate Alzheimer's disease. *N. Engl. J. Med.* **370**, 311–21 (2014).
  153. Salloway, S. *et al.* Two phase 3 trials of bapineuzumab in mild-to-moderate Alzheimer's disease. *N. Engl. J. Med.* **370**, 322–33 (2014).
  154. Tayeb, H. O., Murray, E. D., Price, B. H. & Tarazi, F. I. Bapineuzumab and solanezumab for Alzheimer's disease: is the 'amyloid cascade hypothesis' still alive? *Expert Opin. Biol. Ther.* **13**, 1075–1084 (2013).
  155. Samadi, H. & Sultzer, D. Solanezumab for Alzheimer's disease. *Time* 787–798 (2011).  
doi:10.1517/14712598.2011.578573
  156. Liu-Seifert, H. *et al.* Delayed-start analysis: Mild Alzheimer's disease patients in solanezumab trials, 3.5 years. *Alzheimer's Dement. Transl. Res. Clin. Interv.* **1**, 111–121 (2015).
  157. Siemers, E. R. *et al.* Phase 3 solanezumab trials: Secondary outcomes in mild Alzheimer's disease patients. *Alzheimer's Dement.* **12**, 110–120 (2016).
  158. Panza, F. *et al.* Amyloid-based immunotherapy for Alzheimer's disease in the time of prevention trials: the way forward. *Expert Rev. Clin. Immunol.* **10**, 405–419 (2014).
  159. Panza, F. *et al.* Efficacy and safety studies of gantenerumab in patients with Alzheimer's disease. *Expert Rev. Neurother.* **14**, 973–986 (2014).
  160. Sevigny, J. *et al.* The antibody aducanumab reduces A $\beta$  plaques in Alzheimer's disease. *Nature* **537**, 50–56 (2016).
  161. Sperling, R. A. *et al.* Toward defining the preclinical stages of Alzheimer's disease: Recommendations from the National Institute on Aging and the Alzheimer's Association workgroup. *Alzheimer's Dement.* **7**, 1–13 (2011).
  162. Castello, M. A. & Soriano, S. On the origin of Alzheimer's disease. Trials and tribulations of the amyloid hypothesis. *Ageing Research Reviews* **13**, 10–12 (2014).
  163. Aisen, P. S. *et al.* Report of the task force on designing clinical trials in early (predementia) AD. *Neurology* **76**, 280–286 (2011).
  164. Demetrius, L. A., Magistretti, P. J. & Pellerin, L. Alzheimer's disease: The amyloid hypothesis and the Inverse Warburg effect. *Front. Physiol.* **6**, (2015).
  165. Lee, Y. J., Han, S. B., Nam, S. Y., Oh, K. W. & Hong, J. T. Inflammation and Alzheimer's disease. *Arch. Pharm. Res.* **33**, 1539–1556 (2010).
  166. Manczak, M. *et al.* Mitochondria-targeted antioxidants protect against amyloid-?? toxicity in Alzheimer's disease neurons. *J. Alzheimer's Dis.* **20**, (2010).
  167. Zlokovic, B. V. Neurovascular mechanisms of Alzheimer's neurodegeneration. *Trends Neurosci.* **28**, 202–208 (2005).

168. LeVine, H. Quantification of  $\beta$ -sheet amyloid fibril structures with thioflavin T. *Methods Enzymol.* **309**, 274–284 (1999).
169. Levine, H. Thioflavine T interaction with synthetic Alzheimer's disease  $\beta$ -amyloid peptides: Detection of amyloid aggregation in solution. *Protein Sci.* **2**, 404–410 (1993).
170. Barrow, C. J., Yasuda, A., Kenny, P. T. M. & Zagorski, M. G. Solution conformations and aggregational properties of synthetic amyloid  $\beta$ -peptides of Alzheimer's disease. Analysis of circular dichroism spectra. *J. Mol. Biol.* **225**, 1075–1093 (1992).
171. Moores, B., Drolle, E., Attwood, S. J., Simons, J. & Leonenko, Z. Effect of surfaces on amyloid fibril formation. *PLoS One* **6**, e25954 (2011).
172. Sikorski, P., Atkins, E. D. T. & Serpell, L. C. Structure and texture of fibrous crystals formed by Alzheimer's A $\beta$ (11-25) peptide fragment. *Structure* **11**, 915–926 (2003).
173. Ono, K., Condrón, M. M. & Teplow, D. B. Structure-neurotoxicity relationships of amyloid beta-protein oligomers. *Proc Natl Acad Sci U S A* **106**, 14745–14750 (2009).
174. Lowe, T. L., Strzelec, A., Kiessling, L. L. & Murphy, R. M. Structure - Function relationships for inhibitors of  $\beta$ -Amyloid toxicity containing the recognition sequence KLVFF. *Biochemistry* **40**, 7882–7889 (2001).
175. Woodruff-pak, D. S. Animal Models of Alzheimer ' s Disease : Therapeutic Implications. **15**, 507–521 (2008).
176. Pallitto, M. M., Ghanta, J., Heinzelman, P., Kiessling, L. L. & Murphy, R. M. Recognition sequence design for peptidyl modulators of  $\beta$ -amyloid aggregation and toxicity. *Biochemistry* **38**, 3570–3578 (1999).
177. Soto, C., Kindy, M. S., Baumann, M. & Frangione, B. Inhibition of Alzheimer's amyloidosis by peptides that prevent beta-sheet conformation. *Biochem. Biophys. Res. Commun.* **226**, 672–680 (1996).
178. Soto, C. & Sigurdsson, E. M.  $\beta$ -sheet breaker peptides inhibit fibrillogenesis in a rat brain model of amyloidosis: Implications for Alzheimer's therapy. *Nat. Med.* **4**, 623–6 (1998).
179. Soto, C., Kindy, M. S., Baumann, M. & Frangione, B. Inhibition of Alzheimer's Amyloidosis by Peptides That Prevent  $\beta$ -Sheet Conformation. *Biochem. Biophys. Res. Commun.* **226**, 672–680 (1996).
180. Chacón, M. a, Barría, M. I., Soto, C. & Inestrosa, N. C. Beta-sheet breaker peptide prevents Abeta-induced spatial memory impairments with partial reduction of amyloid deposits. *Mol. Psychiatry* **9**, 953–961 (2004).
181. Kumar, J. & Sim, V. D-amino acid-based peptide inhibitors as early or preventative therapy in Alzheimer disease. *Prion* **8**, 1–6 (2014).
182. Miller, S. M. *et al.* Comparison of the proteolytic susceptibilities of homologous L-amino acid, D-amino acid, and N-substituted glycine peptide and peptoid oligomers. *Drug Dev. Res.* **35**, 20–32 (1995).
183. Sievers, S. A. *et al.* Structure-based design of non-natural amino-acid inhibitors of amyloid fibril formation. *Nature* **475**, 96–100 (2011).
184. Austen, B. M. *et al.* Designing peptide inhibitors for oligomerization and toxicity of Alzheimer's  $\beta$ -amyloid peptide. *Biochemistry* **47**, 1984–1992 (2008).
185. Taylor, M. *et al.* Development of a proteolytically stable retro-inverso peptide inhibitor of  $\beta$ -amyloid

- oligomerization as a potential novel treatment for Alzheimers Disease. *Biochemistry* **49**, 3261–3272 (2010).
186. Zorko, M. & Langel, Ü. Cell-penetrating peptides: Mechanism and kinetics of cargo delivery. *Adv. Drug Deliv. Rev.* **57**, 529–545 (2005).
187. McGonigle, P. Peptide therapeutics for CNS indications. *Biochemical Pharmacology* **83**, 559–566 (2012).
188. Parthasarathy, V. *et al.* A Novel Retro-Inverso Peptide Inhibitor Reduces Amyloid Deposition, Oxidation and Inflammation and Stimulates Neurogenesis in the APP<sup>swe</sup>/PS1 $\Delta$ E9 Mouse Model of Alzheimer’s Disease. *PLoS One* **8**, (2013).
189. Poduslo, J. F., Curran, G. L., Kumar, A., Frangione, B. & Soto, C. ??-Sheet breaker peptide inhibitor of Alzheimer’s amyloidogenesis with increased blood-brain barrier permeability and resistance to proteolytic degradation in plasma. *J. Neurobiol.* **39**, 371–382 (1999).
190. Robert, R. & Wark, K. L. Engineered antibody approaches for Alzheimer’s disease immunotherapy. *Arch. Biochem. Biophys.* **526**, 132–138 (2012).
191. Yu, Y. J. *et al.* Boosting brain uptake of a therapeutic antibody by reducing its affinity for a transcytosis target. *Sci. Transl. Med.* **3**, 84ra44 (2011).
192. Couch, J. a. *et al.* Addressing Safety Liabilities of TfR Bispecific Antibodies That Cross the Blood-Brain Barrier. *Sci. Transl. Med.* **5**, 183ra57-183ra57 (2013).
193. Robinson, M., Lee, B. Y. & Leonenko, Z. Drugs and drug delivery systems targeting amyloid-  $\beta$  in Alzheimer ’s disease. **2**, 332–358 (2015).
194. Chen, Y. & Liu, L. Modern methods for delivery of drugs across the blood-brain barrier. *Advanced Drug Delivery Reviews* **64**, 640–665 (2012).
195. Abbott, N. J., Patabendige, A. A. K., Dolman, D. E. M., Yusof, S. R. & Begley, D. J. Structure and function of the blood-brain barrier. *Neurobiology of Disease* **37**, 13–25 (2010).
196. Abbott, N. J., Rönnbäck, L. & Hansson, E. Astrocyte–endothelial interactions at the blood–brain barrier. *Nat. Rev. Neurosci.* **7**, 41–53 (2006).
197. Cucullo, L. *et al.* A new dynamic in vitro model for the multidimensional study of astrocyte-endothelial cell interactions at the blood-brain barrier. *Brain Res.* **951**, 243–254 (2002).
198. Pardridge, W. M. Drug transport across the blood-brain barrier. *J. Cereb. Blood Flow Metab.* **32**, 1959–72 (2012).
199. Mehta, D. C., Short, J. L. & Nicolazzo, J. A. Memantine transport across the mouse blood-brain barrier is mediated by a cationic influx H<sup>+</sup> antiporter. *Mol. Pharm.* **10**, 4491–4498 (2013).
200. Tsuji, A. Small molecular drug transfer across the blood-brain barrier via carrier-mediated transport systems. *NeuroRx* **2**, 54–62 (2005).
201. Gao, B. *et al.* Organic anion-transporting polypeptides mediate transport of opioid peptides across blood-brain barrier. *J. Pharmacol. Exp. Ther.* **294**, 73–79 (2000).
202. Pan, W. & Kastin, A. J. Polypeptide delivery across the blood-brain barrier. *Curr. Drug Targets. CNS Neurol.*

- Disord.* **3**, 131–6 (2004).
203. Yu, Y. J. *et al.* Therapeutic bispecific antibodies cross the blood-brain barrier in nonhuman primates. *Sci Transl Med* **6**, 261ra154 (2014).
204. Prades, R. *et al.* Delivery of gold nanoparticles to the brain by conjugation with a peptide that recognizes the transferrin receptor. *Biomaterials* **33**, 7194–7205 (2012).
205. Kim, J. Y., Choi, W. Il, Kim, Y. H. & Tae, G. Brain-targeted delivery of protein using chitosan- and RVG peptide-conjugated, pluronic-based nano-carrier. *Biomaterials* **34**, 1170–1178 (2013).
206. Xie, L. *et al.* Alzheimer's beta-amyloid peptides compete for insulin binding to the insulin receptor. *J. Neurosci.* **22**, RC221 (2002).
207. Zhao, W.-Q. *et al.* Amyloid beta oligomers induce impairment of neuronal insulin receptors. *FASEB J.* **22**, 246–260 (2007).
208. Jones, A. R. & Shusta, E. V. Blood-brain barrier transport of therapeutics via receptor-mediation. *Pharmaceutical Research* **24**, 1759–1771 (2007).
209. Wiley, D. T., Webster, P., Gale, A. & Davis, M. E. Transcytosis and brain uptake of transferrin-containing nanoparticles by tuning avidity to transferrin receptor. *Proc. Natl. Acad. Sci.* **110**, 8662–8667 (2013).
210. Lee, H. J., Engelhardt, B., Lesley, J., Bickel, U. & Pardridge, W. M. Targeting rat anti-mouse transferrin receptor monoclonal antibodies through blood-brain barrier in mouse. *J. Pharmacol. Exp. Ther.* **292**, 1048–1052 (2000).
211. Bien-Ly, N. *et al.* Transferrin receptor (TfR) trafficking determines brain uptake of TfR antibody affinity variants. *J. Exp. Med.* **211**, 233–44 (2014).
212. Pardridge, W. M., Buciak, J. L., Kang, Y. S. & Boado, R. J. Protamine-mediated transport of albumin into brain and other organs of the rat. Binding and endocytosis of protamine-albumin complex by microvascular endothelium. *J. Clin. Invest.* **92**, 2224–2229 (1993).
213. Hervé, F., Ghinea, N. & Scherrmann, J.-M. CNS Delivery Via Adsorptive Transcytosis. *AAPS J.* **10**, 455–472 (2008).
214. Brambilla, D. *et al.* PEGylated nanoparticles bind to and alter amyloid-beta peptide conformation: Toward engineering of functional nanomedicines for alzheimer's disease. *ACS Nano* **6**, 5897–5908 (2012).
215. Sharma, G., Modgil, A., Zhong, T., Sun, C. & Singh, J. Influence of short-chain cell-penetrating peptides on transport of doxorubicin encapsulating receptor-targeted liposomes across brain endothelial barrier. *Pharm. Res.* **31**, 1194–1209 (2014).
216. Farkhani, S. M. *et al.* Cell penetrating peptides: Efficient vectors for delivery of nanoparticles, nanocarriers, therapeutic and diagnostic molecules. *Peptides* **57**, 78–94 (2014).
217. Bechara, C. & Sagan, S. Cell-penetrating peptides: 20 years later, where do we stand? *FEBS Letters* **587**, 1693–1702 (2013).
218. Akdag, I. O. & Ozkirimli, E. The uptake mechanism of the cell-penetrating pVEC peptide. *J. Chem.* (2013).

doi:10.1155/2013/851915

219. Herce, H. D. & Garcia, A. E. Molecular dynamics simulations suggest a mechanism for translocation of the HIV-1 TAT peptide across lipid membranes. *Proc. Natl. Acad. Sci.* **104**, 20805–20810 (2007).
220. Fosgerau, K. & Hoffmann, T. Peptide therapeutics: Current status and future directions. *Drug Discovery Today* **20**, 122–128 (2015).
221. Opore, S. K. A., Petoyan, A., Mehrazma, B. & Rauk, A. Molecular dynamics study of the monomers and dimers of N -AcA $\beta$  ( 13 – 23 ) NH<sub>2</sub>: on the effect of pH on the aggregation of the amyloid beta peptide of Alzheimer ' s disease. *Can. J. Chem.* **94**, 273–281 (2015).
222. Porat, Y., Mazor, Y., Efrat, S. & Gazit, E. Inhibition of islet amyloid polypeptide fibril formation: A potential role for heteroaromatic interactions. *Biochemistry* **43**, 14454–14462 (2004).
223. Cohen, T., Frydman-Marom, A., Rechter, M. & Gazit, E. Inhibition of amyloid fibril formation and cytotoxicity by hydroxyindole derivatives. *Biochemistry* **45**, 4727–4735 (2006).
224. Gordon, D. J., Tappe, R. & Meredith, S. C. Design and characterization of a membrane permeable N-methyl amino acid-containing peptide that inhibits Abeta1-40 fibrillogenesis. *J. Pept. Res.* **60**, 37–55 (2002).
225. Buser, C. a, Sigal, C. T., Resh, M. D. & McLaughlin, S. Membrane binding of myristylated peptides corresponding to the NH<sub>2</sub> terminus of Src. *Biochemistry* **33**, 13093–13101 (1994).
226. Nelson, A. R., Borland, L., Allbritton, N. L. & Sims, C. E. Myristoyl-based transport of peptides into living cells. *Biochemistry* **46**, 14771–14781 (2007).
227. Charron, G. Protein Lipidation and Lipid Trafficking. *Acc. Chem. Res.* **44**, 699–708 (2011).
228. Aicart-Ramos, C., Valero, R. A. & Rodriguez-Crespo, I. Protein palmitoylation and subcellular trafficking. *Biochimica et Biophysica Acta - Biomembranes* **1808**, 2981–2994 (2011).
229. Mitchell, R. W., On, N. H., Del Bigio, M. R., Miller, D. W. & Hatch, G. M. Fatty acid transport protein expression in human brain and potential role in fatty acid transport across human brain microvessel endothelial cells. *J. Neurochem.* **117**, 735–746 (2011).
230. Hane, F. T., Lee, B. Y., Petoyan, A., Rauk, A. & Leonenko, Z. Testing synthetic amyloid- $\beta$  aggregation inhibitor using single molecule atomic force spectroscopy. *Biosens. Bioelectron.* **54**, 492–498 (2014).
231. Hane, F. PhD Dissertation: Single Molecule Force Spectroscopy Investigations of Amyloid- $\beta$  Aggregation. (University of Waterloo, 2013).
232. Robinson, M. *et al.* Pseudo-peptide Amyloid- $\beta$  Blocking Inhibitors: Molecular Dynamics and Single Molecule Force Spectroscopy Study. *BBA Proteins Proteomics In Press*, (2017).
233. Binnig, G., Quate, C. F. & Gerber, C. Atomic force microscope. *Phys. Rev. Lett.* **56**, 930 (1986).
234. Butt, H. J., Cappella, B. & Kappl, M. Force measurements with the atomic force microscope: Technique, interpretation and applications. *Surf. Sci. Rep.* **59**, 1–152 (2005).
235. Drolle, E., Hane, F., Lee, B. & Leonenko, Z. Atomic force microscopy to study molecular mechanisms of amyloid fibril formation and toxicity in Alzheimer's disease. *Drug Metab. Rev.* **46**, 207–23 (2014).

236. Shlyakhtenko, L. S. *et al.* Silatrane-based surface chemistry for immobilization of DNA, protein-DNA complexes and other biological materials. *Ultramicroscopy* **97**, 279–287 (2003).
237. Davis, J. B. & Maher, P. Protein kinase C activation inhibits glutamate-induced cytotoxicity in a neuronal cell line. *Brain Res.* **652**, 169–73 (1994).
238. Liu, J., Li, L. & Suo, W. Z. HT22 hippocampal neuronal cell line possesses functional cholinergic properties. *Life Sci.* **84**, 267–271 (2009).
239. Gursoy, E., Cardounel, A. & Kalimi, M. Pregnenolone Protects Mouse Hippocampal (HT-22) Cells against Glutamate and Amyloid Beta Protein Toxicity. *Neurochem. Res.* **26**, 15–21 (2001).
240. Wu, M. *et al.* Cannabinoid Receptor CB1 Is Involved in Nicotine-Induced Protection Against A $\beta$  1-42 Neurotoxicity in HT22 Cells. *J. Mol. Neurosci.* **55**, 778–787 (2014).
241. Mosmann, T. Rapid colorimetric assay for cellular growth and survival: Application to proliferation and cytotoxicity assays. *J. Immunol. Methods* **65**, 55–63 (1983).
242. Ulloth, J. E., Casiano, C. A. & De Leon, M. Palmitic and stearic fatty acids induce caspase-dependent and -independent cell death in nerve growth factor differentiated PC12 cells. *J. Neurochem.* **84**, 655–668 (2003).
243. Pensalfini, A. *et al.* Intracellular amyloid and the neuronal origin of Alzheimer neuritic plaques. *Neurobiol. Dis.* **71**, 53–61 (2014).
244. Vetrivel, K. S. & Thinakaran, G. Amyloidogenic processing of beta-amyloid precursor protein in intracellular compartments. *Neurology* **66**, S69-73 (2006).
245. Kumar, J. & Sim, V. D-amino acid-based peptide inhibitors as early or preventative therapy in Alzheimer disease. *Prion* **8**, 119–124 (2014).
246. Choi, S. H. *et al.* A three-dimensional human neural cell culture model of Alzheimer's disease. *Nature* **515**, 274–278 (2014).
247. Freir, D. B. *et al.* Interaction between prion protein and toxic amyloid  $\beta$  assemblies can be therapeutically targeted at multiple sites. *Nat. Commun.* **2**, 336 (2011).
248. Nicoll, A. J. *et al.* Amyloid- $\beta$  nanotubes are associated with prion protein-dependent synaptotoxicity. *Nat. Commun.* **4**, (2013).

## Appendix A: Supplemental Information

### 1. Single peak fit to force distributions

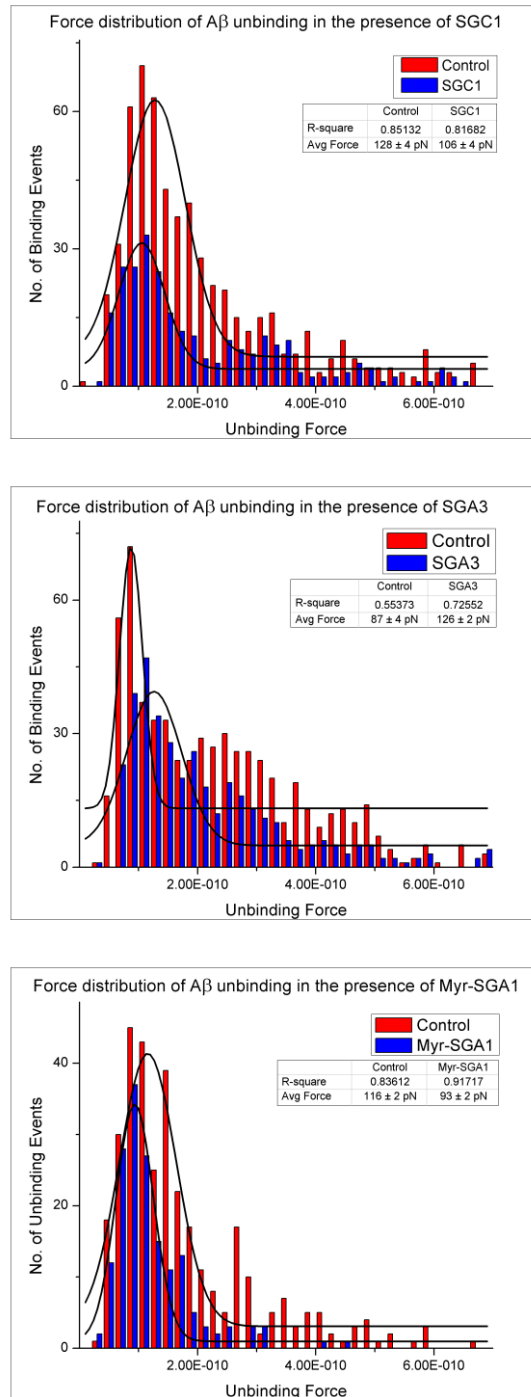


**Figure 18: A $\beta$  force distribution with single peak fit** for inhibitors top to bottom: SGC1, SGA3 and Myr-SGA1. The R-square value for the distribution of control A $\beta$  unbinding forces using a single peak fit were 0.85, 0.55 and 0.84 respectively, as such multiple peak analysis was performed to better fit the data.



## 2. Effects of SG inhibitor on generic A $\beta$ solution

Cell viability of HT22 to A $\beta$  prepared at 37° C for 2 hours

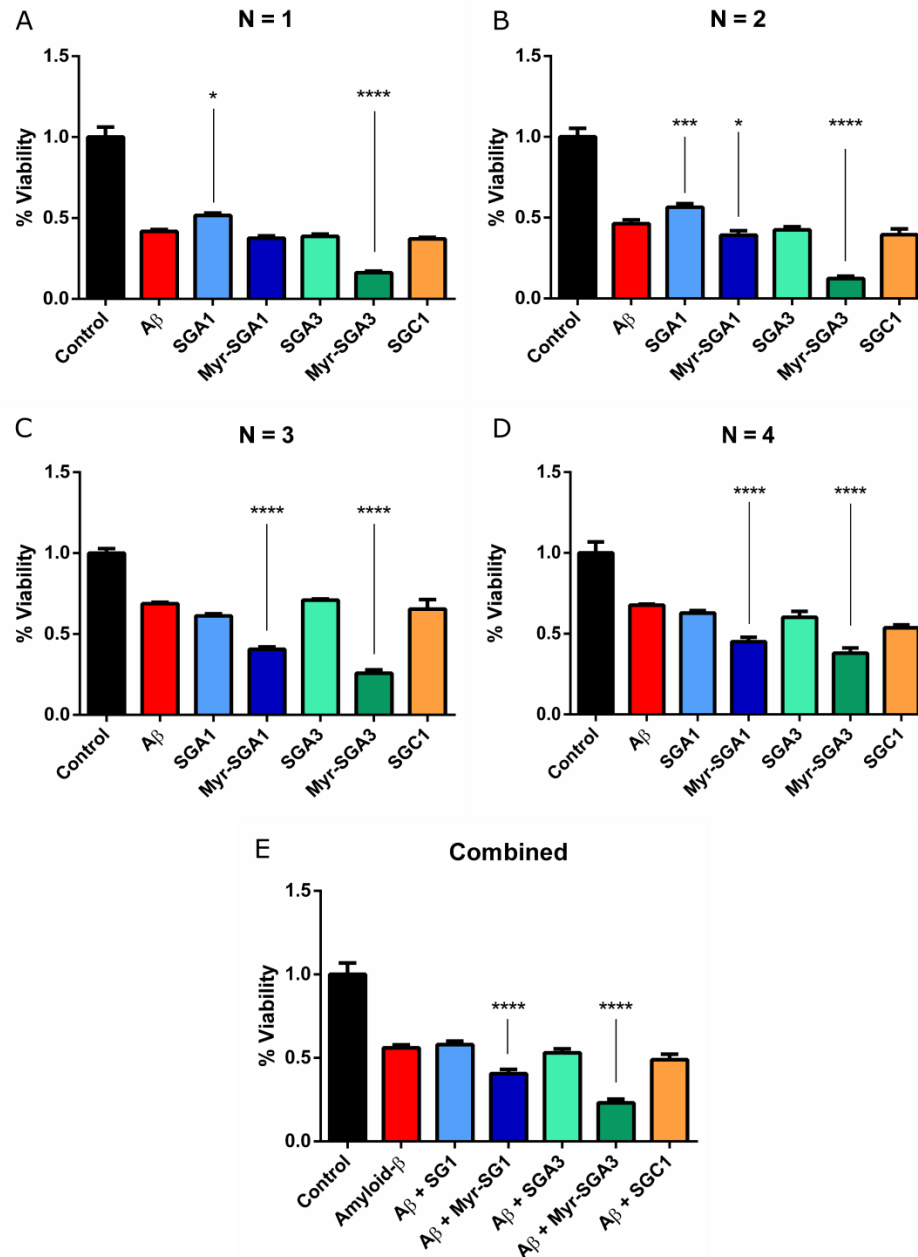


**Figure 19: Cell viability of HT-22 cells to A $\beta$  prepared at 37° C for 2 hours.** The effects of SG inhibitors at equal concentration to A $\beta$  toxicity when prepared at 37 C for 2 hours before exposure to HT-22 cells, the exposure time was 24 hours as in other MTT assays. This solution is expected to produce a large distribution of A $\beta$  aggregate sizes ranging from small oligomers to protofibrils and even short mature fibrils. This A $\beta$  preparation caused highly inconsistent toxicity at 5 $\mu$ M, with only half of the trials (A and B) exhibiting less than 50 % reduction in neuronal viability, of these trials SG1 caused minimal neuroprotection ( $P < 0.05$  and  $P < 0.001$ , respectively). When taken all together (E) the only significant effect was the increase in toxicity of Myr-SGA1 and Myr-SGA3 ( $P < 0.0001$  for both). Similar results would be expected for 0 hour incubation, which would be equivalent to addition of monomeric A $\beta$  at time of exposure.

**Appendix B: Additional Research Projects**

1. The structural biology of A $\beta$ -lipid membrane interactions with real-time high-speed atomic force microscopy – Travelled to the University of Bristol, U.K. on two separate occasions for a total of 9 weeks to collect high-speed AFM images capturing the real-time dynamics of A $\beta$  with model lipid membranes
2. Performed proof of principle experiments towards development of lipid biosensors for the study of membrane-A $\beta$  interactions based on Surface Enhanced Raman Spectroscopy (SERS) and Surface Plasmon Resonance (SPR) techniques.
3. Use of AFM combined fluorescence imaging and SPR to study the binding of affinity tags to various A $\beta$  preparations (monomer, oligomer, fibrils) for MRI AD diagnostic probes.
4. Single molecule force spectroscopy of antigen-adjuvant interactions – This is part of collaboration between Dr. Zoya Leonenko and industry partner the subject of which is confidential and secured by NDA.
5. Performed computational modeling of CO<sub>2</sub> injection wells for long-term atmospheric carbon storage using MATLAB software by writing a program to calculate the real-time pressure distribution within old oil and gas reservoirs as it is filled with compressed liquid CO<sub>2</sub> for climate control engineering applications.